The University Of Sheffield.

Investigating electric vehicles as energy storage systems for an urban tram network to promote the energy efficiency

Teng Zhang

A thesis submitted in partial fulfilment of the requirements for the degree of

Doctor of Philosophy

The University of Sheffield

Faculty of Science

Department of Electronic and Electrical Engineering

September 2021

Abstract

Electrification of the transport sector is a necessary measure required to lower greenhouse gas emissions. However, electrified light rail systems suffer energy efficiency problems due to the ineffective recovery of the braking energy regenerated during train or tramcar braking events. Utilizing the growing number of electric vehicles (EVs), and therefore the increasing number of EV batteries, as energy storage for the rail could provide a novel solution to address the challenge.

Using tramcar operational data collected with a GPS data acquisition system, and the Matlab and Simulink modelling and simulation environment, this research initially gains insight into the energy balance of a local tram system, highlighting that the unrecovered and thereby wasted braking energy could be equivalent to approx. 50% of the overall energy consumption. This research later simulates the addition of a stationary energy storage system (SESS) to the tram network, and demonstrates the energy-saving achieved. Additionally, the simulation also suggests that a small but optimal capacity, and an installation on the mid-stop of an energy supply section, are beneficial to achieving better energy-saving and economic returns. Subsequently, this study designs two energy storage systems (ESSs), the EV energy storage system (EVESS), which solely exploits EV batteries for energy storage, and the combined ESS (CESS), which integrates the EVs with a sub-system of a stationary battery. Both ESS arrangements were found to successfully deliver energy-saving to the tram system. Moreover, a control approach was designed for the CESS to prioritise the charging of the EVs. The CESS could therefore refresh the capacity of the stationary battery more frequently and achieve a better overall energy-saving. Finally, this work compares the energetic and economic performance of the SESS and CESS addition to the network, and concludes that the CESS is more advantageous than the SESS alone. A network-wide CESS installation was therefore examined to assess its economic feasibility, and it was found economically viable if the electricity delivered to the EVs was charged at a reasonable price.

Acknowledgment

I would like to give my deepest and sincerest gratitude to my supervisor Professor David Stone and my co-supervisor Dr Erica Ballantyne. Right from the beginning of this doctoral program, they have been giving me first-class supervision, prompt and endless support, and most importantly, a great deal of patience. There have been many ups and downs in the past four years, and my supervisors always put trust in me and guide me to the next level. I am greatly appreciative of everything they have done for me.

I would like to acknowledge the Grantham Centre and the Mong's Family Scholarship. Their funding support allows me to entirely focus on my research with no stress on the financial issue. Also, I am appreciative of the training, seminar, and conference organized by the Grantham Centre as these activities are educative, informative, and entertaining enough to help me learn more stuff out of my research area and relax. I am also always grateful to be a member of the Grantham scholars family.

I am incredibly thankful for all the support given by my parents and my families. Many many thanks for their love and patience. Also, I would like to thank my husband, Dr Ziye Dai, for his love and his full support of my study.

Last but not least, I would like to express my gratitude to all the staffs and fellow students at the University of Sheffield. Thank you so much for the advice, help, and the fun time spent together.

List of Publications

Part of the content presented in this thesis has been published, the publications are as follows:

Journal Publications

[1] T. Zhang, R. Zhao, E. E. F. Ballantyne, and D. A. Stone, "Increasing urban tram system efficiency, with battery storage and electric vehicle charging," Transportation Research Part D: Transport and Environment, vol. 80, 2020.

[2] T. Zhang, E. E. F. Ballantyne, R. Zhao, and D. A. Stone, "Technical and economic feasibility of increasing tram system efficiency with EV batteries," Transportation Research Part D: Transport and Environment, vol. 91, 2021.

Conference Proceedings

[3] T. Zhang, E. Ballantyne, and D. Stone: "Fully integrated EV energy storage using transport infrastructure," in 2019 International Conference on Clean Electrical Power (ICCEP), 2019, pp. 337-344: IEEE.

[4] T. Zhang, E. Ballantyne, and D. Stone: “Fully integrated EV energy storage using transport infrastructure”. All Energy Conference, Glasgow, May 2019

[5] T. Zhang, E. Ballantyne, and D. Stone: “Lineside storage optimisation for DC light-rail / Tram networks”. Paper S2-0011-A, International conference on Smart Grids and Energy (ICSGE). April 2019, Singapore.

Manuscript under Preparation

[6] T. Zhang, E. E. F. Ballantyne, and D. A. Stone, "Applying electric vehicles as mobile energy storage systems to promote the energy efficiency of an urban tram system," Applied Energy, 2022.

Table of Contents

Table of Contents i

List of Figures v

List of Tables viii

Glossary of Abbreviations and Acronyms x

Chapter 1. Introduction 1

1.1 Background of the electrified transportation network 1

1.1.1 Drivers and key players of the electrification of the transportation network 1

1.1.2 The electrification of rail transport 3

1.1.3 The electrification of road transport 4

1.2 The integration of the electrified rail and road 6

1.2.1 The energy efficiency of the electrified rail system 6

1.2.2 Potential benefits of electrified roads 8

1.3 Aims and objectives 11

1.4 Thesis structure 12

Chapter 2. Literature Review 14

2.1 Energy balance of electrified Transit Systems 14

2.1.1 Applications to analyze energy balance of electrified transit systems 15

2.1.2 Overview of modelling and simulation methods to obtain energy balance 17

2.2 Braking energy recovery of the rail system 20

2.2.1 Overview of braking energy recovery methods 20

2.2.2 Application of wayside ESS 24

2.3 The exploitation of EV batteries for energy storage 27

2.3.1 The Vehicle-to-Grid approach 27

2.3.2 Existing research on electrical energy exchange between rail and road transport 29

2.4 Chapter summary 32

Chapter 3. Modelling of energy trend of the tram network 34
3.1 Tram operation system 35
3.1.1 The Supertram layout 35
3.1.2 Energy supply of tram system 35
3.1.3 Braking mechanism 37
3.1.4 The system data of Supertram 38
3.2 The origin of the input data 38
3.2.1 Overview of input data 38
3.2.2 Data collection 39
3.2.3 The traction force of the tram 44
3.3 Simulation model of energy balance 47
3.3.1 Introduction of the entire model 47
3.3.2 Data calculation module 50
3.3.3 Substation module 51
3.3.4 Line resistance module 53
3.3.5 Tramcar module 53
3.4 Energy balance on tram system 55
3.4.1 Result verification 55
3.4.2 Energy balance of separate system 56
3.4.3 Energy balance of common system 57
3.4.4 Comparison between the separate system and common system 58
3.4.5 Comparison between Sheffield Supertram with other light rails 59
3.5 Chapter summary 60
Chapter 4. Application of energy storage for a tram system 62
4.1 Energy storage system structure and simulation 63
4.1.1 Design principles of energy storage systems 63
4.1.2 Overview of Energy Storage System Model 66

4.1.3 The charging and discharging threshold 67
4.2 Application of energy storage in the separate overhead catenary system 70
4.2.1 Model of the power supply section with ESS installed 70
4.2.2 Factors affecting the ESS performance 71
4.2.3 Applying the ESS onto the whole network 74
4.3 Application of energy storage system in the common overhead catenary system 75
4.3.1 Introduction to ESS installation 76
4.3.2 Single ESS installation 78
4.3.3 Multiple ESS installations 81
4.4 Economic feasibility of applying ESS on tram system 84
4.4.1 Method of economic evaluation 85
4.4.2 Cost and income 88
4.4.3 Economic feasibility 89
4.4.4 Sensitivity study 90
4.4.5 The potential merit of using EVs for energy storage to the tram network 99
4.5 Chapter summary 103
Chapter 5. Impact of the implementation of EV Energy Storage System 105
5.1 Hourly energy balance of tram system 106
5.1.1 Analysis of operational data 106
5.1.2 Simulation method 107
5.1.3 Hourly energy balance 108
5.2 Electric vehicle energy storage system 111
5.2.1 Design of model 111
5.2.2 The influence of variables of electric vehicles parking status 112
5.2.3 The influence of the number of connection devices 117
5.3 Combined energy storage system 118
5.3.1 Introduction of the design concept 118

5.3.2 The smart control 119
5.3.3 Scenario simulation 120
5.4 Comparison of the three systems 121
5.4.1 Energy saving features of the three systems 121
5.4.2 The effect of the three systems in application 123
5.5 Applying the energy storage system on the whole tram network 127
5.5.1 The energy-saving and energy recovery delivered by ESSs 127
5.5.2 The economic feasibility of the addition of ESSs 130
5.5.3 Sensitivity study of the economic evaluation of the CESSs' addition 135
5.6 Chapter summary 139
Chapter 6. Conclusions and future work 141
6.1 Conclusion 141
6.2 Future work 146
References 148
Appendix A Tram travelling profile 158

List of Figures

Figure 1-1 The yearly GHG emissions from all sectors and the transport sector [2, 3] 2
Figure 1-2 Growth of plug-in cars and LGVs [34] 4
Figure 1-3 The predicted profile of vehicles (EVs and non-EVs) of the fastest and slowest decarbonization studied in the Future Energy Scenario [38] 5
Figure 1-4 A schematic of the braking mechanism: (a) regenerative braking and (b) resistive braking 7
Figure 1-5 UK trips by car as driver per person per year 10
Figure 2-1 The schematic of utilization of braking energy via inverter feedback storage 21
Figure 2-2 The schematic of the utilization of braking energy via energy storage: (a) on-board storage, (b) wayside storage 23
Figure 3-1 The route map of the Sheffield Supertram [125] 35
Figure 3-2 Schematic of supply system (a) common OCS and (b) seperate OCS 36
Figure 3-3 Schematic of the modelling and simulation process 39
Figure 3-4 The Speed data and acceleration data collected via iPhone apps “Speedmeter” ...39
Figure 3-5 Garmin GARMIN eTrex® 10 40
Figure 3-6 The speed data and acceleration data collected via GARMIN eTrex® 10 41
Figure 3-7 Tram journeys taken in the sampling campaign 41
Figure 3-8 The change of height above mean sea level and distance over time during the journey from ‘Halfway’ to ‘Malin Bridge’ (Dots highlight tram stop locations) 42
Figure 3-9 The speed and distance profile of the tram journey 43
Figure 3-10 The bend located between Park Grange and Arbourthorne Road (Screen captured from Google Maps) 46
Figure 3-11 The traction force of the tram of journey from Halfway to Gleadless Townend .47
Figure 3-12 The model of a separate OCS that carries two lines 49
Figure 3-13 The model of a common OCS that carries two lines 50
Figure 3-14 The external characteristics (a) and the simplified schematic model (b) of the substation 52
Figure 3-15 The model of the separate OCS substation (a) and common OCS substation (b)52
Figure 3-16 The line resistance model 53
Figure 3-17 The tramcar model 54
Figure 3-18 The power profile of the Gleadless Townend substation 55
Figure 3-19 Energy balance of the separate OCS 56

Figure 3-20 Energy balance of common system.....57
Figure 4-1 The circuit of the DC-DC converter in the ESS.....64
Figure 4-2 The schematic of ESS's double-closed loop control.....65
Figure 4-3 The model of the ESS in Simulink.....66
Figure 4-4 The model of the control module inside the ESS.....67
Figure 4-5 The profile of traction current of tram journey from Halfway to Gleadless Townend 68
Figure 4-6 The battery current simulated based on different CTVs and DTVs.....69
Figure 4-7 Simulink model illustrating a section of the tram network model Model of ESS installation on an energy supply section with separate OCS setup.....70
Figure 4-8 Energy use for a single journey from Halfway to Crystal Peaks with 6 scenarios for the ESS placement 71
Figure 4-9 Energy use for a single journey from Halfway to Crystal Peaks with 5 current limits for a 200Ah battery at the Waterthorpe tram stop.....73
Figure 4-10 Simulated battery current for a single journey from Halfway to Crystal Peaks with a 10C current limit applied to a 200Ah ESS at the Waterthorpe tram stop. 73
Figure 4-11 Simulated Daily Energy trends with a 1,000Ah ESS installed at ideal tram stop locations on the tram network.....74
Figure 4-12 Simulated Daily Energy trends with a 200Ah ESS installed at ideal tram stop locations on the tram network.....75
Figure 4-13 The substation stops and the centre stops of the energy supply sections in the Supertram network.....76
Figure 4-14 Model of ESS installation on substation stop with common OCS setup 77
Figure 4-15 Mean values (with percentage error bars) of the change of energy balance of substation ESS and centre stop ESS 80
Figure 4-16 Daily electricity saving of centre stop ESS installations with different battery capacity 84
Figure 4-17 The spider-plot of the NPV of ESS additions with different battery capacity 95
Figure 4-18 The breakdown of CAPEX and OPEXs of using Stationary ESS and EV battery for energy storage for the tram network 102
Figure 5-1 The speed profile of tram journey between Halfway and Gleadless Townend....107
Figure 5-2 The schematic of simulation method 108
Figure 5-3 The hourly energy balance of the Supertram 109
Figure 5-4 The daily energy balance obtained from different operational data.....110

Figure 5-5 The schematic of the configuration of EVESS 112
Figure 5-6 The scenarios studied for understanding the influence of variables in EV parking status to energy balance 114
Figure 5-7 The SoC of EVs battery of the EVESSs equipped with on connection device but with different EV parking status 115
Figure 5-8 The energy saving and recovery delivered by the EVESSs equipped with one connection device, but with different EV parking status 116
Figure 5-9 The energy saving and recovery delivered by the EVESSs with different number of connection devices and different EV availabilities 117
Figure 5-10 The schematic of the configuration and control of the CESS 119
Figure 5-11 The SoC of the batteries in the CESS with a 100Ah stationary battery 120
Figure 5-12 The profile of energy lost in dump resistor with different ESS scenarios 122
Figure 5-13 The SoC of the EV's and the battery in the CESS with a 500Ah stationary battery 126

List of Tables

Table 1-1 The battery capacity and range of the popular EVs 9
Table 2-1 The generic system specification and the energy balance ratios in the published studies 16
Table 3-1 Supertram system data 38
Table 4-1 Energy usage for a single journey from Halfway to Crystal Peaks with 6 scenarios for ESS placement 71
Table 4-2 Energy usage for a single journey from Halfway to Crystal Peaks with maximum current ratings from 0.5C to 10C, for a 200Ah battery at the Waterthorpe tram stop. 72
Table 4-3 The change of daily energy balance caused by using ESS with different battery capacities 79
Table 4-4 Options for four ESSs installations 83
Table 4-5 Options for five ESSs installation 83
Table 4-6 The costs per ESS 88
Table 4-7 The economics of different numbers of ESS installation with different ESS battery capacity 89
Table 4-8 The undiscounted annual income and annual cash flow related to the ESSs installed on Shalesmoor 91
Table 4-9 The economic evaluation based on different electricity price 91
Table 4-10 The economic evaluation based on different battery price 92
Table 4-11 The economic evaluation based on different battery life 92
Table 4-12 The economic evaluation based on different installation cost 93
Table 4-13 The economic evaluation based on different OPEX to CAPEX ratio 93
Table 4-14 The economic evaluation based on different discount rate 94
Table 4-15 The ranking of the $\pm\%NPV$ on each ESS addition with different numbers of installation 96
Table 4-16 The economics of the multiple ESS additions obtained at a 20% lower battery price 97
Table 4-17 The economics of the multiple ESS additions obtained at a 20% higher electricity price 98
Table 4-18 The economics of the multiple ESS additions obtained at a 20% longer 98
Table 4-19 The costs per ESS without a stationary battery 99

Table 4-20 The economic evaluation based on ESS battery gets replaced by the EV battery 101
Table 5-1 The daily energy saving by different EVESS, SESSs and CESSs 124
Table 5-2 the energy saving and recovery delivered by the SESS and CESS 129
Table 5-3 The economics of each individual SESS and CESS installations 132
Table 5-4 Economic of CESSs excluded the selling of electricity to EV users 134
Table 5-5 The economic evaluation based on different cost relating variables 136
Table 5-6 The economic evaluation based on income relating variables 138
Table 5-7 The economic evaluation based on income relating variables 138

Glossary of Abbreviations and Acronyms

AC/ac	Alternating current
ACF	Annual cash flow
BC	Battery capacity
BEV	Battery electric vehicle
CAPEX	Capital expenditure
CESS	Combined energy storage systems
CTV	Charging threshold voltage
DC/dc	Direct current
DoD	Depth of discharge
DPP	Discounted payback period
DTV	Discharging threshold voltage
ESS	Energy storage system
EV	Electric vehicle
EVESS	Electric vehicle energy storage systems
FD	Fastest decarbonization
GHG	Greenhouse Gas
HGV	Heavy Goods Vehicle
IGBT	Insulated-gate bipolar transistor
IRR	Internal return rate
LatA	Latitude Point A
LatB	Latitude Point B
LGV	Light Goods Vehicle
LonA	Longitude of Point A
LonB	Longitude of Point B
LV	Low voltage
$MtCO_2$	Million tonnes CO_2
NPV	Net present value
OCS	Overhead catenary system
OPEX	Operational expenditure
OPOD	Off-peak period operational data
PHEV	Plug-in hybrid electric vehicle
PPOD	Peak period operational data
PV	Photovoltaic

PWM	Pulse width modulation
RoI	Return on Investment
SD	Slowest decarbonization
SESS	Stationary energy storage systems
SoC	State of charge
TOM	Train Operations Model
ULEV	Ultra-low emission vehicle
V2B	Vehicle to building
V2G	Vehicle to grid
V2H	Vehicle to home
V2L	Vehicle to load
V2X	Vehicle to everything

Chapter 1. Introduction

This thesis focuses on the electrical engineering infrastructure behind electrified rail and road transport, to improve the energy efficiency of the electrified transportation. This chapter aims to introduce the general context and the potential opportunities in this related research area, the driver, aims and objectives of this research, and the thesis structure. Hence,

- Section 1.1 - introduces the drivers and current status of the electrification of the transportation sector.
- Section 1.2 - introduces the issues within electrified light rail and the potential benefits of electrified road transport, and the potential linking of the two to achieve additional energy efficiency benefits.
- Section 1.3 - proposes the aims and objectives of this research.
- Section 1.4 - presents an overview of the thesis structure.

1.1 Background of the electrified transportation network

1.1.1 Drivers and key players of the electrification of the transportation network

The UK government set its target to cut Greenhouse Gas (GHG) emissions to 80% below the 1990 level by 2050 [1]. The UK has already reduced its overall GHG emissions from the 1990 level of 794 million tonnes CO_2 equivalent ($MtCO_2$), to 414 $MtCO_2$ in 2020 [2, 3]. However, from 1990 to 2019, the emissions from the transport sector remained approximately 120-140 $MtCO_2$, and hence the proportional emissions of the transport sector has increased from 15.8% in 1990 to 26.6% in 2019 (as shown in Figure 1-1). Therefore, reducing the GHG emissions from the transportation sector is crucial for tackling the GHG emission reduction goal [4].

Considering that between 75-85% of GHG emissions are attributed to CO_2, decarbonization becomes a key measure for emissions [2, 3]. Decarbonization of the electricity grid in the UK is conducted via the adoption of renewables, such as hydro, solar, wind and bioenergy, etc. The share of renewables in the total electricity generation has increased from 3.6% in 2004 to 37.1% in 2019, while the share of fossil fuels has decreased from 75.5% to 43.3% during this period [5]. Due to this countrywide electricity generation mix, electrified transportation is not technically zero emission. However, in the example of electric vehicles (EVs), they still have a lower CO_2 footprint than a vehicle with a combustion engine powered by fossil fuel, primarily due to the electricity used containing some renewable elements [5, 6]. Hence, electrification of

vehicular transport is one of the important approaches to reduce GHG emissions from the transport sector [6].

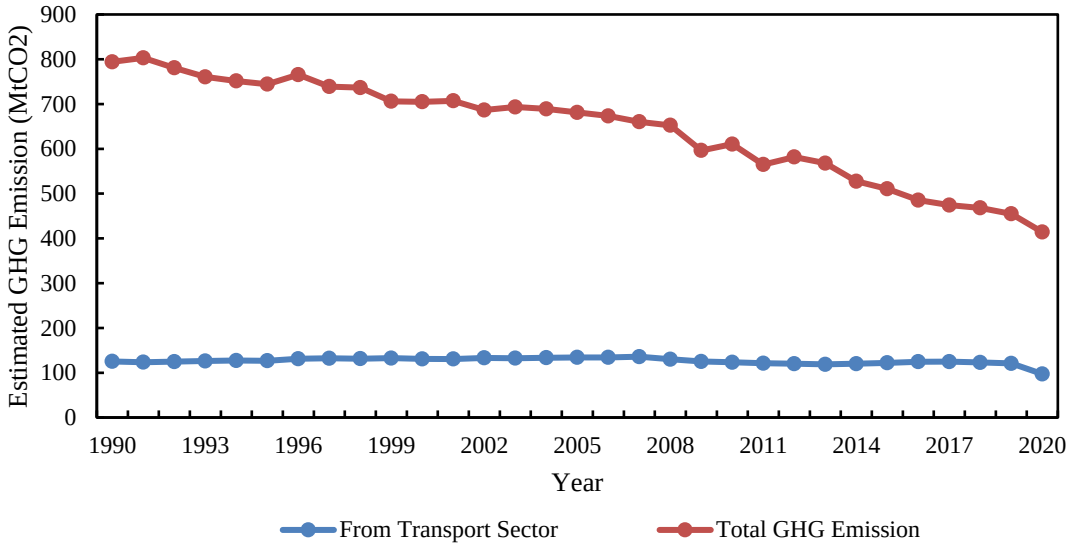

Figure 1-1 The yearly GHG emissions from all sectors and the transport sector [2, 3]

There are four modes of transport, road, waterborne, airbourne, and rail [4]. Based on the passenger travelling distance, from 1952 to 2019, road transport contributed 82.0 - 94.0% of the distance travelled, rail contributed 5.1-17.4% and air and other transport modes contributed less than 0.1-1.5% [7]. For domestic freight transport in the UK, from 1952 to 2019, 71.9 - 89.6% of goods (by weight) were handled via road and 3.9 - 23.8% were handled by rail transport, with only 3.8 - 15.4% being handled via waterborne and other modes [8]. Road and rail together are therefore responsible for the majority of both passenger and freight transport. Coincidentally, examination of the extent to which electrification can be applied in different transport modes shows that electrification of rail and road transport is technologically possible and close to meeting the needs of potential customers, particularly the rail transport has been widely electrified [4]. For rail transport, by 2017, 60% of the rail network in Europe has been electrified, and is responsible for 80% of the total traffic [4]. From 2010 to 2019, in the 27 EU countries, Norway and United Kingdom, the number of registered battery electric cars and plug-in electric cars has increased from 734 to 534,583, and the proportion of electric cars in the total vehicle population increased from 0.01% to 3.46% [9]. Due to the forthcoming UK ban on the sale of new petrol and diesel vehicles in 2030, the number of EVs is expected to grow, and therefore, the electrification of road transport is expected to expand [10-12].

However, the electrification of waterborne and airbourne transportation has only been applied to short range operations, due to the lack of mature energy storage capacity to facilitate longer journeys, and this situation is not expected to change in the next decade [4]. Moreover, from the point of view of distance with regards to goods transport, waterborne and airbourne modes of transport only form a much smaller contribution to the total when compared to the road and rail [7, 8]. Hence, waterborne and airbourne transportation are not considered as key players or targets for GHG emission reduction in the near future. Therefore, the following sections 1.1.2 and 1.1.3 will only review the current and future electrification of rail and road transport modes in the UK, where this research is targetted.

1.1.2 The electrification of rail transport

The UK rail infrastructure mainly comprises of three key bodies, the mainline network that is responsible for the national train travel, the underground railway that provides urban rail travel that operates both above and underground, and the light rail and tramways that offers the urban rail travel at ground level, on elevated structures, in tunnels and on streets [13-15].

Within electrified rail transport, electricity is typically supplied at nominal voltage levels of $750V_{dc}$, 1.5 kV_{dc}, 3 kV_{dc}, 15 kV_{ac}, and 25 kV_{ac} [16]. Generally, an urban rail system, for example the Sheffield Supertram light rail, is supplied at 750 V_{dc} [17]. Conversely, the East Coast Main Train Line, which is a mainline system, is supplied at 25 kV_{ac} [18].

During the period from 1985 to 2020, the mainline rail track in the UK that was open for traffic ranged between 15,500 km and 17,000 km, of which, electrification has increased from 3,809 to 6,049 km [19]. Moreover, the percentage of electrified rail tracks (by length) has increased from 23% in 1984-1985, to 38% in 2019-2020 [19]. For purely rail transport, the yearly electricity consumption grew by 35% from 3,139 GWh in 2005-2006 to 4,257 GWh in 2019-2020 [20]. During this period, the electricity consumption of rail freight transport reduced from 118 GWh to 70 GWh, but increased for the passenger rail transport from 3,021 GWh to 4,186 GWh [20]. From 2017 to 2020, the yearly increases in total train transport and passenger transport have been greater than 3% [20]. By 2020/2021, the two underground railway systems and the ten light rail and tramways systems in the UK together provided 792 km routes for passenger travel. All these routes are electrified [21-31]. In conclusion, a considerable length of rail has been electrified to date and has resulted in an increase in electricity consumption.

1.1.3 The electrification of road transport

Road transport consists of cars, motorcycles, tricycles, quadricycles, Light Goods Vehicles (LGVs), Heavy Goods Vehicles (HGVs), buses and coaches [4]. The level of electrification amongst different vehicles types varies. Long-range trucks and coaches are still not able to be solely powered by electricity due to their high energy demand for moving heavy cargos continuously for long periods of time, to cover the long distances travelled. This is primarily due to the limited energy density of the available battery packs [4]. However, current battery technology enables electrified buses and trucks to operate in urban areas where typically shorter journeys facilitate frequent recharging of the battery [4]. Through the available technology, and incentives offered by the UK government, the number of plug-in vehicles such as cars and LGVs in the UK has grown rapidly in recent years, from 6,227 at the end of 2011, to 413,642 by the end of 2020 with a yearly growth rate (comparing to the previous year) of 130-200% [32]. The proportion of plug-in cars and LGV in the total licensed vehicle population has grown from 0.02% to 1.07% [32, 33]. The rapid growth of the plug-in vehicles is mainly driven by plug-in cars, especially battery electric cars and plug-in hybrid electric cars, as shown in Figure 1-2 [34].

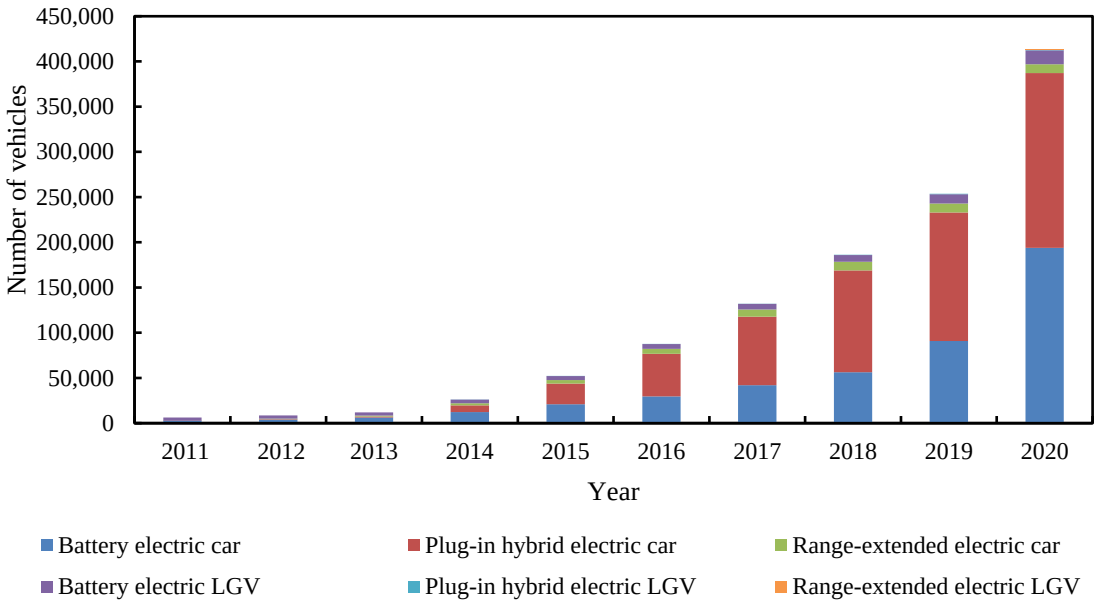

Figure 1-2 Growth of plug-in cars and LGVs [34]

The rapid growth of EVs could be attributed to the available UK government support, as incentives of up to £8,000 per vehicle have been provided to assist with the purchase of 7 categories of cars and vehicles that have emissions lower than 75 g/km since 2011 [35]. Moreover, the UK government considers decarbonization of road transport as one of the

measures for carbon reduction and mitigation of air pollution [36]. In this sense, the UK government aims to make almost every car and van in the UK an ultra-low emission vehicle (ULEV), expected to be plug-in vehicles or hydrogen fuel cell electric vehicles by 2050 [36]. Furthermore, the UK government announced a ban on the sale of new petrol and diesel cars by 2030 [10]. Likely the sale of the new hybrid cars, which include internal combustion engines and emit GHG during their operation due to fossil fuel usage, could also be banned by 2035 or earlier [12, 37]. Hence, the overall electrification of road transport, especially the number of battery electric cars, is expected to continue to grow.

The Future Energy Scenario 2021 published by the National Grid ESO predicts the growth of electric vehicles in a number of different scenarios [37]. These scenarios are assumed to meet the net-zero emission targets by 2050, but have various consumer engagement on energy saving and carbon reduction, the availability of investment and decarbonization technologies, the change on supply side of the energy system, and the reliance on the fossil fuels, etc [37]. Hence, the rate of decarbonization and the predicted growth of EVs according to the different scenarios varies.

The Future Energy Scenario 2021 predicts the total number of vehicles to remain between 28 to 41 million from 2020 to 2050 [38]. The predicted profile of vehicles (EVs and total vehicles) of the fastest decarbonization (FD) and slowest decarbonization (SD) are shown in Figure 1-3.

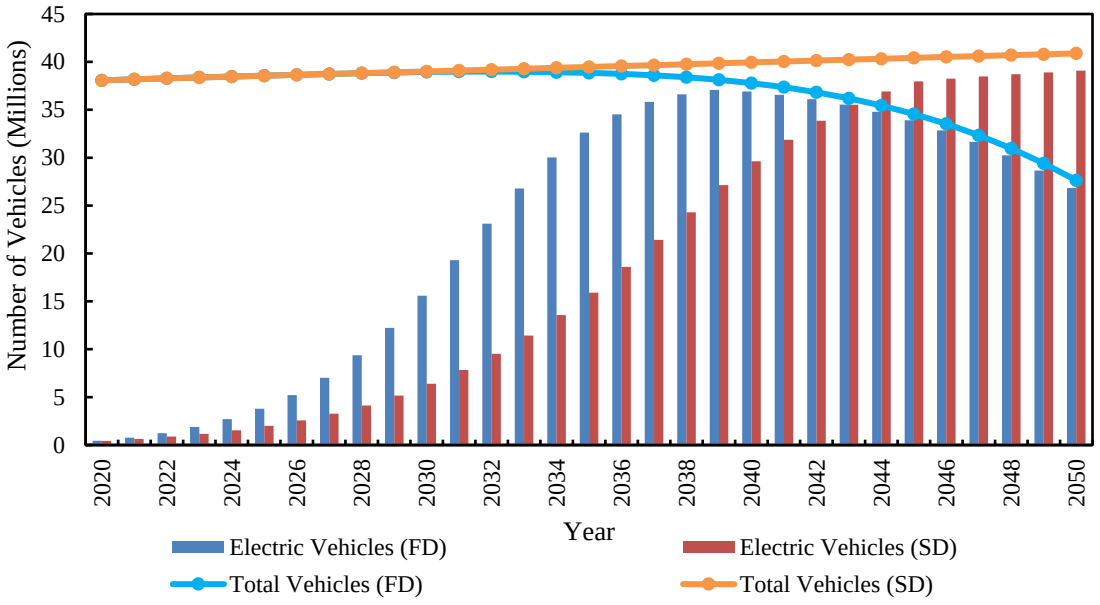

Figure 1-3 The predicted profile of vehicles (EVs and non-EVs) of the fastest and slowest decarbonization studied in the Future Energy Scenario [38]

As can be seen in Figure 1-3, the fastest decarbonization scenario has a steeper growth of EVs from 2020 to 2040 than the slowest decarbonization does. The fastest decarbonization scenario assumes consumers are highly engaged in reducing energy consumption, and prefer public transport. Therefore it has fewer vehicles and EVs on road than the slowest decarbonization scenario. Combining with other scenarios studied, by 2050, 91-98% of the total vehicles are predicted to be electric, and 74-81% of the total vehicles are predicted to be battery-electric cars [38]. The electrification of the road transport in the UK is predicted to have a different growth pattern but eventually reach a high penetration level.

1.2 The integration of the electrified rail and road

The electrification of rail and road is expected to help tackle GHG emissions. At the same time, it also substantially increases electricity demand, and therefore, it is important to improve the system's overall energy efficiency. Since EVs are commonly equipped with a battery to power the electric motor, the growing number of EVs will lead to a growing number of mobile batteries, and thereby a growing energy storage capacity. This energy storage capacity could provide a suitable add-on to the rail infrastructure that suffers energy wastage due to an ineffective recovery of the regenerated braking energy. In detail, when the braking energy generated by the rail system can not be re-used within the system, it can be transmitted to and be stored in the EV battery. The stored energy could then be returned to the rail system or taken away by the EVs. Thus, the integration of rail and road could encourage the bi-directional energy exchange between the two parties and could be the solution for improving the energy efficiency of the rail and road simultaneously.

1.2.1 The energy efficiency of the electrified rail system

Since rail transport consumes a substantial amount of electricity, improving the energy efficiency, such as utilizing lighter material or applying regenerative braking, are considered key measures to deliver those goals [4]. Generally, in rail-based applications, while motoring, the electric motor in the train obtains electrical energy from the supply network and converts this into kinetic energy that drives the train/tram. While braking, there is a potential for the electric motor to act as a generator, that not only slows down the train / tramcar but also converts the kinetic energy of motion into electrical energy [39], which is in-turn fed back onto the rail network. This electrical energy produced during the braking event is therefore referred to as the ‘braking energy’.

In all the electrified mainline rail, light rail and tram, and metro systems, this braking energy could then be used by another tram/train that is accelerating in the same electrical section as the braking event, as shown in Figure 1-4 (a). However, in current practice, the energy supply from the substations is unidirectional, only flowing from the substations to the tram/train, hence the substation operates unidirectionally and thereby only supplies energy to the tram/train but cannot receive energy generated from the tram/train. Therefore, if there is no other train accelerating in the same electrical section as the train which is decelerating, the braking energy will cause the catenary voltage to rise, because it has nowhere to go other than the DC link capacitors of the train/tram drive (connected to the catenary via the pickup). If the voltage rise is too high, it will damage the drive system by over-voltaging the capacitors and semiconductors. In addition, it may damage the catenary and substation rectifiers, causing serious problems. Therefore, in order to dissipate the braking energy, a 'crowbar' protection resistor is introduced into the system (usually mounted on the tram roof), which is turned on when the voltage at the tram exceeds a predetermined voltage threshold. The unused braking energy will then have a path to flow via the resistor where it will be dissipated as heat [39], as shown Figure 1-4 (b).

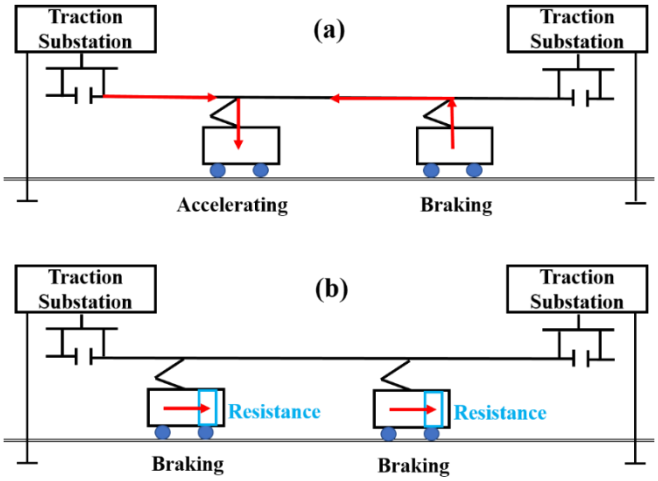

Figure 1-4 A schematic of the braking mechanism: (a) regenerative braking and (b) resistive braking

This braking energy dissipation (often as heat in resistor banks on the roof of the train / tram) is extremely wasteful. In the case of an urban tram system, the distance between tram stops is relatively short leading to a large number of braking events. This is exacerbated by the tram tracks being inlaid into the road surface in places, leading to the tram sharing its route with the normal vehicles, and is therefore subject to normal traffic congestion, which results in frequent braking and accelerating during a journey. Therefore, recovering this wasted braking energy

could improve the overall energy efficiency of the system, and also stabilize the voltage seen on the catenary, preventing possible over-voltage events.

In addition to the issue of wasting valuable braking energy, the electrification of the rail network also has an influence on the utility power grid. Passenger travels account for more than 98.3% of electricity consumption in the mainline rail network [20], and the passenger travels by light rail, tram and metro are all powered by electricity [21-31]. These services are commonly operated from early morning till around midnight. Therefore, part of the rail's operation period overlaps with the peak energy demand period (from approximately 07:00 to 20:00) of the grid [40]. As the electrified rail network is powered by the electricity grid, the growing electrification of the rail network may stress the national grid to some extent during the peak operating periods.

The effective recovery of braking energy can help to address the above two issues, and adding energy storage system (ESS) to the rail network is one of the commonly applied measures [41, 42]. After an ESS is introduced onto the rail / tram system, the regenerated, but unused, energy will be stored in the ESS. When the tram is moving off or accelerating, the ESS will return the stored electricity to the tram [41, 42]. Although an ESS is able to deliver an energy saving to the system and thereby bring in cost savings, it also adds in extra capital and operational costs. In some cases, the high capital cost of the ESS could compromise the economic benefit brought by the energy-saving and lower financial return [41, 43]. Therefore, in order to promote the implementation of ESS for better braking energy recovery and reuse for the rail, it is crucial to discover the way to lower the cost of ESS.

1.2.2 Potential benefits of electrified roads

Rechargeable batteries are one of the key components of EVs. They provide energy storage to the EV, storing the electricity taken from the grid when recharged and feeding the electricity to the electric motor as the vehicle travels. As the number of EVs grows, the number of the batteries installed in the EVs will also grow, thus increasing the overall energy storage capacity available from EVs. Further, as battery technology continues to evolve, improvements will lead to a higher stored energy density from batteries. If the available storage capacity is large enough to exceed the normal expected daily usage, then spare capacity might be available for other purposes. For example grid support, that could potentially provide another income stream for

the vehicle owner. Therefore, the capacity of the vehicle battery, and the routine consumption due to commuting or vehicle use are the two key factors that determine how much spare energy storage capacity in the EV battery could be made available for other uses when the vehicle is parked.

Based on the make / model and type of the Plug-in EVs available, the capacity of vehicle batteries varies widely. If the vehicle is only equipped with an electric drive, for instance the Nissan Leaf and the Tesla model 3, these are defined as battery EVs (BEVs). In order to keep the autonomy within a reasonable range, around 200 miles for both Tesla Model 3 and for the Nissan Leaf, the battery packs on both types of cars are tens of kWhs. If a vehicle has an electric motor, which is powered by an on-board battery plugged in to the grid for recharge, and an internal combustion engine also for the drive, for instance the BMW 330e saloon or the Mercedes-Benz A250e, these are defined as Plug-In Hybrid EVs (PHEVs). The electric motor of a PHEV is more likely to drive the vehicle at a low speed or for a limited range, and hence, its battery pack is smaller than the ones seen in the BEVs. The battery capacity (BC) and range of a number of popular EVs (from top 20 new registrations by model in the UK on 2019) are shown in Table 1-1 [44].

Table 1-1 The battery capacity and range of the popular EVs

Car Model	EV Type	BC (kWh)	Range (mile)	Reference
BMW I3	BEV	42.2	182-190	[45]
Kia Niro	BEV	39-64	180-282	[46]
Nissan Leaf	BEV	40-62	168-239	[47]
Renault ZOE	BEV	52	245	[48]
Tesla Model 3	BEV	50-76	278-360	[49-51]
Jaguar I-Pace	BEV	90	258-292	[52]
BMW 330e	PHEV	12	37	[53]
Mercedes-Benz A 250e	PHEV	15.6	44	[54]

According to the Department for Transport, from 2010 to 2019, in England, the average annual trip distance by car as a driver was 3,198-3,388 miles per person, hence the daily average traveling distance by car as a driver is calculated as 8.8-9.3 miles per person [55]. Figure 1-5 shows the breakdown of car trips made per person (as driver) per year from 2010 to 2019 [56]. As can been seen, the number of trips by car/van, as a driver, was 380-402 per person per year

[56]. Trips between 2-5 miles had the biggest share of miles covered at 32.6-34.7%. More than 77% of the trips are under 10 miles, and more than 93% of the trips were under 25 miles [56]. Therefore, the majority of the car trips were over short distances.

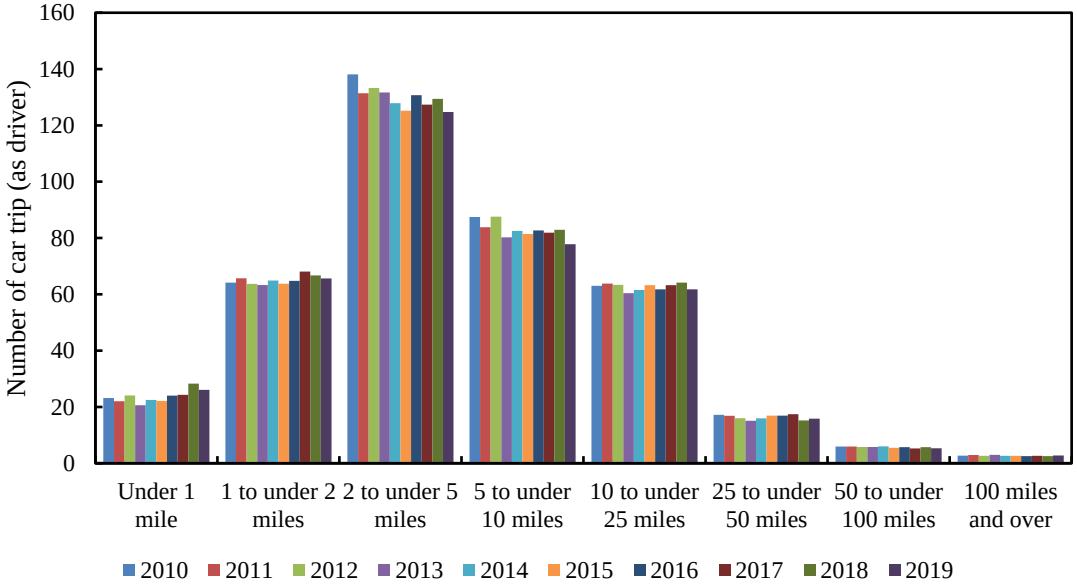

Figure 1-5 UK trips by car as driver per person per year

Cross referencing Table 1-1, if the EV is fully charged every night, both the BEV and the PHEV are able to cover the average daily travel distance of approx. 9 miles without a second charge. For the BEV which has range more than 150 miles, the majority of the battery capacity remains unused with normal daily travel. Thus, there could be some unused capacity in the EV battery which could be offered for other services. Although this energy storage capacity only becomes accessible if the EVs are stationary, studies suggest that approximately 90% of vehicles are parked at any given time within a 24 hour period [57]. Therefore, EVs can potentially be utilized and integrated into energy storage systems. As predicted in the Future Energy Scenario 2021 published by the National Grid, the number of EVs on the road in the UK could reach 27-39 million by 2050 [38]. Assuming each EV is equipped with a 50 kWh battery, the total battery capacity available in the EV population would be equivalent to 1,350-1,950 GWh. Meanwhile, the Future Energy Scenario 2021 also predicted the annual end consumer demand in 2050 would be 388-494 TWh, which is equivalent to a daily end consumer demand of 1,063-1,353 GWh. If all the EV batteries would be used a energy storage and would be fully charged, the electricity stored can provide a supply that meets 1.0-1.8 days of the end consumer demand [38].

As an EV holds great potential for energy storage, the vehicle-to-grid (V2G) concept was first proposed in early 2010, and aimed to provide the power from EVs to specific electricity markets [58, 59]. In recent years, the concept has been developed into V2X, which uses EVs to provide energy storage to any electric devices, facilities and markets [60-62]. In essence, V2X uses EV batteries as an energy storage device to store the electricity that is produced when the grid has low stress and/or has over generation capacity, for reuse later in daily routine applications, especially when the grid is at peak demand, and the EV is not in use. Tarroja, et al. [63] discusses the advantages of using EVs as energy storage over the conventional stationary ESS. The study consideres complementary energy storage for meeting the GHG reduction or renewable energy that might be required in the future, and the exploitation of EVs as energy storage could delay, avoid, or reduce the cost of the purchase of those complementary stationary ESS. Such a concept inspires this research to explore the possibility of connecting the EV to a light rail (tram) network and allowing the EVs to serve as energy storage systems for the rail network in order to recover braking energy and improve overall energy efficiency.

1.3 Aims and objectives

The rail and road sectors are the two key players in the development of electrified transportation networks. However, there are issues with the electrified rail network, particularly the braking energy, which is sometimes dissipated as heat rather than recovered. This is because the produced electrical energy could not be consumed at the point of regeneration. This offers an opportunity for energy storage, and thus utilizing the increasing availability for energy storage capacity offered by the growing number of EVs that could potentially be offered for storing the braking energy from the electrified rail network. EVs can store the braking energy when the train/tram is decelerating and then provide that energy back when the train/tram is accelerating. Furthermore, the EVs could also provide electrical energy to the rail network when the grid is at peak demand, enabling peak lopping of the load presented to the grid. EVs are the key component that connects the rail and road, and deliver the bidirectional energy exchange between the rail and road. Potentially, the energy exchange between rail and road not only improves the energy efficiency of the rail network but also reduces the peak stress on the grid. A further advantage of this, in the case of tram / light rail systems, is that the rail power supply is direct current (dc), therefore dc-dc conversion between the rail and the vehicle battery is more efficient than dc–ac conversion for vehicle-to-grid or standard charging of the EV battery [64]. Among different rail systems, the light rails and trams, operated in an urban area and

commonly at ground level, have the best chance to allow convenient connection with the EVs and hold a greater possibility of enabling the successful connection and subsequent energy exchange between rail and road.

Therefore, this research aims to demonstrate the bidirectional energy exchange between light rail and road using the Sheffield Supertram as the research subject. The objectives of the project are therefore:

- Objective 1 - To investigate the energy balance of the tram network, especially the energy demand for traction and the distribution of the braking energy, via an adequate methodology.
- Objective 2 - To add ESS into the system and examine its impact on energy balance and to determine the optimal configuration of stationary ESS with regards size and location and consideration of economic feasibility.
- Objective 3 - To explore the technical feasibility and the optimal solution for including EVs into the rail network via a full or partial replacement of the stationary ESS, and to assess its merit on the energy balance and the economic feasibility.

1.4 Thesis structure

The remaining five chapters of this thesis are organized as follows:

- Chapter 2 - A literature review focusing on the investigation of the energy balance in light rail systems, the study of the technical and economic performance of adding ESS into a light rail system, and the applications of EVs as energy storage.
- Chapter 3 - An introduction of the energy operation / operating energy balance of a typical tram network, an explanation of the simulation method used, an introduction of the tram network model built, and results and discussion of the energy balance accross the tram network.
- Chapter 4 - An introduction to the stationary ESS model, a comparison of the energetic performances of the ESSs installed on the systems with different energy supply set-ups, investigation of the optimal addition of ESS onto the network based on energy-saving delivered, and the economic feasibility study of the whole or partial network-wide ESS installation.
- Chapter 5 - The study of the tram system's hourly energy balance, the introduction of modelling and features of the EV only ESS, and combined ESS that includes the EV and a stationary battery, a comparison of different ESS systems based on energy-saving

performance, and the study of the energetic and financial impact of the network-wide combined ESS installation.

- Chapter 6 - Conclusions and recommendations.

Chapter 2. Literature Review

As introduced in Chapter 1, the electrification of the rail and road is a good measure to tackle the GHG emission and both are expected to expand. Electrified rail transport suffers an undesirable loss of braking energy and would benefit from good recovery measures to reuse the braking energy to improve the rail's energy efficiency. The fast-growing number of EVs and thereby the growing number of batteries (equipped in the EVs) is expected to bring in a considerable energy storage capacity, which could be potentially used as the energy storage for the rail network for braking energy recovery. Among different electrified rail systems, light rails and trams are considered to have the most convenient connection with the EVs and thereby a better chance towards the successful connection and energy exchange. Thus, this investigation aims to research the bidirectional energy exchange between electrified rail and road transport based on a light rail system. To fulfil such an aim, it is important to:

1) Investigate the energy balance of the light rail network via an adequate methodology.
2) Understand the impact of the addition of ESS on the energy balance and the optimal configuration of added stationary ESS.
3) explore feasibility and merit of exploiting EVs as the ESS for the tram network.

Prior to conducting any experimental research, it is crucial to conduct a literature review to understand the current research progress of the relevant area first, and subsequently, to propose the objectives accordingly to fill knowledge gaps. Thus, in this chapter,

- Section 2.1 - reviews the findings of the existing energy balance studies of the urban light rail network and the methods used in the relevant studies.
- Section 2.2 - introduces and reviews the measures for braking energy recovery and the impact that could be made on the energy and cost-saving.
- Section 2.3 - introduces the exploitation of EVs as energy storage in a different area and reviews its exploitation on the energy exchange between rail and road.
- Section 2.4 - identifies the knowledge gaps of the research areas and proposes the objectives.

2.1 Energy balance of electrified Transit Systems

One of the key objectives of this research is to study and compare the energy balance of the light rail network both before and after the introduction of EVs as ESS. Therefore, the primary aim of this research is to understand the energy balance of the tram system. The observation of

this energy balance could be done either via experimental measurement of the rail vehicle dynamics and system parameters, or modelling of the vehicle dynamics into electrical energy flow. As no direct access to the tram system has been possible within this study, a simulation approach, based on comparison with published results for validation, has been taken. With this in mind, it is prudent to review the approaches of other studies into electrified tram systems, and their respective outputs.

2.1.1 Applications to analyze energy balance of electrified transit systems

A number of studies have examined energy efficiency on urban light rail networks , where the current or original energy balance of the system is used as the baseline for demonstrating the efficacy of improvement measures.

- Destraz, et al. [65] studied a tram line located in Mannheim, Germany, and the simulation result predicted that for a round trip, one tramcar journey consumed 73.36 kWh energy for traction and produced 22.47 kWh of braking energy, which was equivalent to 31% of the traction energy used.
- Açıkbaş and Söylemez [66] investigated the tramway in Istanbul and showed that 81-93% of braking energy could be reused for traction and thereby contributing 32-37% of the traction energy.
- Chymera, et al. [67] modelled and simulated the Blackpool Tramway located in England. It predicted that the energy loss occurred during the operation, i.e. in mechanicals, in braking, etc., and indicated that the braking energy loss contributed to 40% of the total energy loss. The simulation results were compared with the experimentally measured results, and was considered valid.
- Kara, et al. [68] also studied the energy balance of the metro transportation in Istanbul, Turkey via modelling and simulation, and found that the braking energy could contribute approximately 44% of the total energy demand.
- Yang, et al. [69] modelled and simulated Line 2 of Shanghai Metro. The study focused on a traction section that has 15 stops, and discovered that braking energy could contribute 64% of the traction energy. The simulation result also predicted that 72% of the braking energy had been reused for traction in other trams on the network. When validated, this prediction was found to be close to the measured percentage of 69%.
- Tian, et al. [70] exploits the power flow algorithm for the energy balance investigation of the Beijing Yizhuang subway. The modelling and simulation results predicted that the

braking energy was equivilant to 68% of the traction energy. As 35-68% of the total braking energy could be reused for traction via regenerative braking, the energy consumption could be reduced by 22-42%.

- Barrero, et al. [71] used the 'quasistatic' backwards looking method, which is commonly used to simulation power flow and energy consumption in vehicle, to study the energy balance of Brussels metro line. Under the moderate condition, the braking energy produced was equivilant to 46% of the traction energy. 39% of the braking energy could be reused for traction via regenerative braking and could contribute 18% of the traction energy.

As found above, braking energy holds a substantial energy reserve for the urban rail system, but commonly has not been well recovered and reused.

From the studies reviewed, the proportion of braking energy to total traction energy (BE: TE), and the regenerative energy to total braking energy (RE: BE) could be highly variable in different systems. This research gathered the generic specification, i.e. track length, nominal voltage, number of substations and stops, of different systems reviewed above and investigated their impact on the BE: TE ratios and the RE: BE ratios. However, as can be seen in , there is no apparent relationship between the generic system specification and the energy balance ratios in Table 2-1.

Table 2-1 The generic system specification and the energy balance ratios in the published studies

Reference	**Mannheim Tram Line [65]**	**Blackpool Tramway [67]**	**Shanghai Metro Line 2 [69]**	**Beijing Yizhuang Subway [70]**	**Brussels Metro Line [71]**
Track Length (m)	8,000	18,000	60,000	227,300	8,000
Nominal voltage (V)	825	550	1500	750	N/A
No. of Substations	2	N/A	4	12	7 to 9
Mean distance between Substations (m)	4,000	N/A	15,000	18,942	1,000
No. of Stops	15	35	15	14	14
Mean distance between Stops (m)	533	514	4,000	16,236	571
Maximum Speed (km/h)	70	32	80	80	72
BE:TE[1]	31%	40%	64%	68%	46%
RE:BE[2]	18%	N/A	69%	35%-68%	39%

[1]: The ratio of braking energy to traction energy, [2]: The ratio of regenerative energy to braking energy

As shown in Table 2-1, the BE: TE ratios vary. That's because in real life, the traction state and the braking state always go hand in hand, and the former always ends up in the latter. The conversion between kinetic energy and braking energy would be impacted by the locomotive efficiency, gearbox efficiency, friction, etc. Thus, the BE: TE ratios are likely to be independent of the system specifications examined in Table 2-1 but could be related to factors of tramcar features such as motor and gearbox models, etc., which are highly varied in different systems. Intrinsically, the BE: TE ratios can not be predicted through the generic system specifications and are expected to be varied in different systems.

As shown in Table 2-1, the RE: BE ratios have high variations. Regenerative braking occurs if one tram/train is braking while another tram/train is also travelling in the same energy supply and is taking energy from the catenary for traction. The length of the energy supply sections and the timetable of the light rail operation could heavily affect the occurrence of regenerative braking [42, 72, 73]. For instance, a longer energy supply section and a timetable with a more frequent departure would allow more tram/train travelling in the same energy supply section, and therefore, more braking and acceleration would happen in the same energy supply section and the possibility for regenerative braking to happen would increase [42, 72, 73]. However, there is not enough information presented in published studies reviewed to support a meaningful investigation that comprehensively examines the synergetic impact of the length of the energy supply sections and the timetable on the RE: BE ratios. Thus, this review considered it is challenging to predict the RE: BE ratios of a system to test via the generic system specifications. Thus, the energy balance of a rail system is case-specific and can not be simply estimated from the system parameters. The investigation of it requires a dedicated study.

2.1.2 Overview of modelling and simulation methods to obtain energy balance

To identify a suitable method to investigate the energy balance of the tram system, this research firstly reviewed the methods used to examine the energy efficiency of DC electric systems.

Firstly, the most intuitive approach would be experimental measurement, via measuring the voltage and current of each energy flow of the power system. Yang, et al. [74] used a relatively straight-forward method in their study of the Shanghai Metro Line II. By installing the voltage and current sensors on the carrier, the voltage and current data of the tram and the traction grid were obtained. Hence, the energy trend of each part of the network was calculated. However,

in practice, not every network operator is able to allow this intrusive measurement, and allow real-time data collection, as all installations have to adhere to rigid safety standards, and also not adversely affect the reliability of the systems.

As experimental measurement is not always practical, modelling and simulation can be used instead. Another merit of modelling and simulation is that, it is able to predict the performance of the system under different operational configurations without changing them in real life, and hence prevent unnecessary capital cost or compromise the safety of the systems. Various simulation methods have been applied in previous studies.

Dedicated commercial software exists for the simulation of rail networks. For example, RAILSIM, developed by an American company called SYSTRA, is capable of traction and operational simulation and is commonly exploited in the North America region. RAILSIM has also been utilised for tram system simulation by Kara, et al. [68] who used it to analyse the regenerative braking energy of the metro system in Istanbul, Turkey. Additionally, TOM (the Train Operations Model) was developed by Carnegie-Mellon University, and SimuX developed by M. Turan Söylemez, have both been used in the simulation and energy balance studies of tram systems powered by a DC supply [66, 75]. Although the software mentioned above are professional and their effectivity and reliability have been proven, due to concerns on commercial confidentiality, some of them are not open for general use, or are just partially available to a certain organization and academic bodies. Hence, these software packages are not fully accessible, and in some cases, their accessibility issue is attributed to the very high purchase cost.

Instead of using the aforementioned dedicated software, many studies use well-proven general platform softwares, to construct models and undertake system simulations. Some of the software platforms focus on studying the whole network's energy supply system. In those studies, the various parts of the tram network (such as substations, trams, etc.) are equivalent to simple circuit components within an analogous circuit simulation representing the tram network. Subsequently, an analogous electric circuit is built to be analysed for its energy operation via a Power Flow Algorithm. In essence, the Power Flow Algorithm commonly uses equations and matrixes to express the operation of the rail system, and exploits the powerful computing ability of a software platform for modelling and simulation.

Lee, et al. [76] and Tian, et al. [70] applied the Power Flow Algorithm to the construction of a model, and conducted simulations for the investigation of the energy balance. The former looked into the Seoul Metro Line 7, and the latter examined Beijing Yizhuang subway. Teymourfar, et al. [77] modelled the Tehran metro network and simulated the energy balance via creating a digital simulation environment through software PSCAD. Chymera, et al. [67] and Yang, et al. [69] applied the Node Voltage method and conducted the modelling and simulation on Matlab to obtain the current and voltage of each tram car at any given time point and location to understand the energy balance of the network. However, this approach is complicated and not intuitive. Firstly, in the case of a substation with uncontrolled rectification, its characteristics are strongly nonlinear, leading to the non-convergence of the DC network power flow calculation when solving the network for regenerative braking. Besides, it is challenging to modify the model to address changes in the system's configuration or to include extra units, and thus further study approaches for improving energy efficiency of the system.

Some of the software applications target studying the efficiency of the energy exchange between the tram and the supply network. These applications firstly focus on modelling each key unit, component or module of the tramcar and the power supply system. For example, the motor in the tram car will be modelled instead of being simplified to a basic current source existing in an electric circuit. The model can then be built to conduct simulations to scrutinize the energy exchange between the tram and the energy supply network. Shahnia, et al. [78] applied PSCAD to the simulation of the traction power supply system and car models. Streit and Drabek [79, 80] used the Labview software package to obtain the key parameter of their proposed control method and simulated the energy efficiency of a tram car. Matlab/Simulink is also one of the most popular software packages because Matlab/Simulink has libraries (such as the Simpower toolbox) with some electrical components programmed in it. Hence, the users can obtain and add different units to their model directly. Du, et al. [81] used this approach to compare traction current used by different types of electric motor while a light rail train car travels between two substations. Yu, et al. [82] studies the current and voltage change when a tram car brakes. Ruigang, et al. [83] and Brazis, et al. [84] both constructed tram car models and simulated the energy exchange between the tram car and the energy supplying facilities. Using such modelling and simulation methods enables examination of the energy change of one tram/train car while it is travelling in the network, but could struggle to analyse the complicated and dynamic energy trend of the entire rail network, which has multiple trains

travelling simultaneously. Still, it can construct models that have a good visualisation and are easy to modify.

In conclusion, various software packages can be used to model the energy balance of the rail system, but the different approaches have their pros and cons. Thus, a methodology which is built on a well-known software platform and is intuitive but still able to model the energy balance of a complicated and dynamic rail system, is required.

2.2 Braking energy recovery of the rail system

2.2.1 Overview of braking energy recovery methods

The recovery of braking energy could be via operational management or technical intervention. For example, in light rail systems, Optimising the departure schedules is one of the commonly applied operational management measures and could help improve braking energy recovery. However, it is out of the scope of this research. To date, the technical intervention for braking energy recovery is two fold, using reversible substations, and the addition of energy storage systems (ESS's) [41, 42, 85].

2.2.1.1 via Reversible substations

Reversible substations are equipped with AC/DC inverters in the place of simple multi-pulse rectifiers, which allow the braking energy to be fed back to the distribution network [41-43]. Inverter feedback is instigated with a high power three-phase inverter. This type of inverter is able to connect its DC link, with the DC line of the traction substation. Via this approach, the regenerated electricity can be inverted into AC, and synchronised to the voltage and phase of the grid. Hence, the regenerated energy can be returned to the network of the grid operator, thus being used in the operator's network or sold to the energy supplier [41]. The schematic of this approach is shown in Figure 2-1. A number of studies have looked into the exploitation of reversible substations in the rail network.

- Cornic [86] presented the findings of the RailEnergy project. The project was funded by the European Commission under the 6th Framework Programme for Research and Development, and aimed to reduce rail energy consumption. It architected the reversible DC substation and modelled / simulated its performance by virtually applying it on a regional service from Utrecht to Zwolle, which has an 87 km track length, 15 stops, and a supply power range from 6-18 MW. The simulation result showed that the application of

reversible substations could deliver an energy saving of 7%. However, in this study, the frequency of stops does not closely reflect that of a busy urban tram system, expecially when this exists in part over the road network, and is thus subject to trafffic flow issues.

- Ibaiondo and Romo [87] developed a new converter topology, which can be applied to the reversible substation. A prototype unit was designed and installed in one of the traction substations of the urban subway network in Bilbao, Spain. The addition of the prototype could reduce daily energy consumption by approx. 8.7% for weekdays, 14.5% for Saturdays, and 24.25% for Sundays.
- Gelman [88] compared the energy-saving and the related economic performance of the reversible substation and the conventional substation. The modelling and simulation found that the reversible substation can lead to the system consuming 44% less energy than the conventional substation. Given the relatively high capital cost of the reversible substation, the work estimated that the investment would be recovered after 12 years.

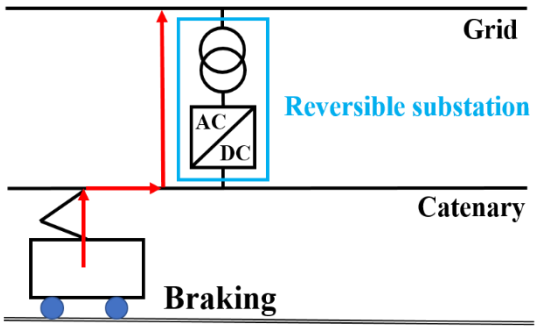

Figure 2-1 The schematic of utilization of braking energy via inverter feedback storage

The application of inverter feedback to the utility supply is good for integrated energy usage and efficiency, as the regenerative energy is directly fed back to the grid. However, it has a weak economic justification, due to high capital cost of the inverters, and the complicated control and maintenance that hinders its wider application. Moreover, the quality of the electricity that is fed back is relatively low as the current harmonics can be high, and the power levels transient. The high harmonic distortion gives rise to interference with communication and control systems on the tram / rail system, and can generate interference with other electric facilities [42, 89]. In addition, the very low price paid by grid operators for electricity returned to the utility supply does not aid the economic case, as the energy has to then be drawn from the grid at a much higher price when it is needed again [90].

2.2.1.2 via Energy storage system

After an ESS is introduced onto the rail / tram system, the regenerated, but unused, energy will be stored 'locally' in the ESS, instead of being returned to the utility supply. When the tram is moving off, or accelerating, the ESS will return the stored electricity to the tram without incurring supply costs from the utility grid. One of the key components of an ESS is the energy storage unit, for which batteries, super-capacitors, and flywheels are popular choices for rail / tram applications [91].

Battery Storage

Battery storage uses a rechargeable electrochemical battery as the energy storage unit. At present, typical battery chemistries under investigation for storing regenerative energy include lead-acid batteries, Nickel-based batteries, and lithium batteries [92]. The advantages of battery energy storage systems are that the energy density is high, the cost is low, and the technology is mature [93]. However, due to the low power densities of common battery chemistries, the charge-discharge time is relatively long [93].

Supercapacitor Storage

The super-capacitor is another method of energy storage. In a super-capacitor, the electrode and the electrolyte compose a binary electrical layer structure. Since the electricity is stored as electrical potential energy, the charge-discharge does not require the chemical conversion that is required within a battery. Such a characteristic enables a super-capacitor to charge and discharge rapidly [93]. Compared to the battery, the super-capacitor has a much higher power density, but a significantly lower energy density [91]. Thus, a super-capacitor stores less energy than a battery that shares the same mass [91].

Flywheels storage

Flywheel energy storage systems store the electrical energy as mechanical kinetic energy in a spinning flywheel. However, the flywheel can only store the energy for a short time, and energy loss occurs during the spinning of the flywheels due to the inevitable friction (bearing friction and windage being typical) [41]. The flywheel system also requires a large volume of space, heavy maintenance, and could create noise and safety concerns [94]. Due to the substantially decreased cost of lithium ion batteries since 2010, Meishner and Sauer [94] predicted that battery ESS would displace flywheel based systems, which were popular between 2000 to 2010.

Based on the location of installation, ESSs can be categorised as either onboard storage, or wayside storage. For the onboard storage, the ESS is installed on the tram / train, and the unit primarily stores and supplies energy to the tram it is located on. With wayside storage, the module can collect the unused braking energy from trams on the system, and it can also provide the electricity back to a nearby accelerating tram. A schematic of the approaches can be seen as Figure 2-2. Previous research related to using onboard ESS for light rail networks includes:

- Steiner, et al. [95] reported that a prototype light rail vehicle with onboard energy storage capacity was offered to the public transportation operator RNV in Mannheim for trial by Bombardier Transportation. Compared to the conventional light rail vehicle with no energy storage, the prototype equipped with a new traction system and energy storage consumed 30% less energy and reduced the peak power demand on the system by 50%.
- Herrera, et al. [96] modelled and simulated the application of a tramcar with onboard ESS on the tramway of Seville, Spain. Through optimising the energy management strategy and also the capacity of the ESS, the daily operational cost of the tram system could be reduced.
- Arboleya, et al. [93] conducted a case study to demonstrate the energy-saving performance of the onboard ESS. Based on an assumed journey, the simulation result found that the light rail vehicle with onboard ESS consumes 11.5% less energy than the one without onboard ESS.

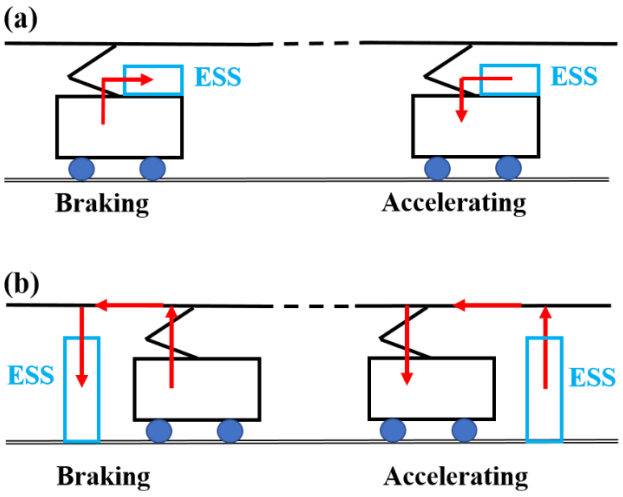

Figure 2-2 The schematic of the utilization of braking energy via energy storage: (a) on-board storage, (b) wayside storage

Therefore, the aforementioned studies prove that the onboard ESS can effectively recover braking energy and thereby achieve energy savings, and that an onboard ESS is also suitable for catenary free networks [93]. However, the onboard ESS is only effective for the light rail

vehicle on which it is installed, and once that light rail vehicle is no longer in operation, the onboard ESS will not provide benefit to other light rail vehicles or the network as a whole. Furthermore, the addition of on-board ESS to the vehicle would increase the weight or volume limits for the vehicle, therefore reducing the vehicle's performance and passenger-carrying capacity. The installation of wayside ESS could avoid such issues. The connection to the rail is then stationary, and similar to our suggested approach about connecting EVs to the network. Thus, this thesis provides a comprehensive review on the wayside ESS in the following Section 2.2.2.

2.2.2 Application of wayside ESS

The wayside ESS is also referred to as the stationary ESS, and is commonly installed on the ground alongside the tracks. Therefore, it avoids the issues associated with an on-board ESS as it doesn't occupy any passenger-capacity (in terms of weight or volume) of the tramcar and it can offer its service to the tram network all the times. Among various methods for recovering the braking energy, the stationary wayside ESS is the one closest to our suggested approach, because when EVs are acting as an ESS, they are connected to a charging point and remain stationary. Therefore, this research reviews the application of stationary ESS in light rail systems.

Barrero, et al. [97] studied the Brussels metro line 2 which has a total length of 8 km, 14 stops, 9 unidirectional power supply substations, and is operated in an open-circuit voltage of 876V. The study develops a simulation program based on the "effect-cause" method in Matlab/Simulink. The study uses a supercapacitor for energy storage and suggests that the ESSs should be installed every 1.5 to 2.0 km. The work achieved an energy saving of 11% in peak hours, and 26% for night and weekend periods, demonstrating the success and applicability of ESS within a tram system.

Teymourfar, et al. [77] studied the Tehran line-3 metro which is operated with a nominal voltage of 750 V. Although the whole network is 33 km long incorporating 26 stops, the study only conducted modelling on a segment which contains 10 stops and 9 unidirectional substations. The study developed an effective method to predict the maximum instantaneous regenerative energy produced at each stop. The study shows that regenerative energy produced at each of the 10 stops varies from 533 MWh/year to 5,900 MWh/year. For each stop, the study tailors

the configuration of the stationary ESS module. For the stop with the greatest regenerative energy production, the maximum energy saving is around 42-44% during peak and off-peak operating hours.

Lee, et al. [76] studied the Seoul Metro Line 7 in South Korea, which comprises 42 stations and 16 substations over 47.1 km of track. The network is operated with a rated voltage of 1,500V and the no-load voltage of 1,650V. The study modelled and simulated a railway system with ESS installed, and calculated the optimal power and capacity of the ESS. The capacity of the ESS was calculated as 478 kWh, and its application to the system was able to improve the efficiency to more than 90%, while saving 7 MWh energy per hour. As energy consumption was predicted to reduce, the operational cost was consequently lowered by 27.7%. Moreover, the wayside ESS was also found to deliver benefits of stabilising the feeder voltage, and the line charging and discharging voltages. As a result, transient overvoltage or under voltage on the catenary is prevented.

Ceraolo and Lutzemberger [98] studied the Bergamo light rail system, which is 12 km long, has 10 power supply substations and is operated with a rated voltage of 750V, via modelling the simulation. With an ESS added to each power supply substation, the simulation result predicted an approx. 43% energy-saving. The study also suggested that 2-4 km is the optimum distance between the ESS's in order to minimise the energy loss due to the line resistance. Additionally, the study compared the influence caused by the storage media, the super-capacitor and lithium ion battery. Although the energy saving delivered by both super-capacitor and lithium ion batteries is comparable, lithium ion batteries are a more competitive option because installation costs are lower, and hence lead to a more rapid Return on Investment (RoI).

Gao, et al. [99] studied the Beijing line-5 metro supply network and trains. Real data from the metro line and its trains were obtained and used to predict the maximum instantaneous regenerative energy of each station via modelling and simulation. The research found that the addition of wayside ESS could lead to a daily energy saving of 12%, which was equivalent to 1,500 MWh per annum.

As mentioned above, the ESS helps deliver energy-savings to a rail network, but installation requires capital investment. The implementation of adding ESS to the rail network thereby needs to be justified based on whether the initial investment can be returned through the

economic benefit created by the energy-saving, and how quick it can be. Some literature has performed economic feasibility studies based on the energy balance.

Teymourfar, et al. [77] investigated the economic benefit of using a wayside ESS and predicted good economic feasibility. The study estimated that the initial investment would be returned after ten months, and the cost-saving through the ESS would be approximately nine times higher than the initial investment, over the ESS lifetime.

Ceraolo and Lutzemberger [98] compared the economics of stationary ESS with a battery or a super-capacitor acting as energy storage media. Assuming the battery and super-capacitor deliver a similar energy-saving, the former showed better economics than the latter since it was assumed to be 50% cheaper in unit price. However, the increase in the number of ESS additions was found not to elevate the energy-saving linearly. Fewer ESS installations improve the speed at which the investment would be recovered. When the number of ESSs ranged from one to ten, the payback period varied from two to 18 years for the system under consideration.

Lamedica, et al. [100] investigated the optimal addition of wayside ESS to a railway line. Its economic study not only considered the payback period, which focused on how long the initial investment is recovered, but also looked into the net present value (NPV), which predicts the economic benefit generated during the useful life of the ESS. The study found that both one and two ESSs could achieve a positive NPV, and so, they are both proven economic additions. However, the addition of two ESSs was found to have a smaller NPV and a longer payback period than just a single ESS.

Park, et al. [101] investigated how the cost and asset life of the battery in the ESS impacts the economic feasibility. Based on the actual load data of a Korean urban light rail substation, the study modelled and simulated the energy saving achieved by adding a battery ESS. It discovered that the predicted annual profit generated through the ESS addditon would increase by 50 US dollars ($) if the unit cost ($ per kWh) of battery was less than $130/kWh and could decrease by $1/kWh. Additionally, the study found that if the battery's asset life could be extended, more profit could be generated over the battery's useful life, for instance, the estimated total profit generated was approx. $23,000 if the battery life was 10 years and coud become $37,500 if the battery life 15 years.

Roch-Dupré, et al. [102] studied the impact of the addition of an ESS on the demand charge, energy consumption and the related economic influence. With the aid of modelling and simulation, this research predicted that the addition of an ESS lowered the cost of the demand charge by 10.02% and lowered energy consumption by 16.93%, therefore leading to a 15.08% reduction in the overall cost. Further, it studied the influence of the ESS cost on the economics and showed that NPV could change from € -6,000 to € 298,000 if the cost of the battery varied from 50% to 150% of its assumed baseline level.

As discussed in the above research, the economics of including ESSs varys substantially between studies and is likely to be case-specific as each case would have a varied energy saving that lead to different cost savings and use different types, capacity and number of ESS that result in highly varied costs. It is worth noting that both the number and size of ESSs influences energy-saving, but the energy-saving might not respond to the two influential factors linearly. Therefore, the ESS's configuration (i.e. the capacity) and implementation strategy (i.e. the location and the number of ESS additions) could also heavily impact the economic appraisal built on energy-saving. Furthermore, the unit cost per ESS, which directly impacts the initial investment, is also found to affect the economic performance.

Although some researches have looked into how different parameters impact the economic feasibility, they did not study these uncertainties in-depth, and consider how and why these uncertainties influence the economic appraisal differently. Therefore, it would be valuable to have a comprehensive study that holistically investigates the impact of the ESS's configuration, the implementation strategy, and the cost element on the energy-saving and economic feasibility of installation. Also, it would be beneficial to conduct a sensitivity study on each cost or income-related element to understand how they influence the economic evaluation.

2.3 The exploitation of EV batteries for energy storage

2.3.1 The Vehicle-to-Grid approach

The V2G approach utilizes the energy storage capacity embedded in the EVs to achieve energy exchange between EVs and grid, and is called vehicle-to-grid (V2G) [103, 104]. V2G technology allows the EVs to provide power to specific electricity markets, for example when the demand is high (peak lopping or load shifting), or to store power from the grid at specific occasions, for example, when the demand is low (or has over generation capacity) [103, 104].

2.3.1.1 The merits of V2G

Studies have suggested that V2G can make a contribution to the regulation of grid frequency, and the overall reduction of the peak demand. With V2G, EVs may be required to provide power to the grid. Since the cost per kWh of electrical energy obtained utilising EVs is high, and the durability of the EVs' batteries is low, the EVs are not suitable for providing based-load power like the large generators [105, 106]. However, because the EV battery is able to quickly respond to demand changes [107], it could be utilized for voltage regulation or for primary and secondary reserves [105, 106].

Studies have been done on applying V2G for grid regulation. Drude, et al. [108] introduces two dispatch strategies to the Brazilian energy market, and proves that V2G operation can help to stabilise the grid. It also suggests that an appropriate policy should be put in place for preventing the conflict between grid operator and EV owners. Udrene and Bazbauers [109] used an advanced energy systems analysis tool called "EnergyPLAN", which can be used to simulate the operation of the different energy system (i.e. electricity, heating, cooling, transport, etc) [110], to examine the feasibility of using V2G enabled vehicles to provide peak-shaving services to the Latvian electricity system. The result shows that, with 11% of the EVs battery capacity available to the grid, a 100 kg annual CO_2 reduction per passenger car can be achieved. Financially, White and Zhang [111] discovered that approaches that enable frequency regulation services, and peak-load shifting, provides significant financial returns as an annual profits of $277-3,080 estimated based on the 2009 New York electricity market price for the vehicle owner.

Various studies suggest V2G can also be used for integration of renewable energy generation [112, 113]. From using the 'EnergyPlan' model, Lund and Kempton [114] found that V2G operation can absorb excess generation from wind power, and increase the overall utilization of wind power in an electricity grid. If EV batteries are a higher capacity, this benefit will be further improved. Haddadian, et al. [115] investigated using V2G to increase the penetration of different renewable resources without harming the system security and stability. The outcome of this research suggests that V2G can smooth the variability of renewable generation, leading to a reduction of overall system operation costs and emissions, and increase the uptake of wind power. Ul-Haq, et al. [116] studies an EV charging station that is either powered by photovoltaic (PV) panels, or the power grid. V2G is used to stabilise the grid during peak load

hours. The simulation result demonstrates the feasibility of the charging station under different operating modes, together with the V2G operation.

In conclusion, the V2G technology has been proven to be viable and can bring benefits in terms of peak demand reduction, grid regulation, and grid stabilisation. This benefit could potentially be delivered to the rail application, when EVs act as the ESS for the light rail system.

2.3.1.2 Issues of using the V2G approach

The degradation of the EV battery is one of the key issues affecting the feasibility of the V2G. Guenther, et al. [117] conducted a model-based study to examine the aging of EV batteries in different load profiles, and considered the battery life would be reduced as the V2G peak-shaving was added to the battery cycling. Uddin, et al. [118] reported there is a disagreement as to whether the V2G will degrade the battery life in different literature, they suggest that the longevity of the battery should not be affected if there is a smart control algorithm that uses an objective of maximising battery life as part of the system operation. Hill, et al. [119] compares the revenue achieved by the EV owners for providing V2G for grid ancillary services (such as frequency regulation) to the cost of the potential battery degradation caused by V2G. The study concluded that, from the owners' perspective, the battery life is a key factor that determines the financial viability of the V2G in practice.

Apart from the financial viability, the battery life also affects the EVs owner's willingness to participate V2G system, as they are the owner of the battery and will be directly impacted by any shortening of battery life that occurs as a result of being used for V2G. Geske and Schumann [120] surveyed EV owners and found that the "Range anxiety" and the "minimum range" are the most important determinants in their consideration of whether to allow V2G operation with their vehicle batteries. Thus, potentially incentives are required to encourage the EV owners to participate in V2G applications [121].

2.3.2 Existing research on electrical energy exchange between rail and road transport

In recent years, many researchers have investigated the technological and economic feasibility of V2G, and have further developed the V2G concept into V2X, which uses EVs to provide power to any electric devices, facilities and markets [60-62]. V2X could have various applications depending on what is linked to and exchanging energy with the vehicle. Examples

of V2X applications include: vehicle-to-load (V2L), vehicle-to-home (V2H), and vehicle-to-building (V2B) [61, 62]. The V2L is considered the least complex and applied on the smallest scales. It primarily aims to use EVs to provide an emergency backup load to facilities experiencing energy shortages and/or lacking a grid connection [61, 62]. In some cases, it is used for recreational or non-urgent usage, i.e. camping and concerts [62]. V2H is the second least complex application among the three examples. It not only uses the EV for load but uses it for energy storage as part of home energy management [61, 62]. The latter application is popular for homes that possess renewable energy generation, such as solar and wind. Since the time of peak energy generation may not coincide with the time of peak consumption, thus the V2H could deliver its energy storage capacity to balance and smooth the generation and load, and prolong the grid independence [61]. V2B is a more complex application and usually occurs on a large scale that involves greater numbers of EVs or an EV fleet. The EVs in the V2B application can provide their electricity charged during the off-peak period to the commercial or industrial user during the peak period. The V2B could help reduce the grid demand during peak [61, 62]. Also, it might deliver cost benefits to the commercial or industrial user due to the potential to purchase the electricity from the EV owner at a lower price rather than from grid [62]. The US air force conducted a three week experiment in Colorado and used two medium duty electric trucks with 95 kW power and 125 kWh capacity for the V2B. The power demand was successfully reduced by 43 kW [122].

In the light of V2X, the charging station of EVs could connect to the rail network, and potentially, EVs could thereby act as the wayside energy storage system of the rail network. The V2X version for rail and road could utilize the EVs to store and balance the generation and usage of braking energy, and offer some of the EV energy to the rail traction to reduce grid demand and stress. It combines the features and the merits of the V2H and V2B. However, studies are limited that investigate the connection and energy exchange between rail and road.

Brenna, et al. [123] studied connecting the rail and EV charging points as using a high-speed railway system to provide power to the fast charging facilities of EVs in service stations located alongside the highway close to the railway lines. When an EV undertakes a long journey on the highway, it requires high power rapid-charging facilities for a quick re-charge in order to extend its traveling range. The fast charging facility requires a high power electrical grid connection which is not commonly available in the remote areas, but can be accessed via the highspeed train power system, which is supplied at the kV level. Thus, Brenna, et al. [123]

proposed to link the rail and road. However, the energy provided to the EV is not related to the braking energy of the rail, and it is just from the high power grid supply initially provided to the rail. Hence, the power supplied to the EV charging has to be limited as if excessive energy is drawn from the rail power supply network, the operation of the rail will be compromised. Moreover, the energy exchange between the rail and road proposed in this study is unidirectional, only from rail to road as found in standard charging systems.

The charging of EVs by the rail network does not always compromise rail operations. Fernandez-Rodriguez, et al. [124] linked a wayside ESS with an EV charging point. The ESS firstly absorbed the excessive braking energy, which was produced but did not get reused immediately. A management system then controlled the discharging of the ESS, to charge up the EV connected to the system or to power the rail in traction load. The study discovered that the connection of the EV charging point and the wayside ESS improved energy saving, and this could be attributed to the EV taking the braking energy originally stored in the ESS and therefore allowing the ESS to receive more braking energy. However, the energy exchange between the EVs and the rail is still unidirectional as it is from the rail to the road.

A bidirectional energy exchange between rail and road, which properly implements the V2X, has been proposed. Radu, et al. [121] analysed the on-board and wayside ESS application in urban DC transport systems and proposed (another) concept about the connection between the rail network and the EV charging point. It suggested using the wayside ESS to connect the rail and EVs. When the wayside ESS has sufficient braking energy reserve collected from the DC transport systems, it could then charge the EVs. When the EVs connected to the wayside ESS that hold available energy to give and the DC transport system has energy demand in traction, the EVs could then sell their energy to the rail through charging the wayside ESS. Such an application enables the charging of EVs with braking energy, elevates the wayside ESS's receiving capacity on braking energy, potentially reduces the traction load (to the grid) and energy bills of the rail, and could also even encourage the use of public transport if the DC transport system operator offers a discount on their service to the EV owners who are willing to connect their vehicle and sell energy to the ESS. Still, the concept proposed has not been well proven for its technical and economic feasibility through actual case studies. It would be valuable to conduct a case study to model and simulate how the exploitation of EVs battery for energy storage could benefit a real rail system from both an energy and financial perspective.

2.4 Chapter summary

This research aims to achieve the bidirectional energy exchange between light rail and road, using the EV battery as the energy storage system for the rail to reduce the rail's energy consumption and peak demand and to potentially recover part of the braking energy to charge the EVs.

Section 2.1 reviewed recent energy balance studies of urban light rail systems. It considered that modelling and simulation have been commonly used for energy balance investigation and is easy to modify based on different research needs. The energy balances used as the baseline to assess the energetic and financial advantages of different energy storage approaches are case-specific and seldomly been studied at a whole network scale. The gap existing in the current knowledge is the lack of a comprehensive understanding of the whole network energy balance and an optimized method for achieving this. Therefore, the first objective of this research is to investigate the energy balance of the tram network, especially the energy demand for traction and the distribution of the braking energy, via an adequate modelling methodology.

Section 2.2 reviewed the current braking energy recovery approaches. As the stationary battery ESS has a good performance on energy saving and shares a similar connection (to the rail) method with the EV, it is considered a suitable starting point for the energy storage study. The energetic and financial benefit delivered by the addition of stationary ESS is expected to vary greatly from case to case and is impacted by the units added, the capacity, the location of installations, etc. It is likely that the strategy used to add stationary ESS to the light rail network could be transferred to the later EV application. However, the gap existing in the current knowledge is that there is no comprehensive understanding of the optimal strategy, which considers both technical and economic feasibility. Therefore, the second objective of the research is to introduce the stationary ESS into the system, examine its impact on energy balance, and determine the optimal configuration of stationary ESS with regards size, location and number of addition and consideration of economic feasibility.

Section 2.3 reviewed the application of the EV as energy storage for different electric facilities and markets. The concept of utilizing EV batteries to provide the energy for rail are considered to have several benefits, such as reducing the rail's energy consumption and peak demand, better recovery of the braking energy, etc. However, the gap existing in the current knowledge

is that such a concept has not been assessed based on an actual system, and the connection and integration of the EV to the rail have not been well researched. Therefore, the third and final objective of this research is to explore the technical feasibility and the optimal solution of integrating EVs into the rail network via a full or partial replacement of the stationary ESS, and to assess its merit on the energy balance and the economic feasibility.

The thesis will now

1) introduce the operation of a typical tram network, propose and explain the simulation method and model used for the energy balance study, and present and discuss the results, in Chapter 3
2) introduce the stationary ESS model designed, compare the performance of the addition of stationary ESS added to the systems with different energy supply modes, discuss the optimal ESS implementation strategy (i.e. number and location) based on the energy-saving and cost-saving delivered, in Chapter 4
3) present the hourly energy balance of the tram network, introduce the model and the inclusion of EVs into the ESSs designed, compares different ESS systems based on their energetic and financial performance on the partial or full network-wide installation, in Chapter 5

Chapter 3. Modelling of energy trend of the tram network

Having examined the various approaches to modelling energy storage on light rail (tram) networks in the previous chapter, this chapter will describe the development of a model, based on travel data logged on the Sheffield Supertram as an example network.

The energy supply system, operational time schedule, and vehicular traffic all impact on the energy consumption of an urban light rail (tram) system. With such a complex interconnected problem, construction of a general model is not possible to suit all tram systems. Therefore, this project aims to utilize the Sheffield supertram as a specific example system for a case study. However, the complex inter-relationships between the factors affecting the energy use are generic to most urban light rail systems, therefore the results are representative of, and can be extrapolated to, similar systems. Throughout this research, there was no access to the energy supply network of the Supertram for experimental monitoring of voltage and current, despite efforts made to engage with Supertram, however design simulations made during the construction of sections of the supertram network were made available to the project by the design contractor, and could be used for model validation. This research therefore aims to investigate the potential improvement in the total energy consumption of the tram system through the introduction of energy storage onto the system. To this end, this research project took a modelling approach to the problem, validated by the small amount of data available, and the results of other studies carried out on similar urban tram systems. To achieve the overall aims of the project, a model was built in Matlab Simulink, based on the actual configuration of the Supertram system (reported in the literature). This was then used to simulate the energy balance of the system, and for subsequent investigations. The core concept of the modelling is to use the actual operational data, distance, speed and acceleration, of sample tram journeys to estimate the real time load of the motor and the tramcar, and ultimately simulate the energy trend with the association of the published operational timetable.

This chapter explains the process of modelling and simulation of the energy trend of the tram network from its operational data, based on Matlab Simulink, and presents the energy trend estimated for the same tram system with different energy supply methods, as described later in the chapter. In detail, the chapter is broken down into the following sections:

- Section 3.1 - introduces the system layout, energy supply mechanism and braking mechanism for the typical urban light rail network of the type studied.

- Section 3.2 - explains the type of data required, the data collection methodology and the data processing for the simulation.
- Section 3.3 - shows the details of the model of the tram network.
- Section 3.4 - presents the intial benchmark results and discussion of the energy trend of the tram network, obtained from the simulation.

3.1 Tram operation system

3.1.1 The Supertram layout

This research focuses on the Sheffield Supertram network, which is a light rail network operated by the Stagecoach company. The Supertram provides an inner-city tram based public transportation service to the city of Sheffield (UK). As a focus of the project, it is considered as a typical urban light rail tram network.

The total route length of the Supertram network is 29 km. It consists of three lines (or routes) which includes 48 stops in total, the blue line, the yellow line and the purple line as shown in Figure 3-1. In the network, each track is a dual rail system allowing inward and outward travel from the city center on separate tracks, and where routes overlap, the dual track is shared between routes (lines), through appropriate timetabling of the services.

Figure 3-1 The route map of the Sheffield Supertram [125]

3.1.2 Energy supply of tram system

The schematic of the energy supply mode of the Supertram is shown in Figure 3-2. The rated nominal voltage of the Supertram system is 750 V dc, and the low voltage (LV) distribution

voltage of the UK utility grid connection is 11 kV ac at the substations. Hence, the substations transform the 11 kV ac into 750 V dc, and provide it to the catenary for supplying power to the trams. The traction electric motor on the tram converts the electricity received from the catenary into kinetic energy that moves the tram. There are 12 substations to supply energy within the tram network, shown with their names underlined in red in Figure 3-1. The substation applies a bilateral power supply methodology. Namely, each substation provides power to the two adjacent rail supply sections.

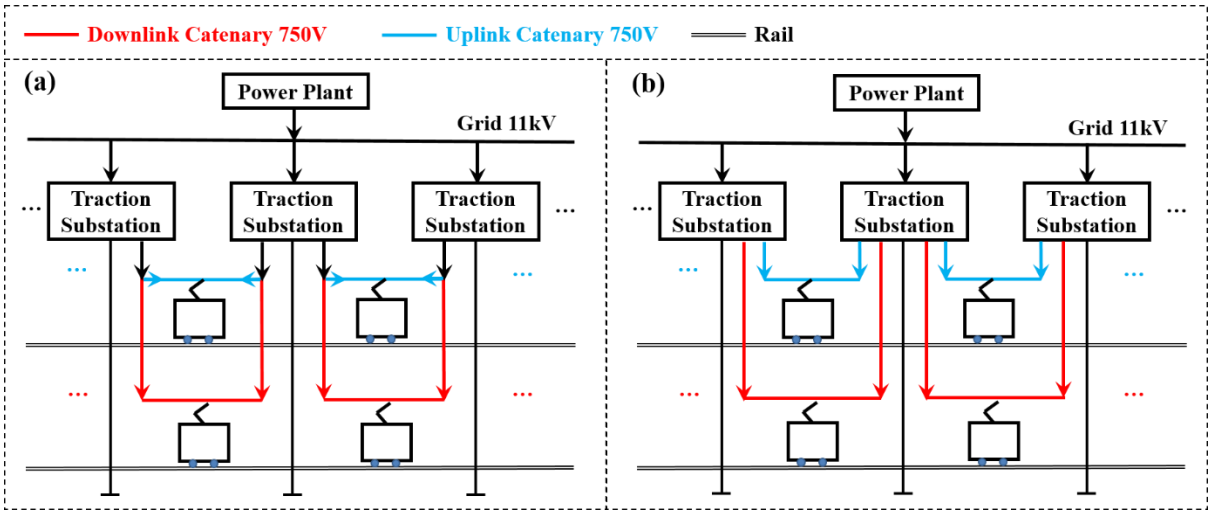

Figure 3-2 Schematic of supply system (a) common OCS and (b) seperate OCS

In real world practice, the urban light rail system can use either a separate overhead catenary system (OCS) or a common OCS to transmit the energy from the substation to the tramcar. For example, the systems studied in [67, 70, 100, 126, 127] exploit a seperate OCS, and the systems studied in [73, 77, 128] exploit a common OCS. In the separate OCS, the substation has two independent cable feeds to power the uplink catenary/tram-travel and downlink catenary/tram-travel, each fed from a separate rectifier. Therefore, the two cables (uplink and downlink) are not electrically connected, as shown in Figure 3-2 (b), and energy cannot be transferred between the uplink and the downlink. However, in the common OCS, the substation uses the same cable to power both the uplink and downlink and hence the uplink and downlink catenaries are connected, as shown in Figure 3-2(a), and energy can be transferred between the two directions.

The use of either the common OCS or the separate OCS determines how energy flows between uplink and downlink, and hence between different tramcars and substations, and furthermore,

between tramcar and tramcar. Consequently, it can lead to different energy usage trends between systems. This project received a report from Supertram for internal use only, and the report contains this crucial system data, the introduction of the common OCS and separate OCS, and some insights into the difference between the two energy supplying methods [129]. Therefore, it is worth studying the effect on the energy trend of the two alternative operational modes. In this project, different models were created to represent the common OCS mode and the separate OCS mode, funadamentally based on the Supertram network. A detailed description of the models is given in Section 3.3.

3.1.3 Braking mechanism

A moving tram can either be accelerating, at constant (uniform) speed, or decelerating. During acceleration and at constant speed, the tram draws current from the catenary and energy is consumed (there is friction opposing the motion even at constant speed). However, whilst decelerating (or braking), electricity is derived from the kinetic energy of the tram, via the electric motor on the tram, which is then regenerated into the catenary system.

While a tram is braking, electricity will be generated. However, the simple rectifiers used at the substations do not allow energy to be fed from the catenary back into the grid. Thus, if another tram is also travelling between the same two substations and is accelerating, the generated electricity would be fed to the accelerating tram. This type of braking is called regenerative braking. If there is no additional tram travelling between the same two substations while the tram is braking, the electricity, which cannot flow to an available tramcar nor back to the substation, will charge the stray capacitance of the catenary and thereby raise the catenary voltage, exceeding the allowable voltage limit and cause problems with voltage breakdown somewhere in the system. Hence, instead of being fed back to the catenary, the generated electricity is diverted to the braking resistors located on the tram, and therefore the energy gets dissipated as heat for safety reasons. This type of braking is called resistive braking.

Therefore, the tram operation not only consumes electricity but also generates electricity due to regeneration. One of the tasks of this research is to seek a solution to maximize the use of the regenerative braking energy, and thereby reduce the energy supply from substations. Hence, it is essential to understand the energy associated with the regenerative braking and resistive braking, and have an overview of the overall energy trend of the tram operation.

3.1.4 The system data of Supertram

This research aims to use modelling and simulation methods to study the energy balance of the Supertram system and this thereby requires gathering the Supertram's system data for the model construction and the subsequent simulation. Part of system data is publically available from Supertram's official website and was collected [130]. With the access to Supertram's internal report, this research validated the data collected from the Supertram official website and supplied some crucial but not publically available extra data [129]. The key system data used in the modelling and simulations is shown in Table 3-1.

Table 3-1 Supertram system data

Sources	Name	Value
Public available data	catenary nominal voltage	750V
	tare weight	46.5t
	passenger capacity	88 seated
	maximum acceleration	1.3 m/s^2
Internal-use only data	Not publically available	

3.2 The origin of the input data

3.2.1 Overview of input data

As mentioned at the beginning of this chapter, this research uses simulation models to estimate the energy trend. The simulation includes the construction of model and the data input. Figure 3-3 presents the general data input process for the simulation, and it can be explained as:

- The distance, speed, acceleration and altitude data of one tram journey that covers all the routes and stops was collected initially on a second by second basis.
- This data was subsequently used to calculate both the distance moved from position to position, and the force generated or absorbed by the electric motor at any moment during the tram journey.
- Both the distance and force data obtained for the single tram journey, and the operational timetable, are used by a Matlab model for integration into the system. The model aims to replicate the operational profile of the tramcar for every tram journey during a single day.

- Based on the operational profile of every tram journey made during a day (from the Matlab model), the Simulink model will simulate the daily energy balance of the tram system.

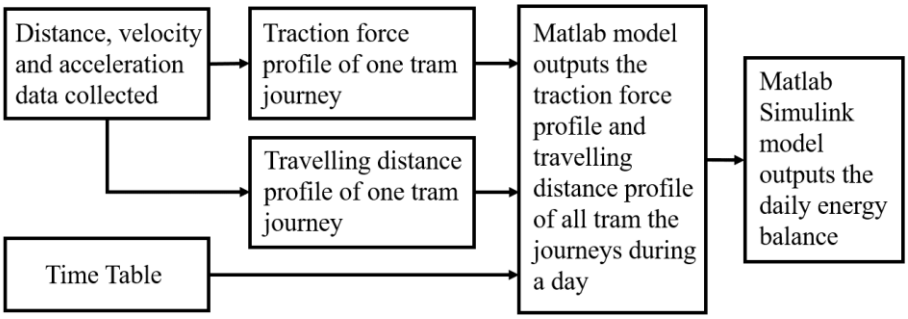

Figure 3-3 Schematic of the modelling and simulation process

3.2.2 Data collection

3.2.2.1 Selection of device

Dedicated GPS devices can be used to collect travel data, including coordinates, speed and acceleration of a moving object. This can also be collected using non-dedicated equipment with GPS function, such as a cell phone. In the initial stage of the project, several mobile applications were tested and proven not to meet our requirement on data accuracy. As an example, data was gathered by the mobile application named "Speedmeter", which was found to be the best among the tested mobile applications. The graphs of the speed and acceleration data collected via "Speedmeter" are shown in Figure 3-4.

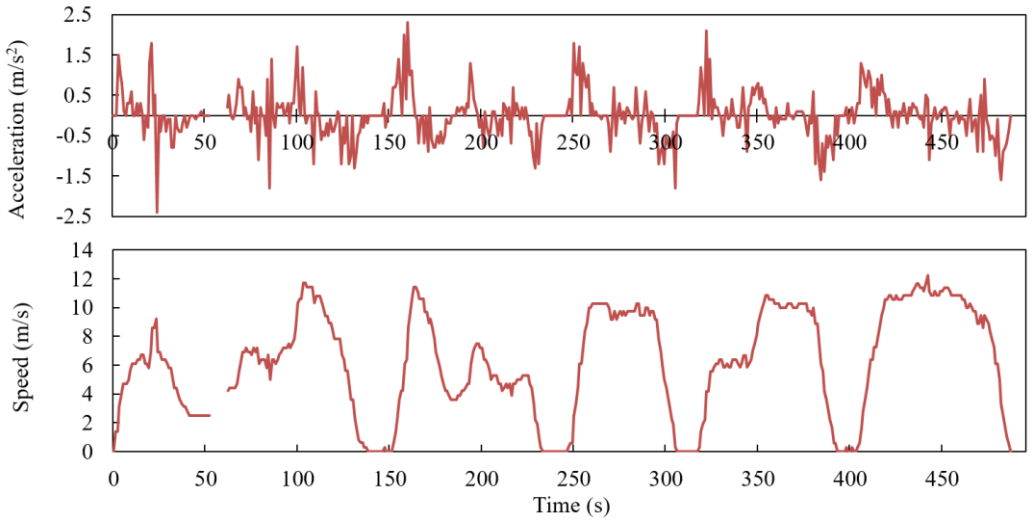

Figure 3-4 The Speed data and acceleration data collected via iPhone apps "Speedmeter"

As can be seen, due to the loss of the cellular signal, the data of the 50th to 60th second in such a journey of under 10 minutes is missed. More importantly, the acceleration collected exceeded the maximum regulated value of 1.3m/s^2 given by the Supertram data. The graph of the speed and acceleration data collected via "Speedmeter" is shown in Figure 3-4.

After consulting the technician from the University of Sheffield School of Geography, a GPS device, GARMIN eTrex® 10 (shown in Figure 3-5), was used for the data collection for this research project.

Figure 3-5 Garmin GARMIN eTrex® 10

The raw data collected by GARMIN eTrex® 10 is latitude and longitude coordinates. The coordinates are collected second by second, and hence, the travelling distance per second can be calculated. If the latitude and longitude of Point A are (LatA, LonA) and of Point B is (LatB, LonB), then the distance between Point A and Point B is calculated via Equation 3-1.

$$S = R \times \arccos[\sin(LatA) \times \sin(LatB) + \cos(LatA) \times \cos(LatB) * \cos(LonA - LonB)] \qquad \text{Equation 3-1}$$

where ***S*** is distance, ***R*** is the radius of the earth which is taken as 6,371,000 (metre).
With the distance acquired, the speed and acceleration can be calculated via Equation 3-2.

$$S(t) = \int v(t)dt = \iint a(t)dt \qquad \text{Equation 3-2}$$

where ***S*** is distance, ***t*** is time, ***v*** is speed, and a is acceleration.

In order to examine the reliability of GARMIN eTrex® 10, the device was used to collect the travelling data of the tram journey alongside the mobile application "Speedmeter". The graphs of the speed and acceleration data collected via GARMIN eTrex® 10 are shown in Figure 3-6. Although the curves of the speed are similar, the acceleration curve collected via GARMIN

eTrex® 10 does not exceed the regulated range, and there are no sections of data loss. Thus, the device meets our requirement on reliability and accuracy, and is used for the subsequent data collection.

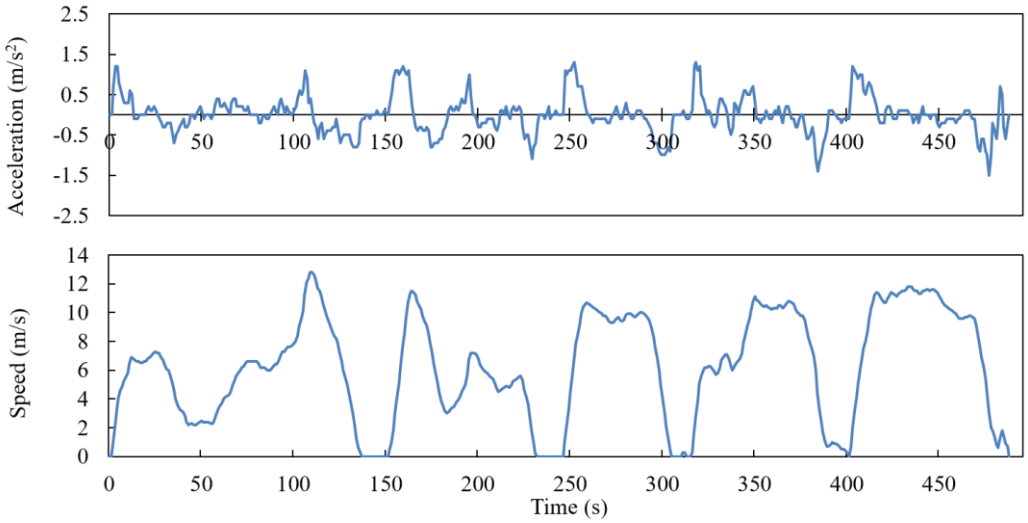

Figure 3-6 The speed data and acceleration data collected via GARMIN eTrex® 10

3.2.2.2 The principle of data collection

Since the Supertram network has three lines, it is impossible to have one single journey that covers all the routes and stops on the uplink and downlink. To understand the energy trend of the entire network, data collected from both travelling directions of each line is required. Therefore, in the sampling campaign, data collection that covers the whole system consisted of 8 different tram journeys as shown in Figure 3-7.

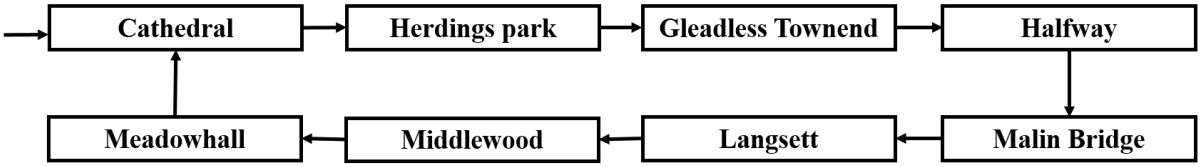

Figure 3-7 Tram journeys taken in the sampling campaign

These journeys covers all of the possible routes and stops on both uplink and downlink of each route, for example, the data sampling tram journey was initially carried out from the Cathedral stop to Herdings Park, then the second journey was from Herdings Park back to Gleadless Townend which is actually a stop on the route from Cathedral to Herdings Park. When the 8th tram journey finished at Cathedral where the sampling started, one sampling campaign was

complete, and the operational data of a tramcar at any place of the network or at any moment during the journey was thereby obtained.

As mentioned initially, the tram journey is affected by the road and traffic conditions as the tram travels for part of its journey on public roads, and its travel pattern is therefore varied due to traffic variations. In order to get more reliable and representative data, data collection events took place on three different days during a week. In those sampling days, data collection took place in both morning and afternoon. Therefore, there are six sets of data collected in total to account for basic variations in traffic.

In detail, data was collected in both mornings and afternoons of June 19th, 20th and 21st 2018. The morning data collection began on the Purple line tram journey which departed at 08:20 from the Cathedral to Herdings Park. The afternoon data collection began on the Purple line tram journey which left at 13:45 from the Cathedral to Herdings Park.

3.2.2.3 Result of the data collection

The six data sets contain the height above mean sea level, distance, speed and acceleration of the tram journeys in both directions for all three lines that took place on both morning and afternoon from June 19th to 21st. Figure 3-8 shows the height above mean sea level profile of the journey collected from Halfway to Malin Bridge in one sampling campaign. In that figure, the tram stops are highlighted with red dots.

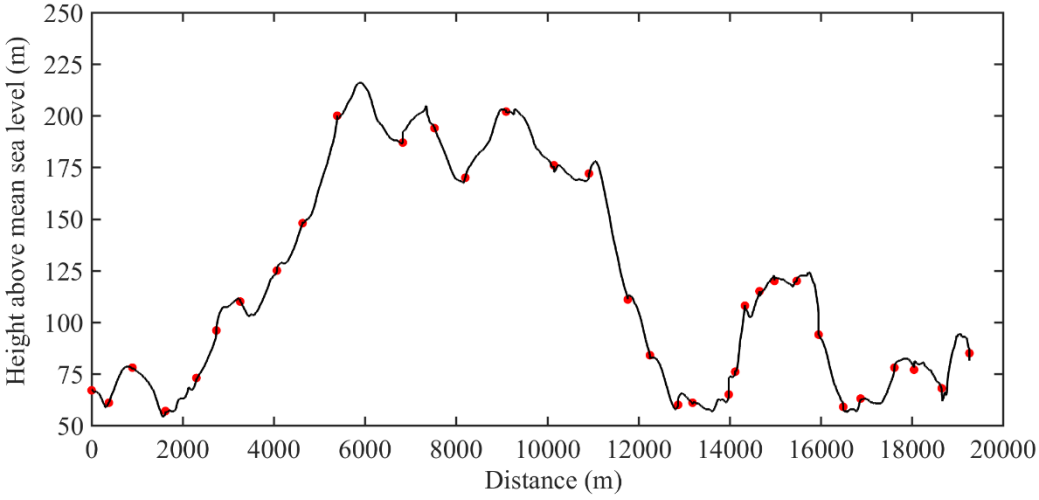

Figure 3-8 The change of height above mean sea level and distance over time during the journey from 'Halfway' to 'Malin Bridge' (Dots highlight tram stop locations)

The six sets of speed and distance data were categorized into Blue Line (from Halfway to Malin Bridge), Yellow Line (from Middlewook to Meadowhall) and Purple Line (from Cathedral to Herding Park) and are shown in the Appendix A. It is worth noting that, although the speed is not identical between journeys with same origin and destination, the overall trends are similar. Three tram journeys were randomly selected to compare their travelling (speed) profiles obtained through the six different sets of travelling data, as shown in Figure 3-9. These three tram journeys are (a) from Spring Lane to Arbourthorne, (b) from Beighton/Drake House Lane to Crystal Peaks, and (c) from Attercliffe to Arena/Don Valley Stadium.

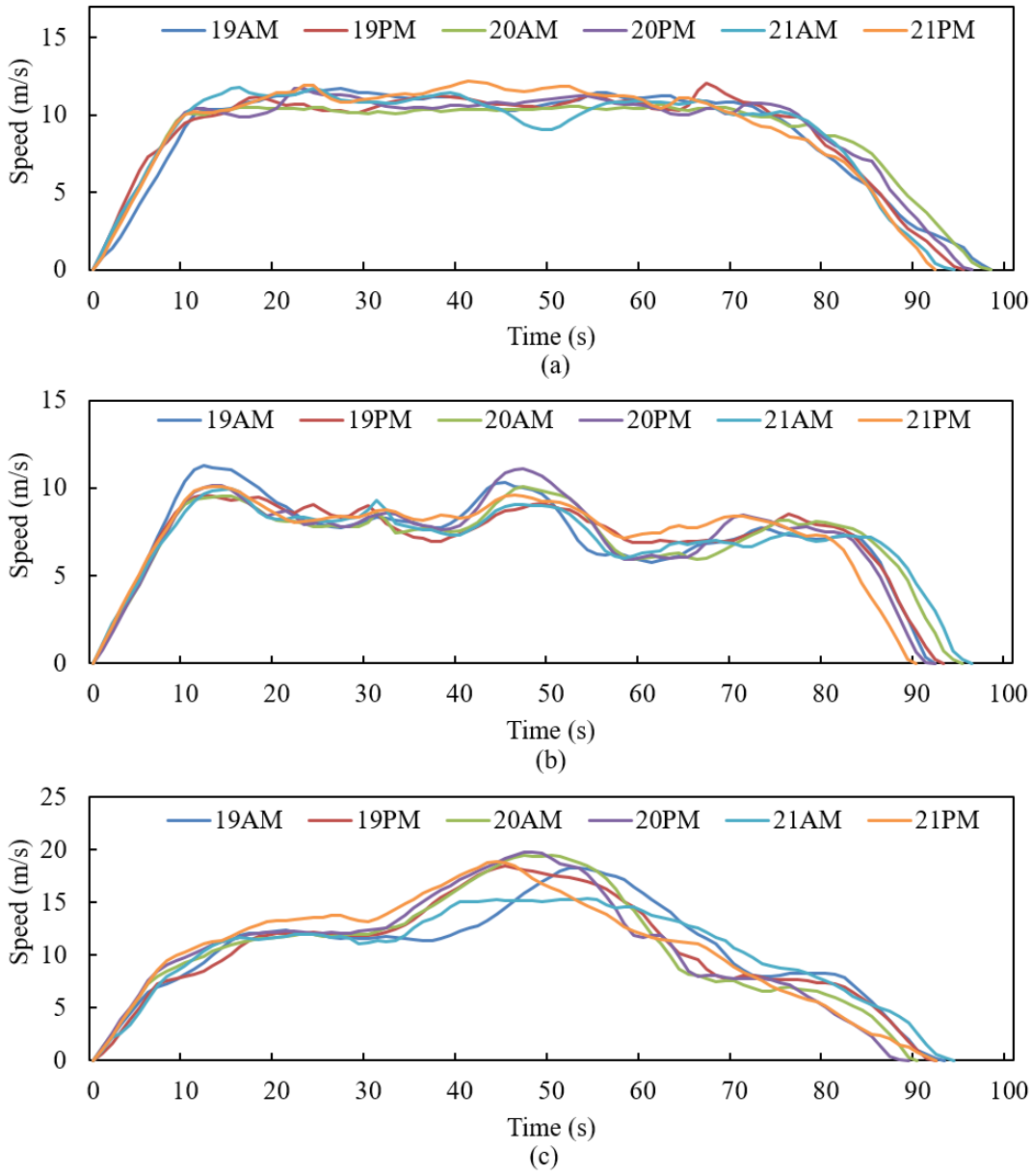

Figure 3-9 The speed and distance profile of the tram journey

3.2.3 The traction force of the tram

The traction and braking of the tram are driven by electricity. The electric motor of the tram is the device that transforms the energy, such as the mutual transformation of electricity and kinetic energy, and consequently, provides force to accelerate or decelerate the tram. In this sense, traction force and braking force are key parameters showing the status of energy transformation in the electric motor, and can be used to calculate the electricity generation and consumption in the tram operation.

From simple first principles, this research analyses the tram movement from a perspective of the mechanics. Generally, while the tram is moving, the force that impacts the tram is the joint force (F_{Joint}) of the traction force ($F_{Traction}$) provided by the electric motor and resistance force opposing the motion ($f_{Resistance}$). Hence, the $F_{Traction}$ provided by the electric motor can be calculated via Equation 3-3.

$$F_{Traction} = F_{Joint} - f_{Resistance} \qquad \text{Equation 3-3}$$

where $\boldsymbol{F_{Traction}}$ is the traction force, $\boldsymbol{F_{Joint}}$ is the joint force, and $\boldsymbol{f_{Resistance}}$ is the running resistance.

All three forces are vectors. During the tram operation, the tram is considered always moving forward. If the force exerted on the tram car is in the same direction to the movement of the tram, it is considered as having a positive magnitude. Otherwise, it is considered as having negative magnitude. In the case of resistance, the $f_{Resistance}$, which is always in the oppositive direction to the movement of the tram, is always considered as having negative magnitude.

3.2.3.1 The Joint force

The F_{Joint} can be calculated from Equation 3-4 by applying Newton's second law.

$$F_{Joint} = M_{tram} \times \mathrm{a} \qquad \text{Equation 3-4}$$

where $\boldsymbol{M_{tram}}$ is the mass of the tram and $\boldsymbol{a}$ is the measured acceleration from the GPS data logging.

Using publically available information from the website of Supertram, the tare weight and the passenger capacity of one tram car is 46,500 kg and 88 seats, respectively [130]. Assuming the average weight of a person is about 60 kg [131], the total mass of a full tram car is

46,500+88×60 = 51,780 kg. According to the information posted on the website of Supertram, the physical acceleration of the tram ranges from 0-1.3 m/s^2. Therefore, the joint force ranges between 0 and 67.3 kN for a full capacity seated tram.

3.2.3.2 The running resistance

During tram operation, the force that impacts the tram and hinders its movement is called the tram resistance. The tram resistance consists of basic resistance and additional resistance [83].

'Basic resistance' consists of motion resistance between the parts of the tram, air resistance, and is also caused by the impact of, and friction between, the wheels and rails. There are many factors that affect the basic resistance of the tram, and some are unable to be accurately quantified. In order to simplify the calculation of the basic resistance, the Davis equation [132] is commonly applied to approximately express the basic resistance, based on empirical data and the type of trams. Hence, the basic resistance can be calculated via Equation 3-5 [132].

$$f_1 = a + bv + cv^2 \qquad \text{Equation 3-5}$$

where v is the velocity, and **a**, ***b***, ***c*** are vehicle-related constants. In this study, ***a*** is taken as 1.01, ***b*** is taken as 0, and ***c*** is taken as 0.0006, values obtained from Supertram's internal report.

'Additional resistance' is caused by the road conditions, and consists of ramp resistance, bend resistance and tunnel resistance [133, 134].

Tunnel resistance

Since the route of Supertram rarely runs through a tunnel, the tunnel resistance was not considered in this modelling.

Ramp resistance

The ramp resistance (f_2) is calculated via Equation 3-6 [135].

$$f_2 = M_{tram} g \sin\left[\tan^{-1}\left(\frac{T_{grad}}{100}\right)\right] \qquad \text{Equation 3-6}$$

where $\boldsymbol{M_{tram}}$ is the mass of the tram, $\boldsymbol{g}$ is the gravity and $\boldsymbol{T_{grad}}$ is the track gradient in percentage and is obtained from the height above mean sea level given by the data logging.

Bend resistance

The bend resistance (f_3) is calculated via Equation 3-7 [136].

$$f_3 = 0.01 * \frac{k}{R} * M_{tram} \qquad \text{Equation 3-7}$$

The variable $\boldsymbol{f_3}$ is the resistance due to track curvature (kN), $\boldsymbol{k}$ is dimensionless parameter depending upon the train, and is taken as 600 in the UK study [136]. $\boldsymbol{R}$ is the curve radius in a horizontal plane (meters), $\boldsymbol{M_{tram}}$ is the mass of the tram.

The value of the *R* is measured via Google maps. As shown in Figure 3-10, using the tram route between Park Grange and Arbourthorne Road as an example, the radius of the bend is measured as 160 m.

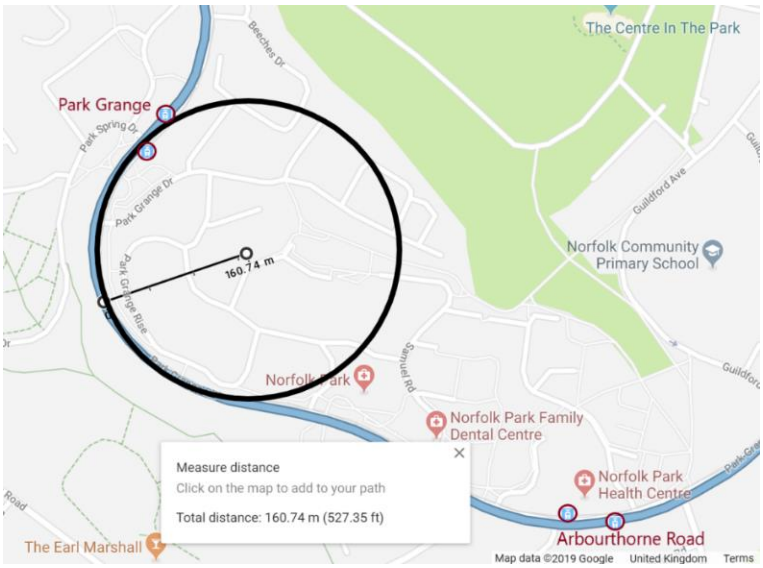

Figure 3-10 The bend located between Park Grange and Arbourthorne Road (Screen captured from Google Maps)

Through GPS data collected, the exploitation of Google maps, and the application of Equation 3-7, this research discovered that:

- There are only seven locations that have a bend with a ≤50 m radius, the time used to travel through these bends is approx. 135s, and the bend resistance calculated is 6.2 kN
- There are eight locations that have a bend with a radius >50 m but ≤100 m, the time used to travel through these bends is approx. 180s, and the bend resistance calculated is 3.1 kN
- There are only two locations that have a bend with a radius >100 m but ≤150 m, the time used to travel through these bends is approx. 100s, and the bend resistance calculated is 2.1 kN

Based on the weight of the tramcar (section 3.2.3) and the nominal maximum acceleration (Table 3-1) the maximum joint force (of the tramcar) during the tram operation, ranges from 0 to 67.3 kN. When compared to the joint force, the bend resistance is not likely to be influential. Travelling all the tracks takes approx. 7,050 s. Hence, the time spent on travelling through the bends mentioned above only accounts for a short proportion of the total travel time. Considering that the bend resistance makes a very small impact on the tram journey is in line with other academic studies [135, 137-139], which also do not include the bend resistance in the traction force calculations for their work.

3.2.3.3 Result of traction force

From Equations 3-3 to 3-6, the traction force of the tram of any moment during the journey can be found, and is an input to the energy trend model. However, due to the limited space here, only the journey from Halfway to Gleadless Townend is shown as an example, and the calculated traction force of the tram during the journey is shown in Figure 3-11. It is worth noting that the positive traction force shown indicates the tram is accelerating and requires traction, and the negative traction force shown indicates the tram is braking and produces braking energy.

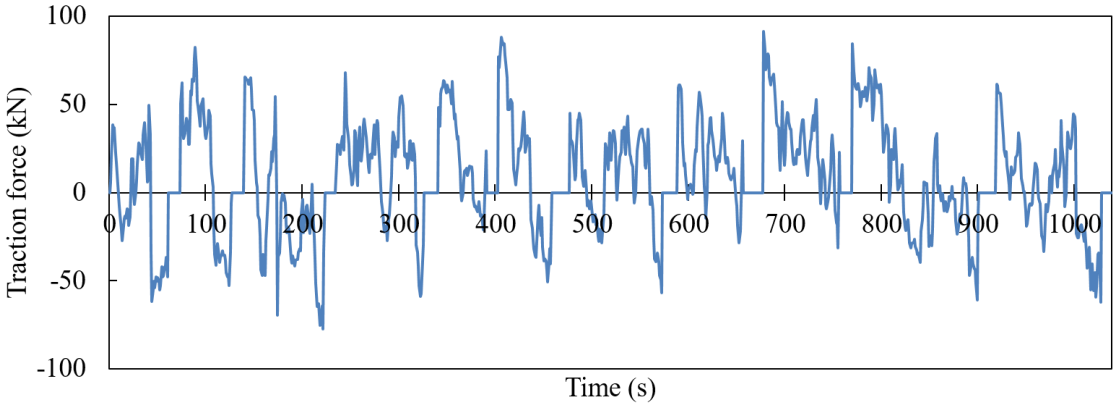

Figure 3-11 The traction force of the tram of journey from Halfway to Gleadless Townend

3.3 Simulation model of energy balance

3.3.1 Introduction of the entire model

As mentioned previously in section 3.1.2, the substations exploit a bilateral power supply method. Each substation only provides energy to the adjacent energy supply section. Since there are 12 substations in the Supertram network (red underlined in Figure 3-1 to show

locations), they segregate the network into 11 distinct energy supply sections. In order to simplify the modelling, and shorten the simulation run time, this research firstly simulates the energy balance of the 11 energy supply sections, and then obtains the energy balance of the entire tram network from a sum of the 11 sections.

According to the Supertram operating timetable, the smallest departure interval of each line is longer than 10 minutes. However, the time used for a tram to travel through two adjacent substations is less than 10 minutes. Therefore, if only one line uses the track between two adjacent substations,

- there is always only one tramcar travelling in the same travelling direction (either uplink or downlink) at any one time,
- there are always two tramcars moving in the opposite direction (one on the uplink, one on the downlink) inside the given energy supply section, at any one time.

If there is more than one line (blue, yellow and/or purple) going through two adjacent substations, it is possible that there could be two tramcars travelling in the same direction at any one time. Hence, there could be four tramcars in any given energy supply section, two travelling in one direction, and the other two travelling in the opposite direction.

From analysis of the timetable and the route map of Supertram (shown in Figure 3-1), the sections that always have two tramcars travelling in one energy section at any one time are:

- Halfway to Gleadless Townend (includes Halfway to Crystal Peaks, Crystal Peaks to Birley Lane, and Birley Lane to Gleadless Townend),
- Herdings Park to Gleadless Townend (in the same energy supply section with Birley Lane to Gleadless Townend),
- Meadowhall to Fitzalan Square (includes Meadowhall to Carbrook, Carbrook to Nunnery Square, and Nunnery Square to Fitzalan Square),
- Langsett to Malin Bridge and Langsett to Middlewood.

The sections that may have up to four tramcars travelling at any one time are:

- Langsett to Fitzalan Square (includes Langsett to University of Sheffield and University of Sheffield to Fitzalan Square),

- Fitzalan Square to Gleadless Townend (includes Fitzalan Square to Abourthorne Road and Abourthorne Road to Gleadless Townend).

Therefore, this research created two models in Matlab Simulink. The first one is for the sections with only one line passing through, and the second one is for the sections with two lines or more passing through. This section (3.3) uses the second model, which is the more complex one, as the example to illustrate the structure of the model.

Figure 3-12 and Figure 3-13 show the model of both the separate OCS and the common OCS, for the sections of the track with two lines passing through it, respectively. The key difference between the two models is whether the power supply cables that feed the uplink and downlink are connected, and therefore whether the substation separately supplies power to the tramcars travelling in different directions. Apart from that, the two models have identical structure and composition. Generally, the model has four main setions, 1) data calculation module， 2) substation module， 3) line resistance module and 4) tramcar module. The “CAL P” and “CAL N” blocks are the main calculation modules. “Substation1” and “Substation2” represent the substations; “tram1P”, “tram2P” “tram1N” and “tram2N” are the tram modules; “R1P” to “R3P’ and “R1N” to “R3N” are the line resistance modules respectively.

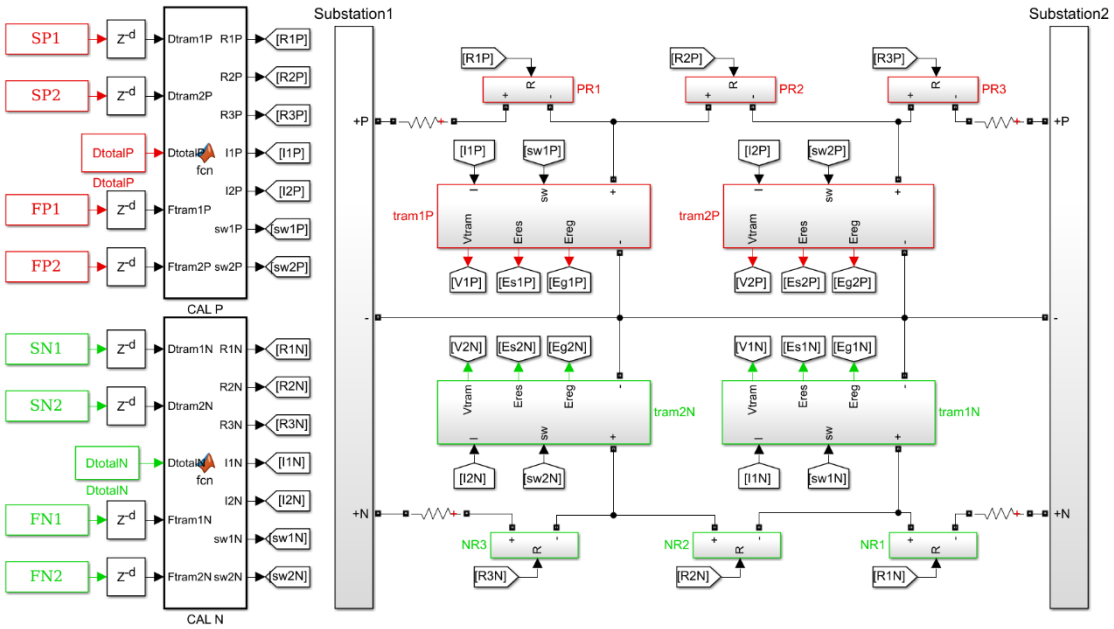

Figure 3-12 The model of a separate OCS that carries two lines

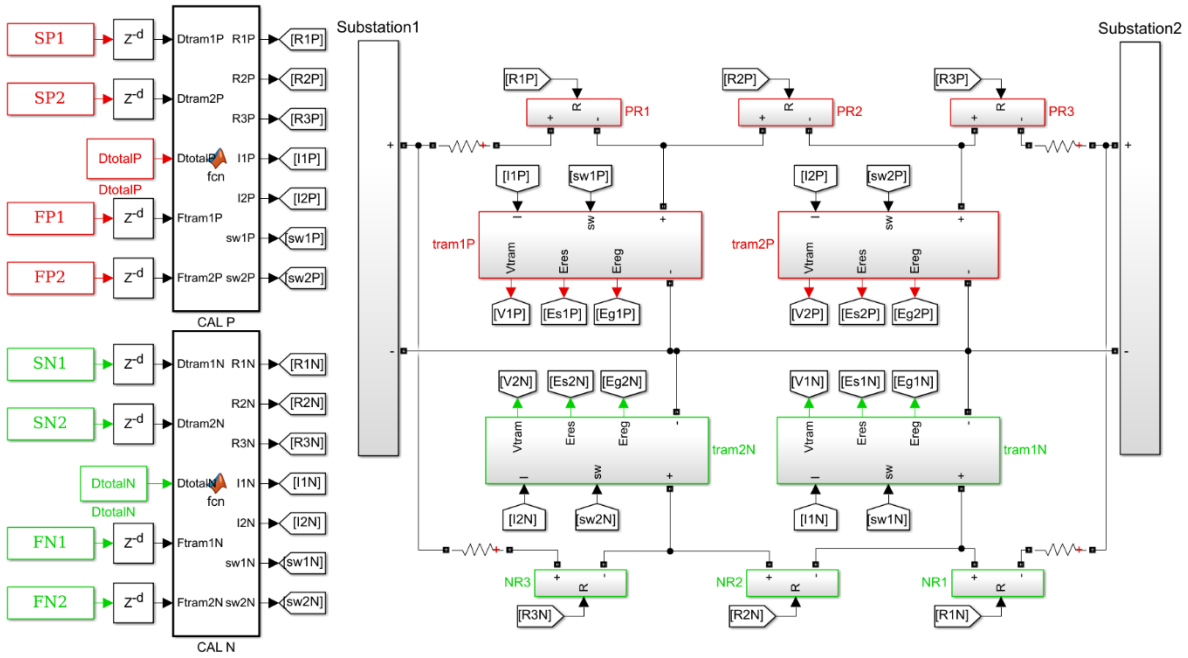

Figure 3-13 The model of a common OCS that carries two lines.

3.3.2 Data calculation module

The data calculation module is responsible for exploiting the Matlab function to process and integrate the input data, and for feeding the processed data to different modules to complete the simulation. The input to this module is the distance and force data, and the output includes:

- The line resistance from the substation at any moment during the tramcars journey ('R1P' to 'R3P' and 'R1N' to 'R3N'),
- The traction current of every tramcar travelling in the energy supply section ('I1P', 'I2P', 'I1N'and 'I2N'), and
- Data that controls which tramcar will connect to the energy supply network ('sw1P' 'sw2P' 'sw1N'and 'sw2N').

The numerical value of line resistance can be calculated via Equation 3-8.

$$R = S * \rho \qquad \text{Equation 3-8}$$

where $\boldsymbol{S}$ is distance and $\boldsymbol{\rho}$ is resistivity of the track and catenary, that is taken as 0.1419×10^{3} Ω/m.

From the force, the current drawn by the tram may be calculated. The traction motors used in the trams are the Siemens 1KB2121 and 1KB2021 [130]. Both motors are Asynchronous AC

motor / drive combinations, which feature a linear relationship between the rated torque and the rated current (I_e) [83]. Therefore, a linear relationship with the I_e and the force from the motor (F_T) is deduced and can be expressed as Equation 3-9.

$$I_e = k * F_T \qquad \text{Equation 3-9}$$

where ***k*** is a constant. The force constant, k, representing not only the motor, but the whole drivetrain of the tram, can be approximated to 14 under traction conditions [81], and to 10 under braking conditions [82] for systems like Supertram. The different k value used for traction condition and braking condition is because the motor, gearbox and other components would impact conversion efficiency. When the tramcar is in traction load, current flows from the supply network to the tramcar and gets converted into traction force that drives the wheel through the motor, gearbox, and other relevant units. A current I_{e_t}, which is supplied from the supply network to the tramcar, will lead to a traction force F_{T_t}, after the conversion efficiency losses. When the tramcar is braking, the motor, gearbox, and other relevant units will convert the braking force from wheel back to the current, and the current flows in the opposite direction, from the tramcar to the supply network. Even though the braking force F_{T_b}, would share the same magnitude with the traction force F_{T_t}, after the loss experienced on the conversion units, the current I_{e_b} obtained from the braking force would be smaller than the current I_{e_t}.

3.3.3 Substation module

In order to reduce the harmonic current injected into the electricity supply system by the substation rectifiers, and the ripple factor of the output voltage, a 24-pulse transformer is applied in the substation model [70, 81, 82]. In the ideal condition, the external characteristics of the substation are shown as below in Figure 3-14(a). In the figure, U_N stands for Nominal rated voltage, I_N stands for Nominal rated current, and U_E stands for No-load DC output voltage. According to Thevenin equivalent principle, the traction substation can therefore be seen as an equivalent DC voltage source and an internal resistance. Based on the simplified schematic the substation model shown in Figure 3-14 (b).

Additionally, the substation system also consists of a diode rectifier unit. As the diode rectifier unit only allows current flow from the alternating (grid) side to the direct (tram) side, current can only be transmitted to the catenary from the substation but cannot be accepted back to substation from the catenary. Therefore, a series diode is added into the model.

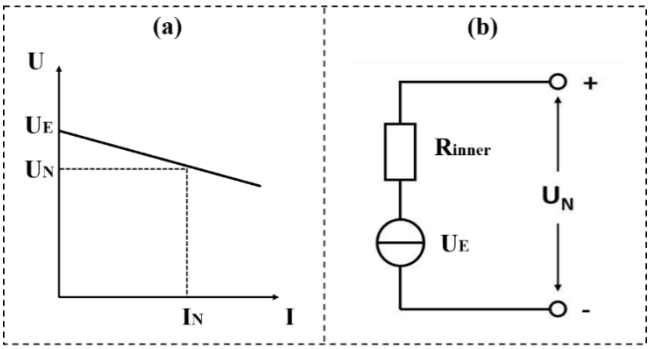

Figure 3-14 The external characteristics (a) and the simplified schematic model (b) of the substation

The separate OCS typically powers the tramcars in the uplink and downlink separately, each fed from its own rectifier. Hence, there are two cathode outputs in the separate OCS. For the common OCS, it uses the same cable to power both the uplink and downlink and it thereby only has one cathode output. The seperate OCS substation model is constructed in Simulink, as shown in Figure 3-15(a) and the common OCS model is shown in Figure 3-15(b).

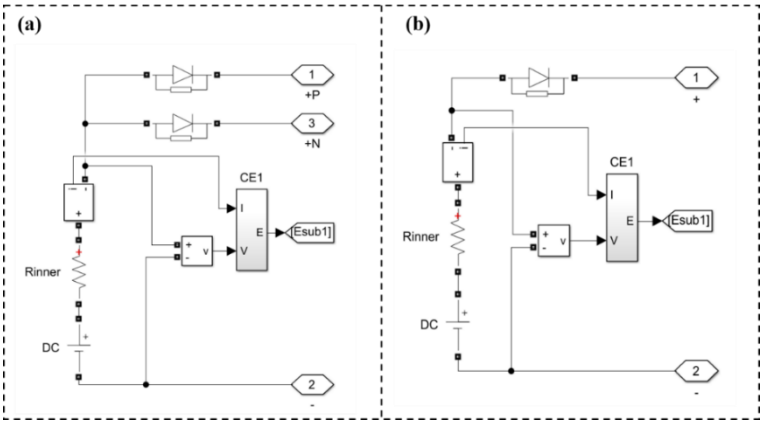

Figure 3-15 The model of the separate OCS substation (a) and common OCS substation (b)

As shown in Figure 3-15, the main components of the substation module are a DC source, a resistor, and a diode, and they are in series. The voltage of the DC source is taken as 750 V, and the series resistance is taken as 0.02 Ω [70, 140]. “CE1” is the unit responsible for the energy calculation. It firstly calculates the energy consumption of the substation based on the input current and voltage data, and subsequently converts the energy result from J to kWh. The calculation is expressed via

$$E = \int IV\,dt \qquad \text{Equation 3-10}$$

where ***E*** is the energy consumption, ***I*** is the current pass through unit, and ***V*** is the voltage across the unit.

3.3.4 Line resistance module

The key feature of the line resistance module is to work out the catenary resistance according to the travelled distance. It is reported that the track resistance is smaller and makes less impact than the catenary resistance [93], and the Supretram internal report considers the catenary resistance only. Therefore, this research only includes the catenary resistance in the modelling and simulation and exploits a variable resistor to mimick the line resistance system. However, as there is no variable resistor unit in the library of the Specialized Technology, the line resistance module has to be built specifically. Commonly, the variable resistor consists of a controllable current source or a controllable voltage source. As this model places the variable resistor in series, but Simulink does not allow controllable current sources in these series connections, a controllable voltage source is chosen. The model of the line resistance module in Simulink is therefore shown in Figure 3-16.

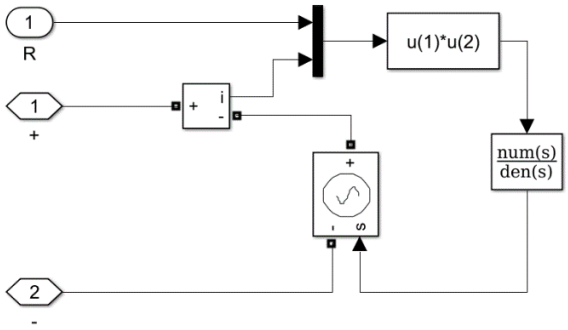

Figure 3-16 The line resistance model

With the resistance set in the model, the voltage of the controllable voltage source is obtained via the function. Ultimately, this module equals the resistance of the catenary resistance at any given simulation timestep.

3.3.5 Tramcar module

The tram is in effect a controlled current source, or sink, on the system as the trams are in effect torque controlled, the driver being ultimately responsible for controlling the speed of the tram. For simplification, the tram system is therefore replaced and represented by a controllable current source. The tramcar model is shown in Figure 3-17.

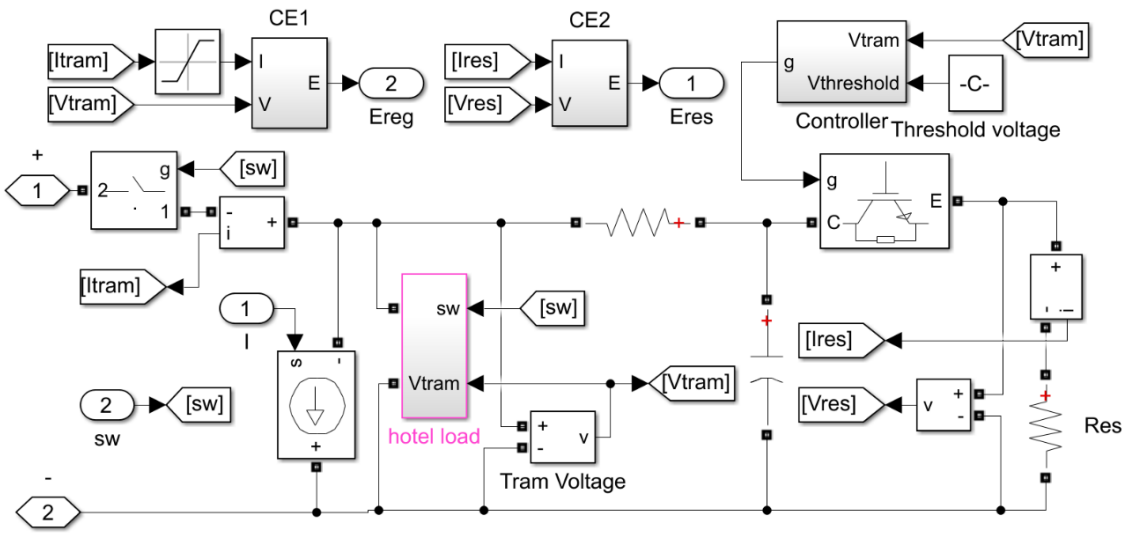

Figure 3-17 The tramcar model

The on-board energy ‘dump’ resistor is to prevent the catenary voltage rising above the line voltage limit while the tram is braking if too much current is returned to the catenary. The on-board dump resistor employs a constant voltage limit approach, using a multiphase IGBT (Insulated Gate Bipolar Transistor) chopper and a dump resistor. As the DC bus voltage (catenary voltage) rises under the braking condition, the conduction ratio of the chopper is adjusted to maintain the voltage below the set maximum limit. Hence, the power dissipated in the dump resistor is controlled. The resistance of the dump resistor is 0.1 Ω, and the upper limit of the catenary voltage is set to 790 V. Additionally, a ‘hotel load’ module, which is used to simulate the hotel load that represents the energy consumption of lighting and heating within the tram, was also added into the tramcar module. The power of the hotel load is 11.5 kW. The power of lighting and the power of heating of the Supertram tramcar is estimated as 5 kW and 13 kW [130], respectively. The lighting stays on all year round, but the heating is provided only 50% of the time during the year. Hence, the power of the hotel load is considered as 11.5 kW throughout the year.

The blocks “CE1” and “CE2” are energy calculation modules. One measures the current from the tramcar to the traction catenary together with the voltage across the tramcar, calculating the regenerative braking energy fed from the tramcar back to the traction catenary. The other is supplied with the current and the voltage across the energy “dump” resistor, they can calculate the resistive braking energy that is wasted in the dump resistor.

3.4 Energy balance on tram system

In order to investigate the energy use within the tram system, this research investigates the energy balance of three aspects of the system:

- Energy supplied to the traction catenary from substation (E_{sub})
- Energy dissipated on resistor through resistive braking (E_{res}), and
- Energy recovered by other tramcars through regenerative braking (E_{reg})

Prior to presenting the result of the simulated energy balance, here we firstly validate the simulated result with the data provided in Supertram's internal report.

3.4.1 Result verification

The Supertram's internal report shows the maximum power (occurred during the operation) of some substations with different OCS set up. Using the substation in Gleadless Townend as a demonstrating example, the maximum power was estimated as 494 kW for a separate OCS and 483 kW for a common OCS, respectively [129]. Our research then simulated a power profile of the substation and shows the profile of a random 3,000s of tram journey in Figure 3-18.

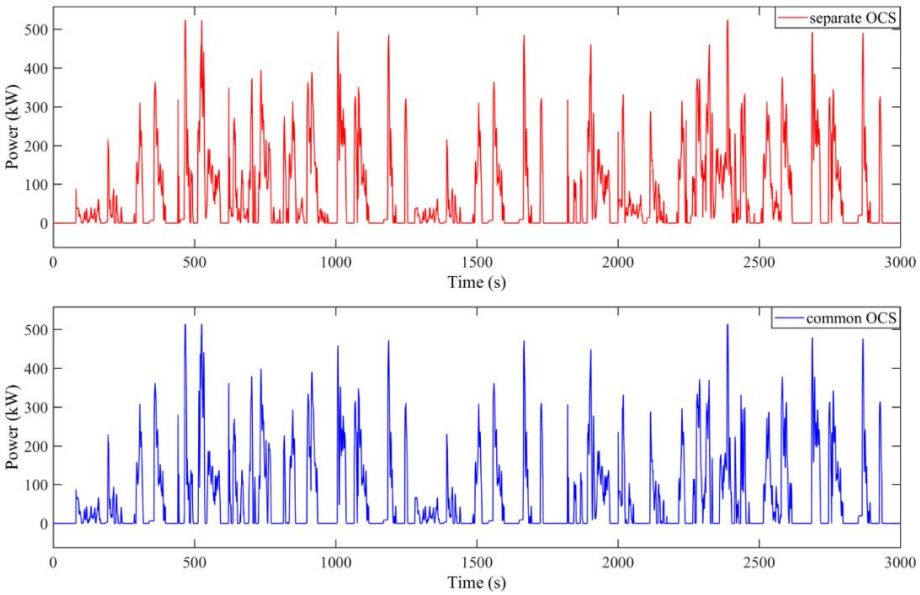

Figure 3-18 The power profile of the Gleadless Townend substation

As can be seen in Figure 3-18, the maximum power of the Gleadless Townend substation simulated in this research was

- 525 kW for a separate OCS, which is only 6.3% higher than the 494 kW estimated in Supertram's internal report, and

- 510 kW for a common OCS, which is only 5.6% higher than the 483 kW estimated in Supertram's internal report

Since the difference between results obtained in this study and shown in Supertram's internal report is less than 10%, the simulated results obtained are considered in alignment with the data presented in Supertram's internal report. Thus, the model used and the simulation conducted in this research is considered reliable.

3.4.2 Energy balance of separate system

For the separate OCS, 6 sets of energy balance data were calculated based on the six sets of tram operational data. From these, the mean value of the six energy balances is calculated. The mean simulated E_{sub}, E_{res} and E_{reg} of the separate OCS were 34,394 ± 401 kWh/day; 17,789 ± 410 kWh/day; and 1,832 ± 198 kWh/day, respectively. Details of the E_{sub}, E_{res} and E_{reg} values simulated based on different sets of data and the mean values are shown in Figure 3-19. The following discussion of the energy balance of the separate OCS (in the current Section 3.4.2) are based on these mean values.

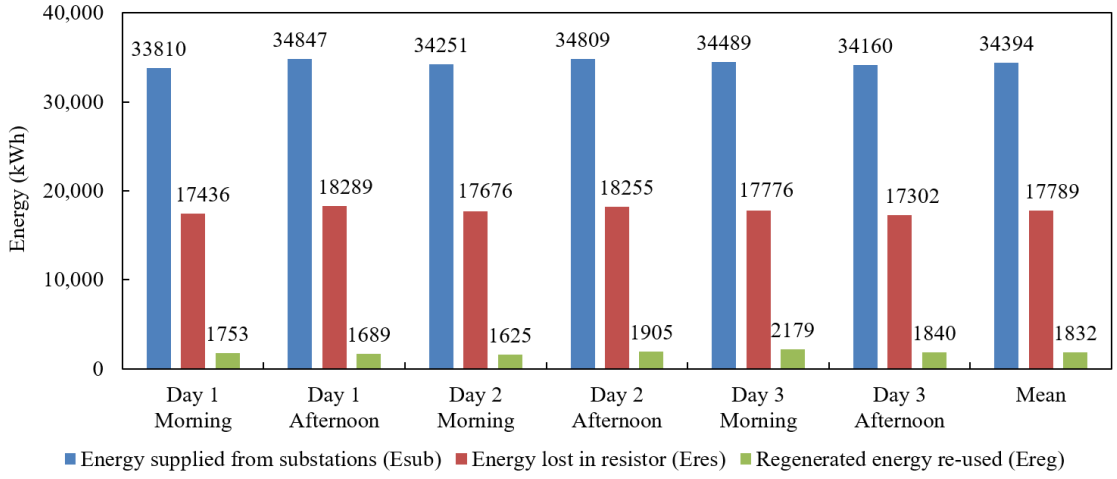

Figure 3-19 Energy balance of the separate OCS

Based on the journey data collected on different dates and times, the energy trends appear to show little variation with traffic conditions and passenger numbers, as the passenger numbers and traffic conditions will not be the same for each journey. Typically, the morning data samples were taken close to the 'rush hour' period, and the afternoon samples were under lighter traffic and passenger number conditions. Thus, the energy supplied from the substations are within ±2% of the average across the six sampled journey sets. This approach to the daily energy

utilization calculations of the separate OCS appears to be an acceptable approximation, based on the consistency of the results shown.

From the data it is possible to see that the mean total traction energy, which was supplied by both the substation and the regenerative braking energy (E_{sub}+E_{reg}), was approx. 36,226 kWh/day. Meanwhile, the mean braking energy, the energy gained from the braking of the tram (E_{res} + E_{reg}) was approx. 19,621 kWh/day. The braking energy was equivalent to approximately 54.2% of the traction energy. However, only 9.3% of the braking energy was recovered for traction as E_{reg}, and the rest 90.7% was lost in the dump resistors as E_{res}. The E_{reg} was equivalent to 5.1% of the total traction energy and 5.3% of the E_{sub}, and the E_{res} was equivalent to 49.1% of the total traction energy and 51.7% of the E_{sub}. This suggests that, in a separate OCS, most of the braking energy is wasted, and the successful recovery of this energy, for re-use, could theoretically save up to half of the total energy consumption.

3.4.3 Energy balance of common system

Six energy balance totals for the common OCS were also simulated, based on the six sets of tram operational data, for comparison with the separate OCS calculations done previously. Similarly, the calculated mean values of the six energy balances were produced. The mean simulated E_{sub}, E_{res} and E_{reg} of the common OCS were 29,517 ± 342 kWh/day; 12,921 ± 272 kWh/day; and 7,271 ± 212 kWh/day, respectively. Details of the simulated E_{sub}, E_{res} and E_{reg} based on the different sets of data and the mean values are shown in Figure 3-20.

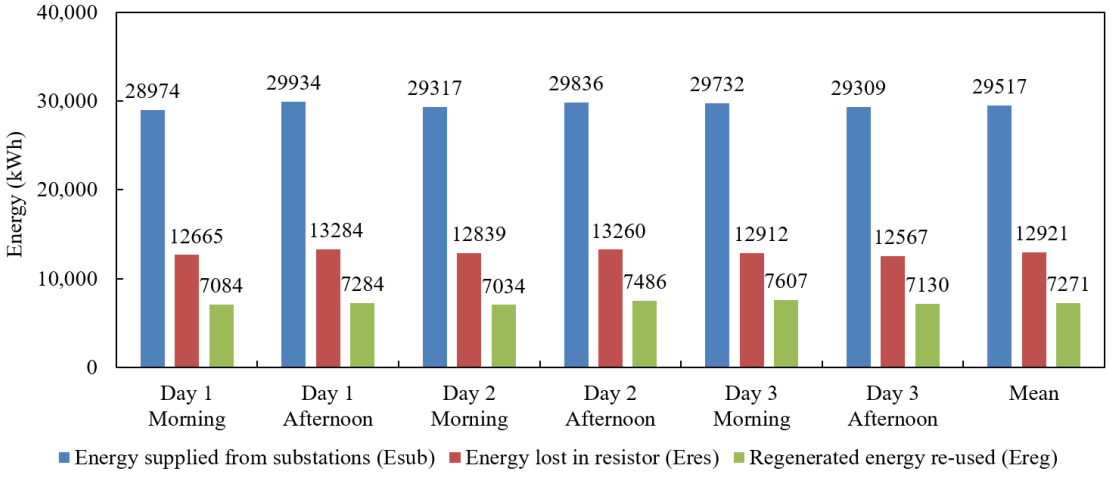

Figure 3-20 Energy balance of common system

Similar to the separate OCS, the simulated results of the common OCS showed a good consistency, with only a less than 3% variation between results obtained from the different data

sets, regardless the variation of traffic conditions and passenger numbers of the different sampled journeys. Therefore, this approach to the daily energy utilization calculations of the common OCS appears to be an acceptable approximation.

In the common OCS, the mean braking energy (E_{res}+E_{reg}) was 20,192 kWh/day and was equivalent to 54.9% of the mean total traction energy (E_{sub}+E_{reg}) as 36,788 kWh/day. Here though, 36.0% of the total braking energy was reused as E_{reg}, and the rest was wasted on the dump resistor. Compared to the separate OCS, this is a much better use of braking energy, being recycled into another tram. The E_{reg} was equivalent to 19.8% of the total traction energy and 24.6% of the E_{sub}, and the E_{res} was equivalent to 35.1% of the total traction energy and 43.8% of the E_{sub}. Similar to the separate OCS, a successful recovery of this wasted energy could theoretically save up to nearly half of the total system energy consumption.

3.4.4 Comparison between the separate system and common system

The data shown in Figure 3-19 and Figure 3-20 suggest that:

1) The total traction energy, which is the sum of the E_{sub} and E_{reg}, and the braking energy, which is the sum of E_{res} and E_{reg}, were similar in separate OCS and common OCS.
2) However, compared to the separate OCS, the common OCS has a higher proportion of braking energy recovered for tram traction and thereby has a higher proportion of traction energy that comes from the regenerative braking energy.
3) The energy from the substations, E_{sub}, for the common OCS is therefore consistently smaller than the E_{sub} of the separate OCS. The mean E_{sub} of the common OCS is also approximately 14% smaller than the mean E_{Sub} of the separate OCS.
4) The wasted energy in the dump resistors, E_{res}, of the common OCS is consistently smaller than the E_{res} of the separate OCS. The mean E_{res} of the common OCS is about 27% smaller than the mean E_{res} of the separate OCS.
5) The energy re-used by another tram in the track section, E_{reg}, of the common OCS is consistently greater than the E_{res} of the separate OCS. The E_{reg} of the common OCS is approximately 297% greater than the mean E_{reg} of the separate OCS.

As mentioned in Section 3.1.2, the separate OCS prevents the energy transferring between the tramcars travelling on the uplink and the downlink, within the same energy supply section, but the common OCS allows it. In the common OCS, more tramcars are therefore able to access

and utilize the braking energy produced, and this leads to a greater value of E_{reg}. A greater E_{reg} then resulted in less energy being required from the substations and thereby a smaller E_{sub}. Additionally, a greater value of re-used energy, E_{reg} also reduces the braking energy to the dump resistors, and hence results in a smaller $E_{res.}$ Hence, the common OCS is considered more energy efficient than the separate OCS.

From the mean results presented in Section 3.4.2 and Section 3.4.3, the energy from the substations, E_{sub} of the common OCS is 34,394-29,517=4,877 kWh/day less than the E_{sub} of the separate OCS, and the re-used braking energy, E_{reg} of common OCS is 7,271-1,832=5,439 kWh/day greater than that of the separate OCS. This suggests that the reduction of the substation energy supply, $E_{sub,}$ can be completely compensated for by the increase in re-use of the braking energy, E_{reg}. Although the increase of the E_{reg} is similar to the reduction of the E_{sub}, the former is still about 12% greater than the latter. This indicates part of additional E_{reg} was potentially lost in the catenary resistance during its transmission to another tramcar.

From the result shown in sections 3.4.2 and 3.4.3, the braking energy, being the sum of E_{reg} and $E_{res,}$ for the two systems were found similar, but the common OCS is slightly higher than the separate OCS. As shown in Figure 3-17, any braking energy generated could also be consumed by the hotel load on the tramcar in addition to the dissipation in the dump resistor. Therefore, some degree of self-consumption will take place for the regenerated braking energy. The largest difference between the common OCS and separate OCS is that the former has more braking energy flow to the catenary and less braking energy flow to the resistor than the latter.

Although a common OCS is found more energy efficient than a separate OCS, the resistive 'dumped' energy, $E_{res,}$ of both systems are still equivalent to about half of their own power supply requirements, E_{sub}. This indicates that there is an enormous unrecovered energy reserve in the tram system, and the successful recovery of this could lead to a great benefit on the energy-saving and potential cost-saving for the tram system operation.

3.4.5 Comparison between Sheffield Supertram with other light rails

The Sheffield Supertram is considered as a typical urban light rail system, and hence, it is worthwhile to compare its energy balance with the other urban light rail systems' for validation. This research studied the Supertram's energy balance based on two different OCSs, and the

total traction energy required and the braking energy produced were found similar in the two different OCSs. Thus, the comparison between the Supertram and other systems primarily focuses on the braking energy to traction energy ratio. Moreover, this research also discovered that applying different OCSs would lead to a different recovery and wastage of braking energy. Although the existing literature barely stated what OCS was used in the urban light rail system studied, this research still included the ratio of the regenerative braking energy to the total braking energy as a comparison parameter.

The energetic performance of an urban light rail system is affected by various factors, such as the timetable, system configuration, and the local traffic condition, etc. and is thereby case specific. Still, the ratio of the braking energy to traction energy of the five light rail systems listed in Table 2-1 ranges between a relatively narrow band of 31% to 68%. In this research, the ratios of both the separate OCS and common OCS studied were at approx. 54%, which is in good agreement with the one of the other systems. Regarding the proportion of regenerative braking energy in the total braking energy, the literature suggested it could range from 18% to 69% (as shown in Table 2-1). In this research, the proportions discovered for the separate OCS and the common OCS were 9.3% and 36.0%, respectively. Thus, the one of the common OCS is in good agreement with the reported findings, but the one of the separate OCS was substantially lower than the reported range. Such a phenomenon could be still valid since the recovery of braking energy could be impacted by various case specific factor; for instance, the reported system would use the common OCS, which has been found more efficient in braking energy recovery than the separate OCS. Still, there is not enough available information to comprehensively discuss the cause of the lower proportion of regenerative braking energy in the total braking energy, however the similarities in results are encouraging.

3.5 Chapter summary

This chapter has applied Matlab modelling and simulation to study the daily energy balance of an urban light-rail system, Supertram in Sheffield. This research successfully collected six sets of tram operational data including speed, distance and acceleration. With the aid of Matlab and Matlab Simulink, models were built for processing the operational data into the force data and for simulating the energy balance based on the processed data. It is worth noting that the models used for the energy balance simulation consist of modules that mimick the operation of critical

components of the Supertram system, i.e. the substations, power supply catenary, and tramcars, etc..

The daily energy balance of a separate OCS and a common OCS were simulated based on six sets of operational data collected from mornings and afternoons on three weekdays. In both cases, the daily energy balances simulated based on different data set shows a good consistency. In detail,

- the mean simulated E_{sub}, E_{res} and E_{reg} of the separate OCS were 34,394 ± 401 kWh/day; 17,789 ± 410 kWh/day; and 1,832±198 kWh/day, respectively, and
- the mean simulated E_{sub}, E_{res} and E_{reg} of the common OCS were 29,517 ± 342 kWh/day; 12,921 ± 272 kWh/day; and 7,271 ± 212 kWh/day, respectively.

In both cases, the amount of braking energy simulated are similar, but the composition varies. In the separate OCS, greater than 90% of the braking energy was dissipated in the dump resistors and the rest was recovered through re-use. Since the common OCS allows more opportunities for tramcars to access and utilize the braking energy, the percentage of braking energy dissipated in the dump resistors was reduced to 64% for this system, and the energy recovered through re-use was increased by approximately 297%. Consequently, the common OCS required approximately 14 % less energy from the substation. In both cases, the braking energy dissipated in the dump resistors was equivalent to nearly half of the energy supplied from the substation. Successful recovery of this energy is crucial to increasing the energy efficiency of the tram network.

Chapter 4. Application of energy storage for a tram system

Having modelled the energy usage trends in a tram network in the previous chapter, the energy consumption results for the tram system indicate that during operation, the tram service suffers a huge braking energy loss, regardless of whichever energy supply method is used. In this chapter the use of a trackside energy storage system (ESS) on the tram network is investigated [71, 77, 94, 96, 98, 100, 121, 141], and it is shown that this trackside storage system is able to recover and reuse some of the braking energy lost on the tram system. The ESS can firstly recover the surplus braking energy in the tram system to reduce the energy dissipated in the tram dump resistors. Additionally, when the tram system requires traction energy, the ESS can provide the braking energy recovered back to the tram via the catenary, reducing the energy supplied from the substations.

Before applying the ESS onto the tram system model, the ESS has to be well designed to fit the purpose and the expected working condition. When an ESS is applied to the tram network, its configuration and installation location are expected to affect the energy balance of the tram network, the performance on energy saving, and the economic feasibility of its implementation. Through the observation of different related phenomena obtained via simulation, an optimal installation solution has been suggested in this chapter.

In real-world applications, both the separate OCS and common OCS are used in the energy supply of urban light-rail systems. Aiming to understand the application of ESS on most light-rail systems, this research now investigates the energy-saving performance of the ESS under both energy supply methods. Hence, this chapter includes:

- Section 4.1 - introduces the structure and composition of the proposed ESS, i.e. the components of the ESS, the operating mechanism and control mechanism, and finally the simulation model of the ESS.
- Section 4.2 - describes how the ESS model is added to the existing tram network with a separate OCS installation, examines the influence of the ESS performance on energy saving, and the possible energy saving delivered through network wide installation
- Section 4.3 - describes how the ESS is added to the existing tram network with a common OCS installation, examines the energy saving performance of different locations for a single ESS installation, and the energy saving delivered by multiple or a network wide installation.

- Section 4.4 - presents the economic feasibility of adding multiple ESS's onto the network, together with a sensitivity study of the most influential factors for the economic evaluation, and the potential merit of using parked EVs as some or all of the ESS
- Section 4.5 - provides a summary of the chapter.

4.1 Energy storage system structure and simulation

In this research, the study on the ESS focuses on optimally applying it to the tram system, for example, determining the best installation location, and the most suitable configuration that can lead to optimal energy-saving and economic feasibility. The research also aims to develop an innovative ESS structure or control mechanism. Thus, to start with, the ESS structure and control mechanism used in this research is initially adapted from published work [126, 142-146].

4.1.1 Design principles of energy storage systems

The ESS design aims to achieve an energy exchange between the ESS and the tram system. Additionally, the design should also make sure the catenary voltage remains stable after the ESS is connected. Hence, the ESS consists of two key components, a DC-DC converter and an energy storage element. The DC-DC converter connects the energy storage element and the tram system. It is responsible for controlling the charging and discharging of the energy storage element and stabilizing the catenary voltage, by presenting a controlled voltage to the catenary whilst allowing the voltage of the ESS to vary with state of charge (SoC).

As previously mentioned, the final aim of the work is to investigate the use of an ESS which may be composed of a single, or number of, EV batteries. Therefore a battery unit is used as the energy storage element of the initial trackside ESS, as opposed to employing other technologies such as flywheels for example. In this way the characteristics of the intial system and the final envisaged system are not too dissimilar. Considering the topology of the DC-DC converter, it should allow bi-directional energy exchange from the tram to the ESS and vice-versa, and there is likely to be a difference between the tram catenary voltage and the voltage across the energy storage element. To this end, the DC-DC converter should be able to operate in Buck mode and Boost mode. The circuit of a suitable DC-DC converter is shown in Figure 4-1.

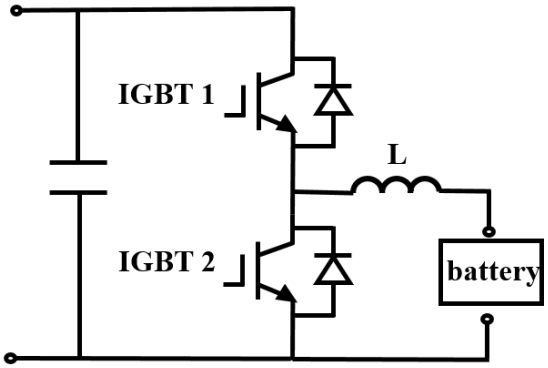

Figure 4-1 The circuit of the DC-DC converter in the ESS

Based on the circuit shown in Figure 4-1, there are three working conditions for the converter, and they fulfill the needs of different operational states of the tram operation. The converter operates through the complementary switching action of the two IGBTs (insulated-gate bipolar transistors), under control of a pulse width modulation (PWM) duty cycle, to achieve the energy flow required.

1) When the tram system has a surplus of braking energy, the catenary voltage rises. The converter will work in Buck mode. Consequently, the braking energy from the tram system will flow into the battery unit, and the battery unit gets charged.
2) When the tram system requires energy for tramcar traction, the converter will work in Boost mode, consequently, the energy will flow from the battery unit to the tram system, and the battery unit gets discharged.
3) When the tram system is stationary, or no tram car is within the supply section, there is no surplus braking energy and no requirement for an energy supply. The converter therefore operates in standby, matching the battery voltage to that of the catenary without transferring energy.

To allow the converter to respond promptly to the different operational status of the tram system, the switching elements of the converter need to be well controlled. In fact, the catenary voltage is a suitable control variable as it can reflect the operational status of the tram system. Since the catenary voltage is chosen as the control variable, but the converter itself employs an inner current control loop for the current in inductor L, this research used a double-closed loop control strategy with a voltage outer loop and an inner current loop. The control strategy is illustrated in Figure 4-2. Figure 4-2 (a) shows the schematic of the connection of the ESS to the tram system, and Figure 4-2 (b) demonstrates the control strategy. In Figure 4-2 (a), the

voltage across the ESS is named U_{dc}, and the current flowing into or out of the battery is named I_L. The control unit will provide two signals, which will be given to the DC-DC converter.

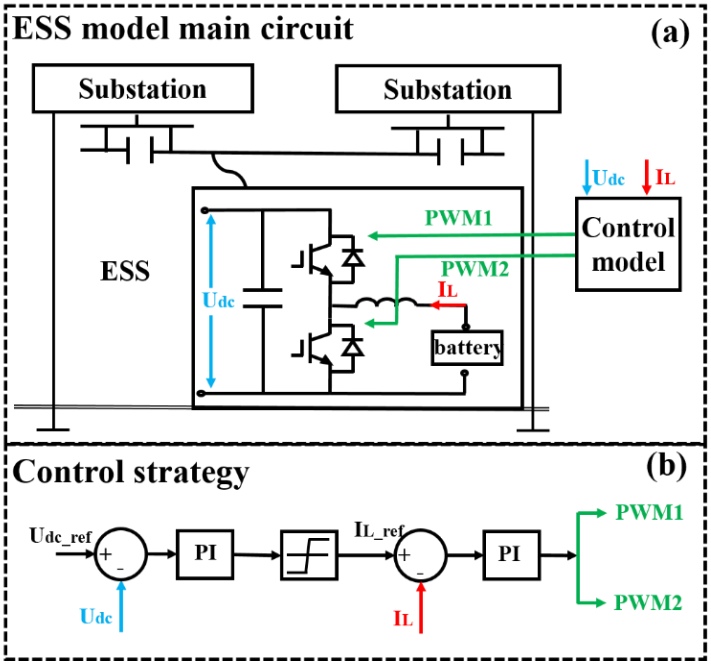

Figure 4-2 The schematic of ESS's double-closed loop control

As shown in Figure 4-2 (b), both U_{dc} and I_L are collected from the ESS module's main circuit. U_{dc_ref} is the reference voltage set for the control strategy. The process of the control can be described as:

1) The U_{dc_ref} will be compared with the U_{dc} to obtain the "voltage error".
2) The PI regulator and the Limiter will process the "voltage error" to get the current reference, I_{L_ref}. It is worth noting that the Limiter limits the maximum charging and discharging current for protection of the ESS battery.
3) The I_{L_ref} will be compared with I_L to obtain the "current error".
4) Another PI regulator will process the "current error" to form the complimentary PWM signals.

Thus, since the catenary voltage at the ESS connection point (U_{dc}) varies, the duty cycle of the converter in the ESS will be adjusted simultaneously, and the current flows into or out of the ESS will therefore change. Such a control strategy can not only stabilize the tram catenary voltage but also charge and discharge the ESS in time, according to the operational status of the catenary / tram system.

4.1.2 Overview of Energy Storage System Model

Based on the structural design described in Section 4.1.1, an ESS model was built in Matlab Simulink and was added to the tram network model, as shown in Figure 4-3. The ESS model includes the control module (blue dashed box), the converter module (green dashed box), and the battery module (red dashed box). It is worth noting that the tram system has an uplink power supply and a downlink power supply. Therefore, the converter module has two converters to serve each power supply line individually in the case of a separate OCS.

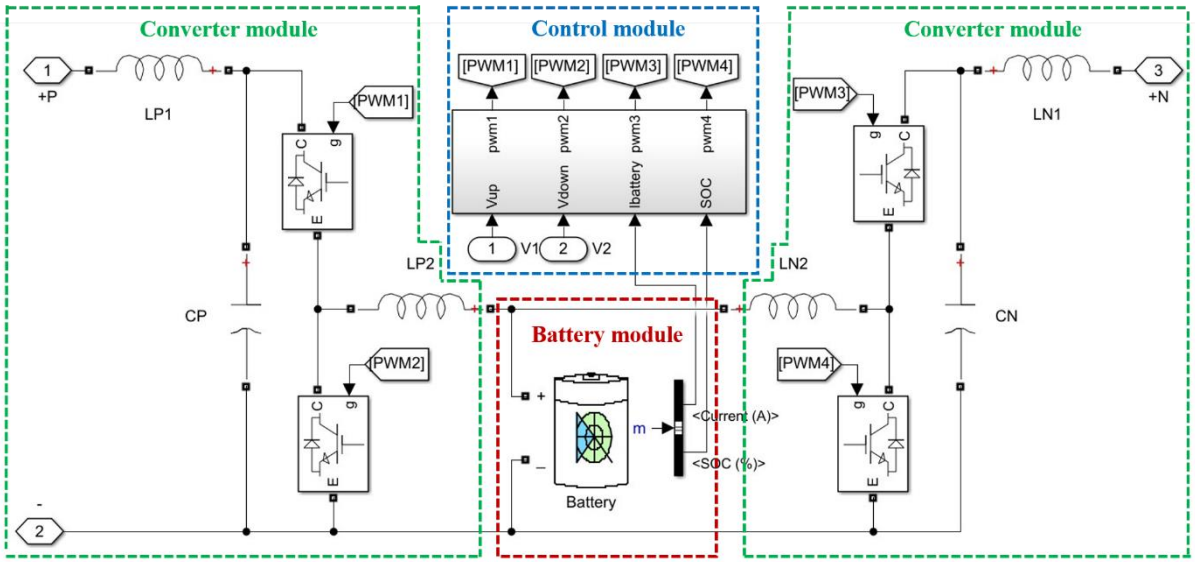

Figure 4-3 The model of the ESS in Simulink

The energy storage unit used in the ESS model is the battery block from the Simulink library. The nominal voltage of the EV battery ranges from 350-400V [47, 147, 148]. To mimic the characteristics of a typical EV battery, the nominal voltage of the battery block was set as 390V. For the converter module, both the converters are identical, and each has two IGBT blocks to receive the PWM signal generated from the control module. Additionally, each converter includes a filter that sits close to the connection point to the tram system. The structure of the control module is shown in Figure 4-4. Both converters are controlled in the same way and use the catenary voltage as the control variable to control the charging and discharging of the battery (as mentioned in Section 4.1.1). The braking energy will flow to and charge the ESS when the catenary voltage exceeds charging threshold voltage (CTV), and the ESS will discharge and supply energy to the tram network when the catenary voltage drops below discharging threshold voltage (DTV). The set thresholds for this operation will be considered later in section 4.1.3.

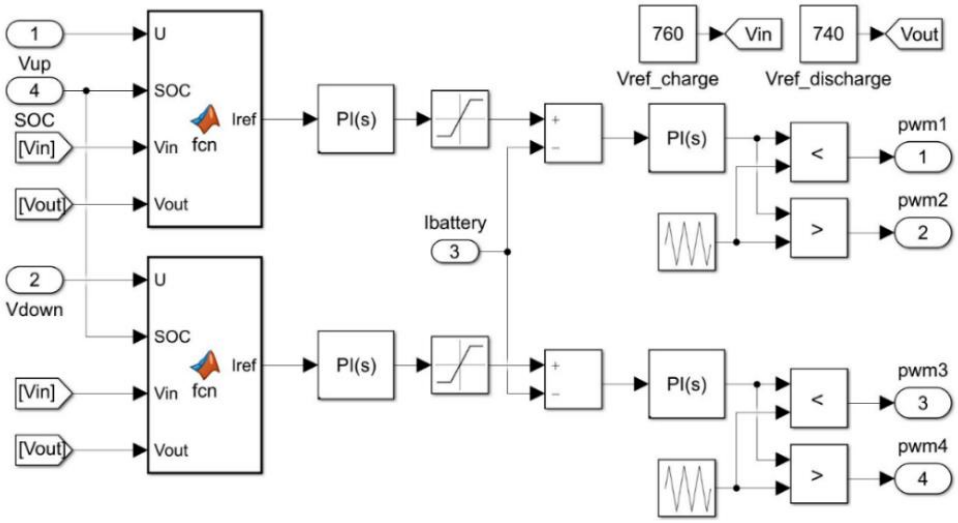

Figure 4-4 The model of the control module inside the ESS

The ESS model described in the sub-section can be configurated with different parameters, such as different battery capacity and different battery discharge limit rates. The following studies related to the ESS exploited this model to investigate how the ESS installation and the ESS configuration impact the energy balance of the tram system.

4.1.3 The charging and discharging threshold

The determination of the CTV and DTV requires a good understanding of the impact of CTV and DTV on the charging and discharging of the ESS. Hence, this research firstly selected a battery with a suitable configuration and used it to study how the different CTV and DTV influence the charging and discharging of the ESS.

In chapter 3, the energy balance of the tram system was simulated, showing that the maximum current drawn by the tram was less than 1,300A at peak traction force. For example, using the tram journey from Halfway to Gleadless Townend for illustration (as shown in Figure 4-5), the traction current remains within 1,000A for the majority of the journey, rarely going above 1,000A or reaching the maximum value of 1,300A. Given the nature of the converters within the ESS model, the maximum practical current likely to be seen by the battery is therefore limited to around 2,000A, given the approximate ratio of the converter being the ratio of the nominal system operating voltage and battery voltage (~2 in this case).

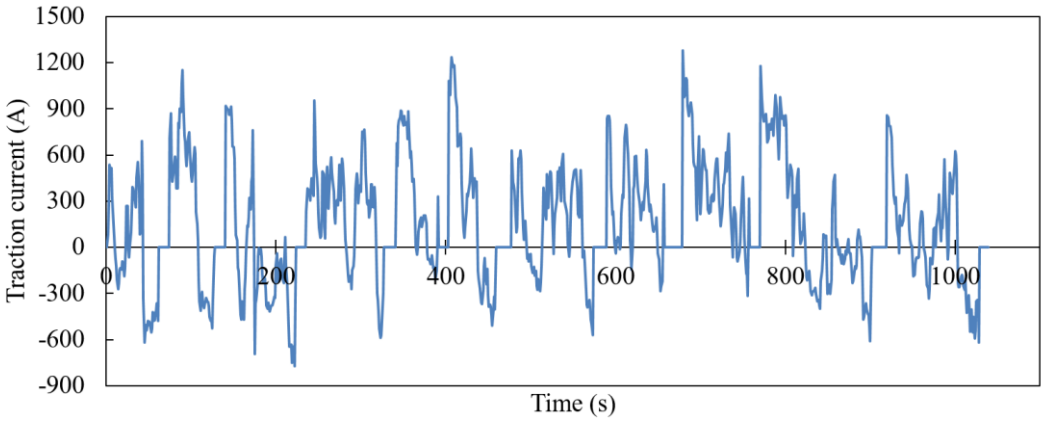

Figure 4-5 The profile of traction current of tram journey from Halfway to Gleadless Townend

This allows the ESS selection to be based on the current rating of the batteries chosen. Normally, a battery operating current can be quoted in terms of its capacity. For example, a 100Ah battery can be expected to supply 100A for 1 hour, termed the 'C' rate, and 100A drawn from the example battery is referred to as 1C. Similarly, if 50A is drawn from the battery, it should supply the current for 2 hours, termed 0.5C or C/2. 200A is similarly termed the 2C rate for the example battery. This then allows comparison between the operating characteristics of battery packs. Normally, lithium-based batteries are limited to a maximum rate of 2C to prevent damage to the cells in the battery packs, or reduced operating lifetime.

As the maximum current seen by the battery is 2,000A, this research intends to limit the battery current to 2C, the initial study was carried out with a 1,000Ah battery pack, with an initial state of charge (SoC) of 50%. The ESS that is equipped with the aforementioned battery was therefore added into the model at the centre stop of a tram section between Halfway and Crystal Peaks on the Blue route.

As mentioned above, the CTV must be greater than the nominal catenary voltage of 750V and must be lower than the upper limit catenary voltage of 790V. Meanwhile, the DTV must be smaller than 750V. There should be a reasonable gap between CTV and DTV to provide room between the charging and discharging in order to ensure the energy supply system operates stably and to give noise immunity. This research chose 760V as the baseline CTV and 740V as the baseline DTV. The DTV was fixed at its baseline level when studying the charging state, and the CTV was set as 760V, 770V, and 780V, respectively. Similarly, the CTV was fixed at its baseline level when examining the discharging state, and the DTV was set as 740V, 730V, and 720V, respectively. A simulation, which was based on a single tram journey from Halfway

to Crystal Peaks, was conducted to understand the current of the battery with different CTVs and DTVs. Results are shown in Figure 4-6.

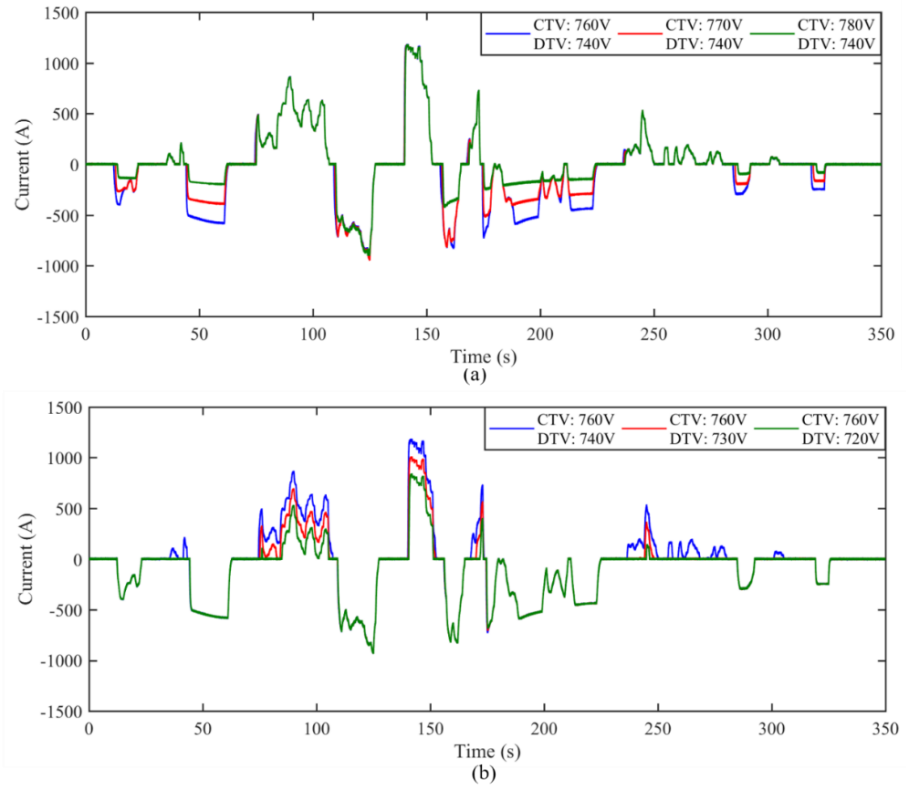

Figure 4-6 The battery current simulated based on different CTVs and DTVs

In Figure 4-6, the positive current shown demonstrates that the energy flows from the battery to the tram system, and vice versa. As can be seen in Figure 4-6 (a), the DTV stays at 740V, and the CTV varies from 760V to 780V. The three simulated cases thereby have the same discharging current, but exploiting higher CTV results in a smaller charging current, leading to lower braking energy absorption. Figure 4-6 (b) shows that the CTV stays at 760V, and the DTV changes from 720V to 740V. The same charging current is found in three cases, but using a higher DTV results in a higher discharging current, leading to more energy exported to the tram system. Thus, the simulation results suggest that the battery will have a better ability to charge and discharge when both the CTV and DTV get closer to the 750V. Given this research aims to used the ESS to absorb as much as the braking energy from the tram and later return the energy back for the tram traction, this research chose 760V as the CTV and 740V as the DTV for the subsequent ESS study in this chapter. It is also interesting to note that control of the CTV and DTV will allow control of the SoC of the ESS if required, with a subsequent affect on the amount of energy which can be captured in the ESS.

4.2 Application of energy storage in the separate overhead catenary system

This section focuses on adding the ESS subsystem onto the tram system having a separate OCS arangement. It firstly introduces how the ESS is included into the tram network model. Subsequently, it investigates the influential factors of the ESS performance if an ESS was installed in an individual energy supply section. Finally, it examines the impact of network wide ESS additions on the energy balance of the tram system and the potential energy savings delivered. It is worth noting that the content presented in this section has been published in Zhang, et al. [149].

4.2.1 Model of the power supply section with ESS installed

In this project, the application of an ESS onto the tram system, two possible scenarios were considered. The first with the ESS added into a single individual energy supply section, the second with ESSs added into all the energy supply sections to explore the network wide advantages of ESS deployment. An example Simulink model of a energy supply section that has an ESS added is shown in Figure 4-7.

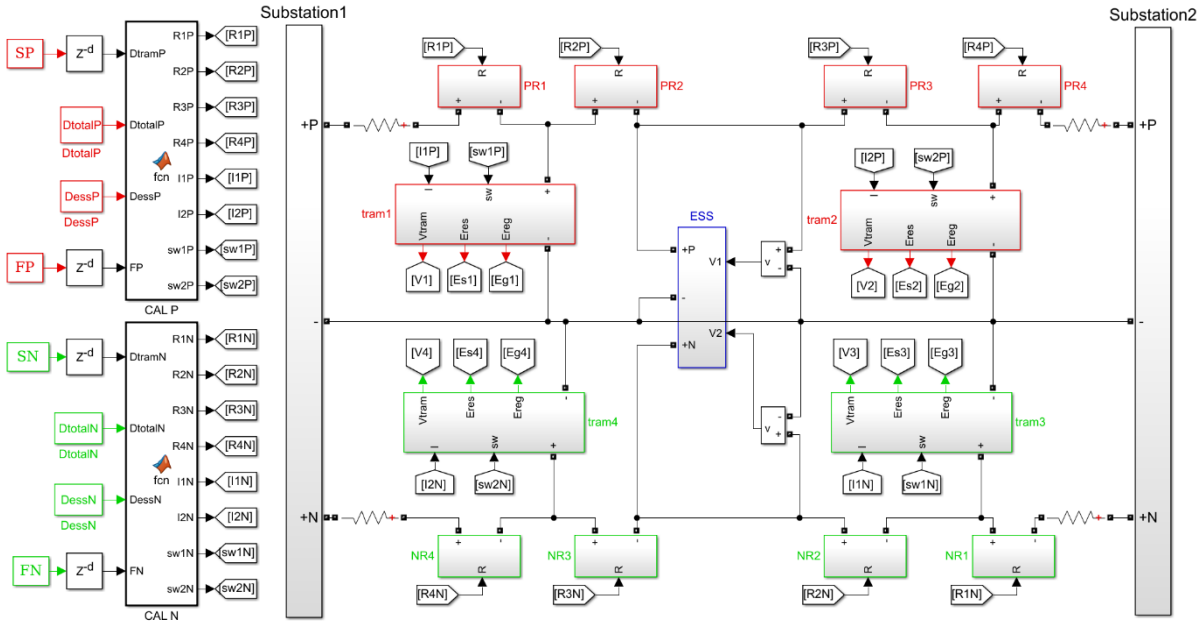

Figure 4-7 Simulink model illustrating a section of the tram network model Model of ESS installation on an energy supply section with separate OCS setup

As can be seen in the figure, the model has more or less the same modules as the base case tram network model (shown in section 3.3), but does include an extra ESS module. In the model, the 'CAL P' and 'CAL N' blocks are the main calculation modules; 'Substation1' and

'Substation2' represent the substations;'tram1' to 'tram4' are the tram modules; 'PR1' to 'PR4' and 'NR1' to 'NR4' are the line resistance modules respectively; and 'ESS' is the energy storage module for this section.

4.2.2 Factors affecting the ESS performance

This thesis firstly studies the impact of the ESS position on performance. The simulation was repeated with an ESS added at every stop in an energy supply section in turn, and subsequently examines the impact of its position on the energy balance of the system. Similar to the study presented in section 4.1.3, the same single journey from Halfway to Crystal Peaks on the Blue route was again chosen. A 1,000Ah ESS with a CTV of 760V and a DTV of 740V was placed at each stop in turn. The results of the energy usage per journey simulated are shown in Table 4-1 and Figure 4-8.

Table 4-1 Energy usage for a single journey from Halfway to Crystal Peaks with 6 scenarios for ESS placement

Location of ESS	Scenario Number	Energy drawn from Halfway substation (kWh)	Energy lost in tram braking resistor (kWh)	Energy drawn from Crystal Peaks substation (kWh)	Total energy from substations (kWh)
without ESS	1	7.457	7.954	6.997	14.454
Halfway	2	6.921	3.375	6.969	13.89
Westfield	3	4.759	2.451	6.146	10.905
Waterthorpe	4	5.142	1.975	5.456	10.598
Beighton	5	6.413	2.157	4.783	11.196
Crystal Peaks	6	7.448	3.914	6.775	14.223

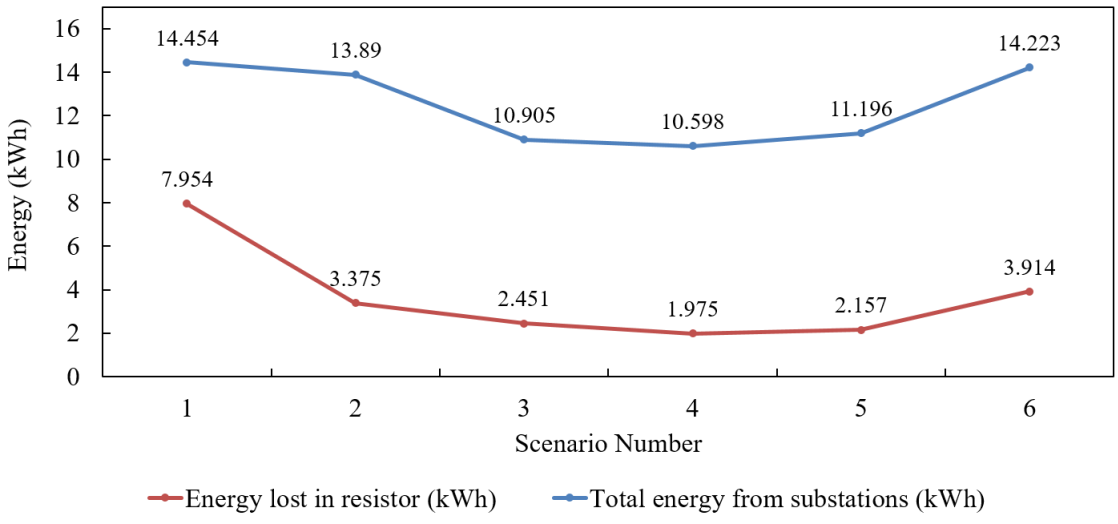

Figure 4-8 Energy use for a single journey from Halfway to Crystal Peaks with 6 scenarios for the ESS placement

From Figure 4-8 and Table 4-1, it can be seen that the least energy is drawn from the utility supply for the single journey shown as Scenario 4, with the ESS being placed at the 'Waterthorpe' tram stop (location 4), which is between the two substations on this track section.

Initially, the ESS placement was constrained to tram stop locations, as these would allow easy track access and could be possible places for EV parking in future study scenarios. In the best scenario, the energy lost in the braking resistors is reduced from 7.954kWh to 1.975kWh per journey, a reduction in loss of approx. 75%. Additionally, the total energy drawn from the utility supply for this single journey is also reduced from 14.454kWh to 10.598kWh, equating to a supply reduction of approx. 27%, due to the re-cycling of the captured energy from tram braking, being used in subsequent accelerations. This therefore points towards the optimum location for an ESS installation, located at existing tram stops, to be as close as possible to the mid-point between any two substations. In this thesis, the tram stop that is located close to the mid-point between any two substations is therefore called the 'centre stop' (of a given energy supply section).

Utilising this ESS position, Table 4-2 shows the effect of using a smaller ESS (200Ah), and applying different current limits to the operation, from 0.5C to 10C, given that the upper value is commensurate with the 1,000Ah, 2C scenario shown above. Whilst this high current rate may not be practical at this time, future developments may not prevent operation at this charge / discharge rate with future battery technologies.

Table 4-2 Energy usage for a single journey from Halfway to Crystal Peaks with maximum current ratings from 0.5C to 10C, for a 200Ah battery at the Waterthorpe tram stop.

Limit discharge rate (C)	Max current (A)	Energy drawn from Halfway substation (kWh)	Energy lost in resistor (kWh)	Energy drawn from Crystal Peaks substation (kWh)	Total energy from substations (kWh)
0.5	100	6.65	5.899	6.451	13.101
1	200	6.306	4.727	6.227	12.533
2	400	5.788	3.091	5.884	11.672
4	800	5.301	1.98	5.561	10.862
10	2000	5.14	1.971	5.454	10.594

Plotting these in Figure 4-9 shows a trend of diminishing returns, with little improvement in energy saving operating the 200Ah battery above 4C. This is anticipated, as it may be seen that the tram current rarely exceeds 4C (800A) while travelling between these substations, as shown by the simulated battery current trace, Figure 4-10.

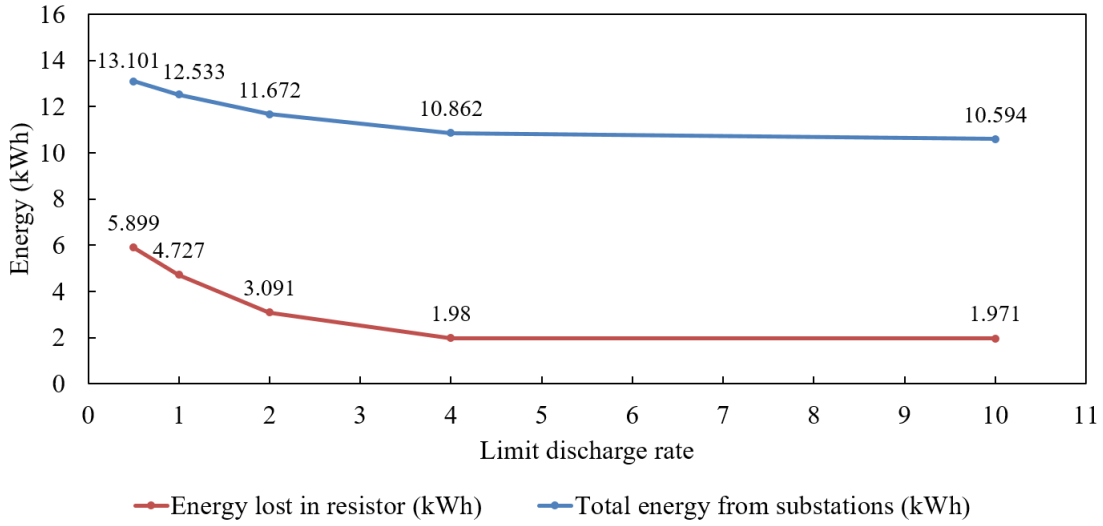

Figure 4-9 Energy use for a single journey from Halfway to Crystal Peaks with 5 current limits for a 200Ah battery at the Waterthorpe tram stop.

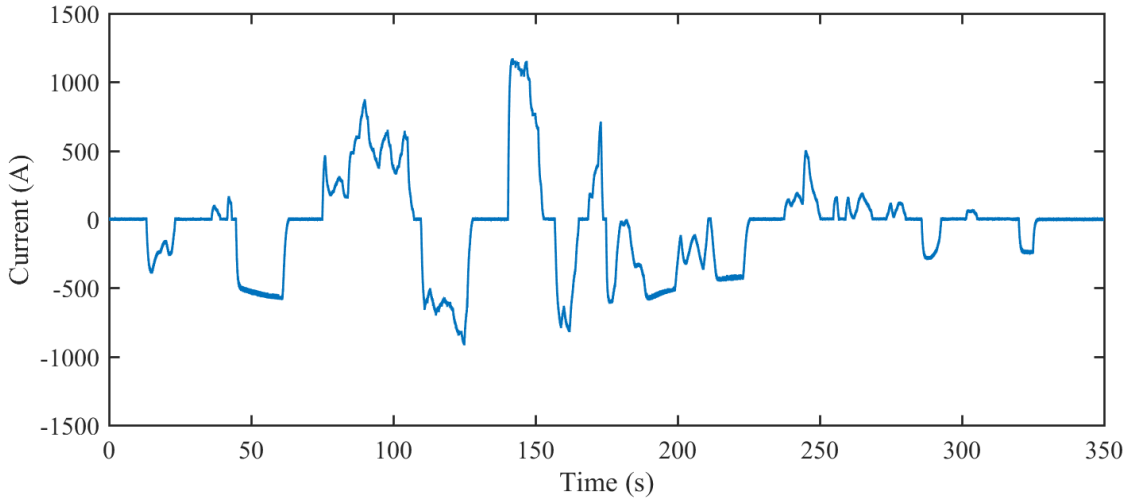

Figure 4-10 Simulated battery current for a single journey from Halfway to Crystal Peaks with a 10C current limit applied to a 200Ah ESS at the Waterthorpe tram stop.

Therefore, the current limit of 4C imposed on the battery is high enough to capture almost all of the energy regenerated from the trams on deceleration and return most of what is available to the tram on acceleration.

4.2.3 Applying the ESS onto the whole network

In order to understand how an ESS can affect the recovery of braking energy on the whole network, 1,000Ah ESSs with a 2C rate limit were added to the network at the 'ideal' locations as discussed previously (i.e. the centre stops), across the whole network, and this results in the overall daily energy trends for the whole network, as shown in Figure 4-11.

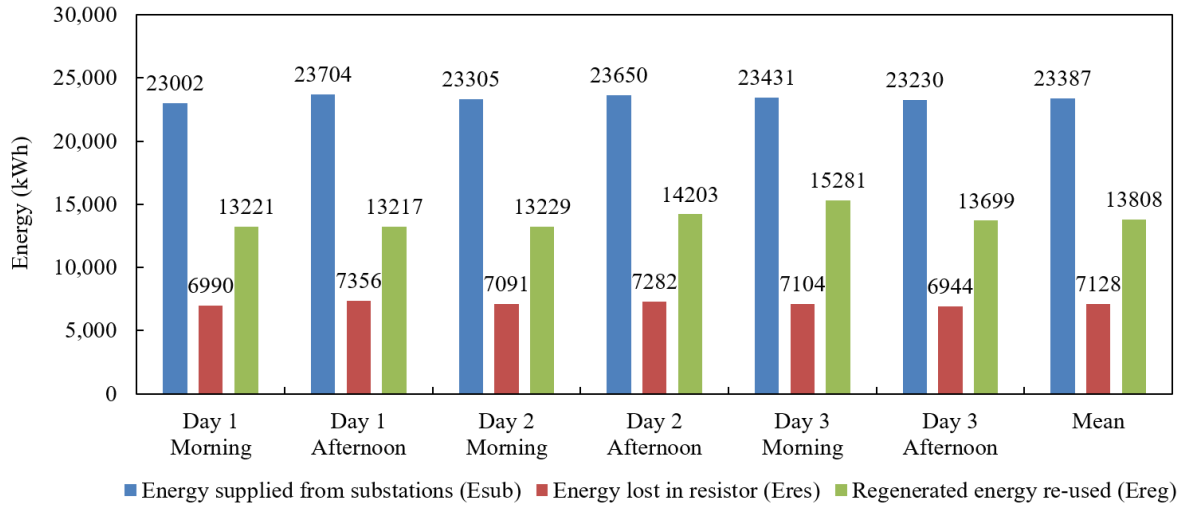

Figure 4-11 Simulated Daily Energy trends with a 1,000Ah ESS installed at ideal tram stop locations on the tram network.

As can be seen in the daily energy balances of the base case tram system (shown in Figure 3-19) compared with Figure 4-11, the addition of the ESS helped to reduce the energy lost in the braking resistors by approx. 60% and increased the regenerated energy re-used by 654%. Consequently, the energy supplied from substation was reduced by approx. 32%. A substantial energy saving of 11,007 kWh/day was delivered across the network, which equates to an annual CO_2 emission saving of 928 tonnes equivalent, as the direct emission of grid electricity is 0.231 kg CO_2/kWh [150].

However, as mentioned in Section 4.2.2, the maximum current drawn by the tram rarely exceeds 1,300A. Besides, Table 4-2 shows that a 200Ah ESS with 4C discharging limited rate that gives a maximum current of 800A could have a comparable energy-saving performance to an ESS that offers a maximum current of 1,000A. Therefore, the proposed ESS capacities were reduced to 200Ah (nominally 78kWh at nominal battery voltage) and an operating current limit of 4C was imposed. The new overall daily energy trends are shown in Figure 4-12.

As can be seen from the mean values in Figure 3-19 and Figure 4-12, the addition of the 200Ah and 4C ESS gave a reduction in the energy lost in braking resistors of approx. 47% and increased the regenerated energy re-used by 511%. The energy supplied from substation was also reduced by 25%. The energy saving delivered by the 200Ah and 4C ESS was approx. 8,694 kWh/day, and that results in an annual CO_2 emission saving of approx. 733 tonnes. Although the energy saving and CO_2 emission saving delivered by 200Ah and 4C ESSs is 21% smaller that the one obtained by the 1,000Ah and 2C ESSs, it is still substantial and was obtained through the use of an 80% smaller battery capacity installation. A smaller ESS with an optimal discharge limit rate could therefore be more preferable, especially when considering return on investment which will be discussed later in this chapter.

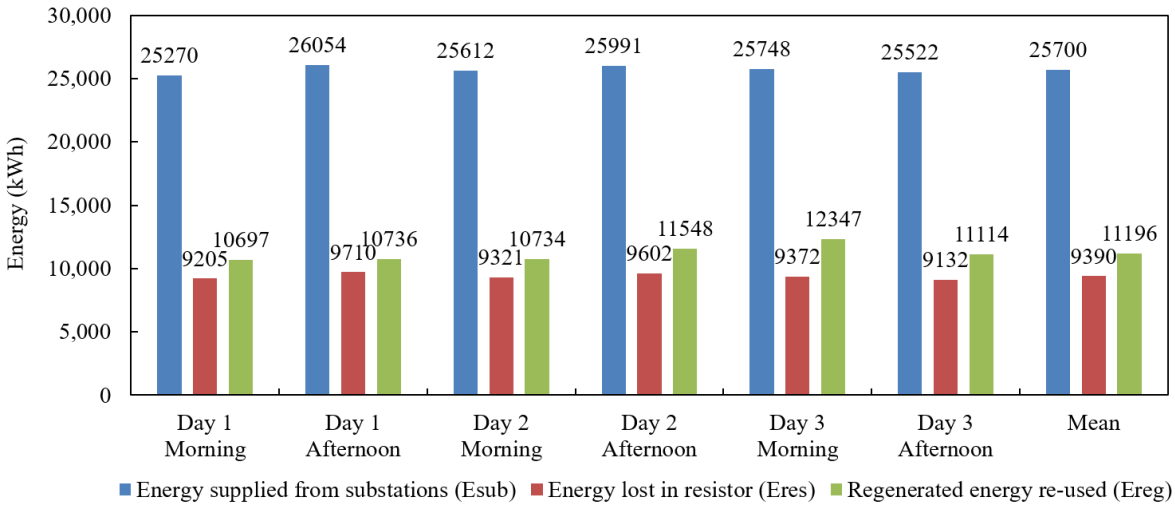

Figure 4-12 Simulated Daily Energy trends with a 200Ah ESS installed at ideal tram stop locations on the tram network.

4.3 Application of energy storage system in the common overhead catenary system

The study on the application of an ESS to the tram system with common OCS was conducted with a similar approach used in the study of applying the ESS in the tram system with separate OCS. However, the study based on the common OCS carried out a deeper investigation on the ESS addition to the stops with substations (called substation stop ESS in this thesis) and explored the possibility of including substation ESS into the network-wide ESS installation. The driver behind this additional investigation is that there is often more land area available at

stops with substations to accommodate an ESS, and additionally, within the Supertram network, five out of seven park and ride facilities are sited in tandem with substations.

This section therefore firstly introduces how the ESS is added into the tram network model with a common OCS arrangement, and how the model allows the substation ESS to serve the two adjacent energy supply sections instead of only one section, as in the case of a centre stop installation. Secondly, it also compares the performance of the different ESS capacities, located at either a centre stop or a substation stop. Finally, it investigates an optimal solution for multiple or even network-wide ESS additions. It is worth noting that the content presented in this section has been published on Zhang, et al. [151].

4.3.1 Introduction to ESS installation

This research considers the implication of locating a possible ESS at various locations within the whole network. To this end, an ESS is modelled at each of the 12 substation stops, and at the 11 centre stops of each energy supply section shown in Figure 4-13, in turn, to assess the overall effect on the whole system energy use.

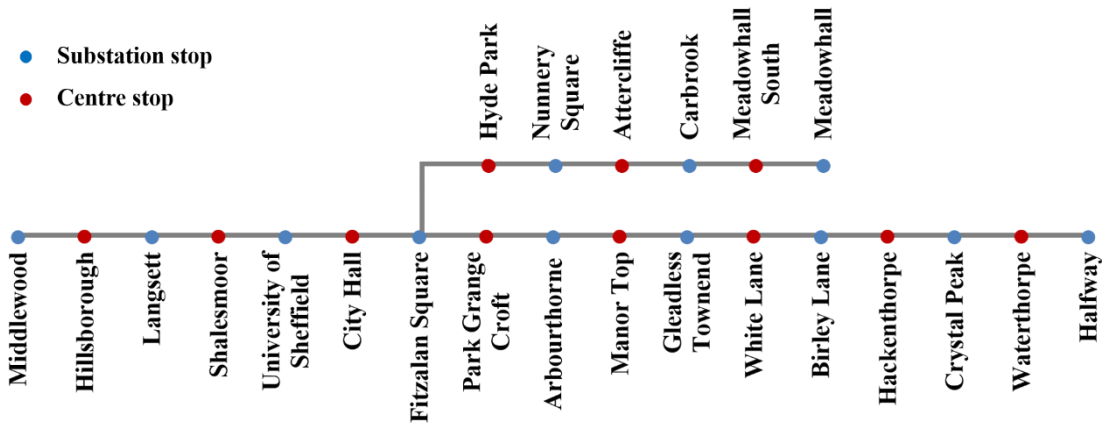

Figure 4-13 The substation stops and the centre stops of the energy supply sections in the Supertram network

The way of adding the ESS onto a centre stop of energy supply section with common OCS setup was similar to the case of adding the ESS onto separate OCS energy supply section (mentioned in subsection 4.2.1). Besides, the Simulink model of ESS installation on a substation stop with common OCS setup (shown in Figure 4-14) also shares similar component modules with the model of ESS installation on a system with separate OCS setup (mentioned in subsection 4.2.1). However, different from the case with separate OCS setup, the substation

stop ESS serves both adjacent energy supply sections instead of only serving the one isolated energy supply section.

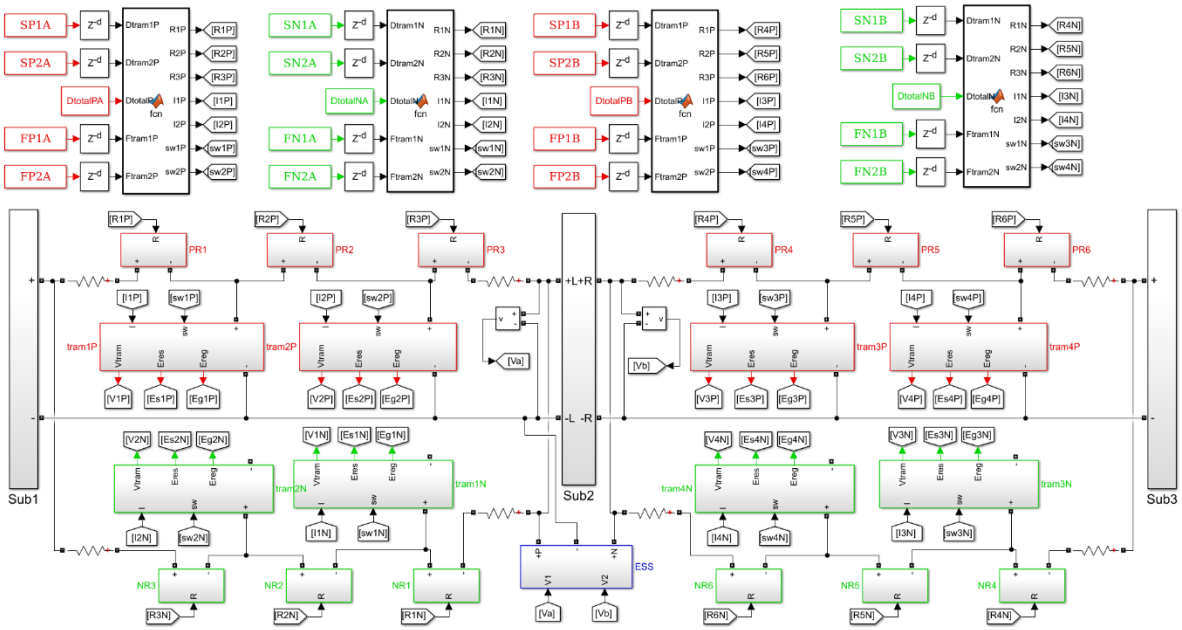

Figure 4-14 Model of ESS installation on substation stop with common OCS setup

As shown in Figure 4-14, the ESS module is able to absorb the braking energy generated from two adjacent energy supply sections. In this section, an ESS with a limited discharge rate of 2C, capacities of 1,000 Ah, 500 Ah, and 100 Ah, and an initial SoC=50% were installed on the substation stop and centre stop of each energy supply section in turn to determine the effect on the system energy use. These example capacities were based on currently available EV battery capacities which range from 40 kWh (i.e. Nissan Leaf) to 100 kWh (i.e. Tesla). Therefore, a 100 Ah battery (39kWh at 390V) can be considered to equate to an EV with a relatively small battery. Multiples of these EVs will give increasingly large available capacity, and Section 4.2 has demonstrated 1,000Ah is a large enough capacity to provide sufficient energy saving capacity to achieve the goals of this research. Hence, the 500Ah is taken as an intermediate value approximately reflective of 5 available EV's for the study.

Similar to Section 4.2, the ESS performance evaluation studied in this section mainly focuses on examining how the introduction of the ESS changes the regenerated energy re-used, the energy lost on the braking resistors, and the energy supplied from the substation on a daily basis. Moreover, this section also investigated how ESS battery capacity and installation location further impacts the ESS performance.

4.3.2 Single ESS installation

The simulation results indicate that the introduction of an ESS, regardless of its placement on either substation stops or centre stops of an energy supply section, increased the re-use of regenerated energy, reduced the energy lost in the braking resistors, and consequently reduced the energy supplied from the substations. Table 4-3 shows the increase in the re-use of the regenerated energy ($+E_{reg}$), the reduction of the energy lost in the resistors ($-E_{res}$), and consequently the reduction of the energy supplied from the substation ($-E_{sub}$) if one ESS, modelled with various storage capacities was installed at either substation stops (n=12) or centre stops (n=11) of the 11 energy supply sections, in turn. Table 4-3 categorizes the results based on the ESS battery capacity, and ranks them in a descending order based on the reduction of the energy supplied from the substations ($-E_{sub}$) in a daily basis, for each of the stops in Figure 4-13.

As shown in Table 4-3, for the same installation location, a higher battery capacity tends to have a greater influence on the amount of regenerated energy re-used, as well as having a greater reduction the energy lost on resistor, and a greater reduction of the energy supplied from the substation. It is worth noting that the ESS state of charge is set to 50% at the beginning of the simulation (namely at the start of a day) regardless of the actual capacity [98]. Assuming the ESS is half full, this would allow the ESS to either store or feed energy from/to the network initially. Additionally, with this initial condition, the ESS has the capacity to either store excess energy, or supply energy to the tram system over the course of the day, this being reflected in the final state of charge of the ESS at the end of the days operation. From the data shown in Table 4-3,

- the ESS could receive a net input of braking energy, if the increase of the regenerated energy re-used (E_{reg}) is greater than the reduction of the energy supplied from the substation (E_{sub}),
- conversely, the ESS could provide its own energy to the tram, if the increase of E_{reg} is less than the reduction of energy from E_{sub}.

Whether the ESS will have a net input or output may be impacted by the number of trams sharing the road network, thus could be attributed to the road traffic condition at different times of day and the frequency of braking and acceleration occurring when a tram passes through a busy area. However, the overall SoC of the ESS could be controlled during operation by varying the CTV and DTV as required.

Table 4-3 The change of daily energy balance caused by using ESS with different battery capacities

Ranking	ESS battery capacity: 1,000 Ah					ESS battery capacity: 500 Ah					ESS battery capacity: 100 Ah				
	Tram Stop	Type*	-Esub (kWh)	-Eres (kWh)	+Ereg (kWh)	Tram Stop	Type*	-Esub (kWh)	-Eres (kWh)	+Ereg (kWh)	Tram Stop	Type*	-Esub (kWh)	-Eres (kWh)	+Ereg (kWh)
1	Park Grange Croft	C	1205	1194	1207	Park Grange Croft	C	1130	1161	1170	Park Grange Croft	C	609	621	630
2	Shalesmoor	C	1084	1155	1156	Shalesmoor	C	964	1048	1042	Shalesmoor	C	607	635	631
3	Manor Top	C	1004	836	844	Manor Top	C	931	829	831	Manor Top	C	566	535	528
4	Hillsborough	C	985	1108	1063	Hillsborough	C	923	1024	979	Fitzalan Square	S	562	608	587
5	City Hall	C	882	1087	1069	City Hall	C	876	984	959	Hillsborough	C	552	637	588
6	Attercliffe	C	833	902	922	Attercliffe	C	770	823	868	The University	S	531	585	538
7	Hackenthorpe	C	678	852	870	Hackenthorpe	C	676	752	772	City Hall	C	518	549	543
8	Waterthorpe	C	675	860	867	Waterthorpe	C	668	753	754	Attercliffe	C	481	488	504
9	Fitzalan Square	S	622	796	773	Fitzalan Square	S	618	726	700	Langsett	S	425	469	439
10	The University	S	607	773	733	The University	S	604	713	669	Hackenthorpe	C	407	410	435
11	Langsett	S	487	656	626	Langsett	S	481	595	566	Waterthorpe	C	401	418	426
12	Hyde Park	C	457	624	651	Hyde Park	C	450	530	560	Arbourthorne	S	370	380	394
13	Arbourthorne	S	435	604	608	Arbourthorne	S	431	533	535	Gleadless Townend	S	337	319	345
14	Gleadless Townend	S	426	527	550	Gleadless Townend	S	423	411	436	Hyde Park	C	326	320	355
15	Meadowhall South	C	386	552	576	Meadowhall South	C	382	472	496	Crystal Peak	S	319	333	350
16	White Lane	C	371	517	546	White Lane	C	368	449	481	Meadowhall South	C	304	311	334
17	Crystal Peak	S	333	538	550	Crystal Peak	S	321	422	438	Nunnery Square	S	299	308	332
18	Nunnery Square	S	318	491	507	Nunnery Square	S	310	408	425	White Lane	C	295	305	322
19	Birley Lane	S	277	400	420	Birley Lane	S	272	338	367	Birley Lane	S	269	275	297
20	Halfway	S	169	384	394	Halfway	S	163	260	275	Halfway	S	160	172	188
21	Middlewood	S	144	330	303	Middlewood	S	141	250	225	Middlewood	S	139	193	171
22	Meadowhall	S	109	304	318	Meadowhall	S	102	198	220	Meadowhall	S	96	107	132
23	Carbrook	S	90	240	262	Carbrook	S	83	176	201	Carbrook	S	61	70	98

*: C = centre stop, and S = substation sto

From Table 4-3 it may be seen that there is little difference in the ranking of the 1,000 Ah category and the 500 Ah category. However, there is a noticeable difference in the rankings of the 100 Ah category from the first 2 columns. Some substation stop ESS installations ranked higher in the 100 Ah category than in the other two categories, for example, an installation on Fitzalan Square went from the 9th to the 4th ranking when comparing the 100Ah column with the other ESS sizes; and the installation on University of Sheffield went from 10th to 6th. To understand how battery capacity impacts the overall savings for the centre and substation stop ESS installations, the mean value of the reduction of energy supply from substation, the reduction of energy lost in the braking resistors, and the increase in regenerated energy re-used was calculated for both centre stop ESS installations and for substation stop ESS's under different ESS battery capacities. Results indicating these mean values and the trends are shown in Figure 4-15.

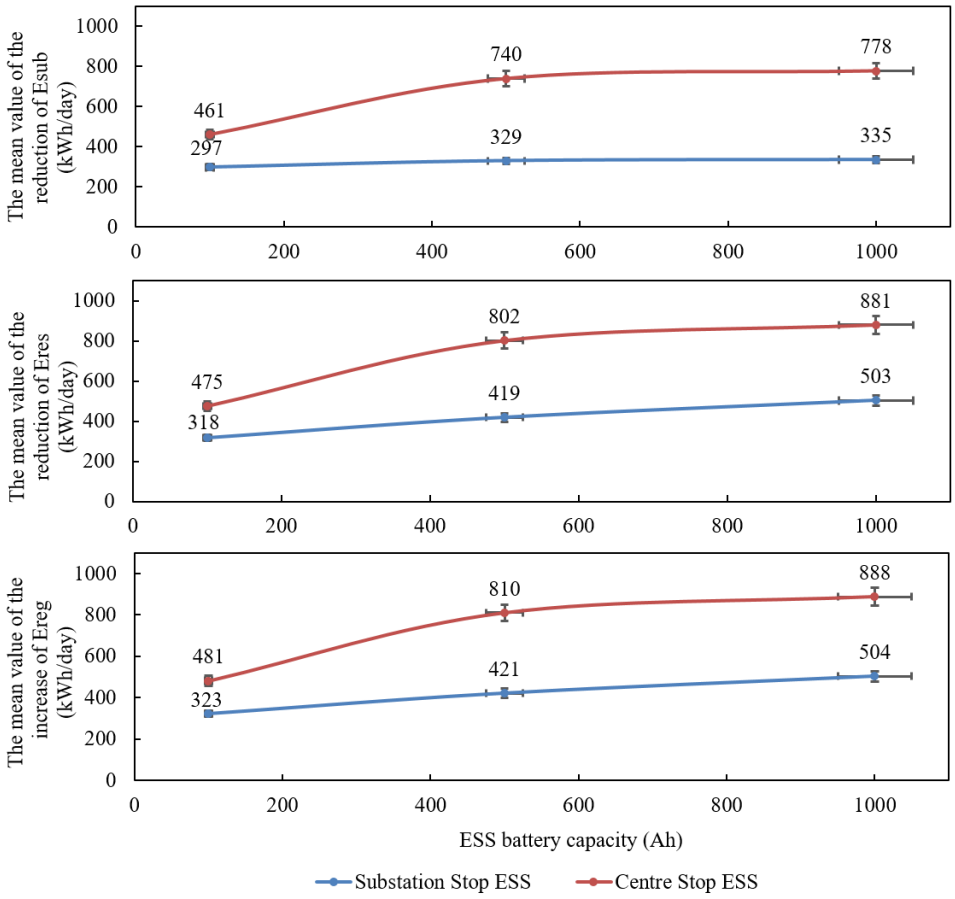

Figure 4-15 Mean values (with percentage error bars) of the change of energy balance of substation ESS and centre stop ESS

As can be seen, the centre stop ESS installations consistently has a greater reduction of E_{sub}, a greater reduction of E_{res}, and a greater increase of E_{reg} than the substation stop ESS installations. The difference varies from 55-132% on the reduction of E_{sub}, 49-91% on the reduction of E_{res}, and 49-92% on the reduction of the E_{reg}. Due to the influence of the catenary resistance, the tramcar braking likely causes more high-voltage-rise events (to the catenary) in the middle of the energy supply section, and hence, the ESS installed near the centre location would absorb more braking energy. Moreover, when the tram (that travels near the centre stop ESS or the substation stop ESS) is accelerating, it is likely that the substation stop ESS will provide less energy than the centre stop ESS does because the substation nearby is a much stronger power source. Therefore, even both ESS could absorb the same amount of energy in the first place, the substation stop ESS could only return less of the braking energy back to the tram network and has a smaller reduction of the energy supplied from the substation. Thus, for the same battery capacity, the centre stop ESS installations lead to a better energy balance than the installations at substation stops.

Although, the accessible braking energy to the substation stop ESS and the centre stop ESS are different, with the latter being likely to be substantially higher than the former. For the substation stop ESS, the lowest simulated ESS capacity of 100 Ah is likely to be sufficient to absorb most of the available braking energy. Thus, increasing ESS battery capacity will only reduce the E_{sub} slightly. However, for the centre stop ESS, this capacity is possibly too small to fully store or utilize the majority of the available braking energy. As shown in Table 4-3, when the simulated ESS capacity was reduced to 100 Ah, the performance of some centre stop ESS degraded, and their ranking dropped. The increasing ESS battery capacity could increase the degree of utilization substantially and thereby the result is a sharper reduction of the E_{sub}..

4.3.3 Multiple ESS installations

In practice, based on the modelling of the entire tram network, multiple ESS could be installed to maximise the energy-saving and cost saving across the network. Table 4-3 could be used to support decision making for determining at which locations to best install an ESS. The working logic is simply to install storage at the higher energy-saving locations (the reduction of energy supplied from substation, E_{sub}) first, namely, to pick the installations shown in Table 4-3 ranked in descending order.

There are two types of ESS installations studied in this project, the ESS at substation stops and the ESS at centre stops. Both types of installation have different distinguishing features, the centre stop ESS is installed inside an energy supply section, and since each energy supply section is isolated from the others, if multiple ESSs are installed on various centre stops respectively, each ESS would work independently. However, if the ESSs are installed on both the substation stop and the centre stop connected to the same energy supply section, they are likely to influence each other, as the braking energy generated could flow to both ESSs simultaneously, and hence each ESS could receive less braking energy than if it is working independently, and ultimately the energy-saving delivered together could be different from the energy-saving delivered independently.

As shown in Table 4-3, the ranking of the 1,000 Ah and 500 Ah capacity ESS are identical and the centre stop ESSs are apparently delivering greater energy-savings than the substation stop ESSs. If a small number of installations are required, the centre stop ESSs are more preferable locations than the substation stop ESSs. However, in the case of 100 Ah capacity ESS, since some substation stop ESSs ranked higher, the small number of installations may involve both the centre stop ESS and substation stop ESS. To address this, simulation results from simultaneous ESS installations on the centre stop and substation stop is presented, illustrating the effects on the total energy saving, based on the 100 Ah ESS.

If only three ESSs are required across the entire Supertram network, the top three locations, Park Croft Grange (1st), Shalesmoor (2nd), Manor Top (3rd) would logically be chosen. If four ESSs are required, Fitzalan Square (4th) would then be initially included as a location. Yet, Park Grange Croft and Fitzalan Square are both located in the same energy supply section as shown in Figure 4-13, the former is the centre stop and the latter is a substation stop. Independently, they can deliver energy-savings of 609 kWh/d and 562 kWh/d, respectively. However, after ESSs are installed on both stops simultaneously, the simulation result suggested the two ESSs would only deliver a saving of 1,078 kWh/d, which is 93 kWh/d smaller than the sum (1,171 kWh) of their independent energy-saving. Therefore, two options for the installation of 4 ESSs have been established as shown in Table 4-4. The difference between these is that option 2 replaces the Fitzalan Square installation (4th) with Hillsborough installation (5th) that is a centre stop and has no conflict with the other centre stops selected for installation. As shown in Table 4-4, option 2 delivers 83 kWh/d more energy saving than option 1.

Table 4-4 Options for four ESSs installations

Option 1			**Option 2**		
Location	**Ranking***	**Type****	**Location**	**Ranking***	**Type****
Park Grange Croft	1st	C	Park Grange Croft	1st	C
Shalesmoor	2nd	C	Shalesmoor	2nd	C
Manor Top	3rd	C	Manor Top	3rd	C
Fitzalan Square	4th	S	Hillsborough	5th	C
Energy Saving (kWh/d)	2,252		Energy Saving (kWh/d)	2,335	

*: Ranking based on reduction of energy supplied from substation shown in Table 4-3
**: C = centre stop, and S = substation stop

In another scenario, if five ESS installations are required, there are three options that could be considered that comprise the top locations (shown in Table 4-3). As shown in Table 4-5, Fitzalan Square and Park Grange Croft in option 1 are in the same energy supply section. Meanwhile, Shalesmoor and the University of Sheffield in option 2 are also in the same energy supply section. Compared to option 1 and option 2, option 3 only consists of centre stop ESS installations and includes a low-ranking location City Hall (7^{th}). However, due to cross influences between ESS in the same energy supply sections, option 3 generates the highest energy saving amongst the three options.

Table 4-5 Options for five ESSs installation

Option 1			**Option 2**			**Option 3**		
Location	**Ranking***	**Type****	**Location**	**Ranking***	**Type****	**Location**	**Ranking***	**Type****
Park Grange Croft	1st	C	Park Grange Croft	1st	C	Park Grange Croft	1st	C
Shalesmoor	2nd	C	Shalesmoor	2nd	C	Shalesmoor	2nd	C
Manor Top	3rd	C	Manor Top	3rd	C	Manor Top	3rd	C
Fitzalan Square	4th	S	Hillsborough	5th	S	Hillsborough	5th	C
Hillsborough	5th	C	University of Sheffield	6th	C	City Hall	7th	C
Energy Saving (kWh/d)	2,804		Energy Saving (kWh/d)	2,743		Energy Saving (kWh/d)	2,853	

*: Ranking based on reduction of energy supplied from substation shown in Table 4-3
**: C = centre stop, and S = substation stop

The two examples provided above indicate that when two ESSs are installed on the substation stop and the centre stop located in the same energy supply section, the energy saving achieved becomes smaller than the sum of their independent installations. Therefore, if multiple ESS

installations are required, the final solution tends to only have centre stop installations regardless of some independent substation stop installations actually ranking higher in terms of energy balance shown in Table 4-3. Thus, this research considers that the best installation locations for multiple ESS on a network are always at the centre stops. Interpreted from Table 4-3, Figure 4-16 shows the potential best daily energy-saving corresponding to each number of ESS installations.

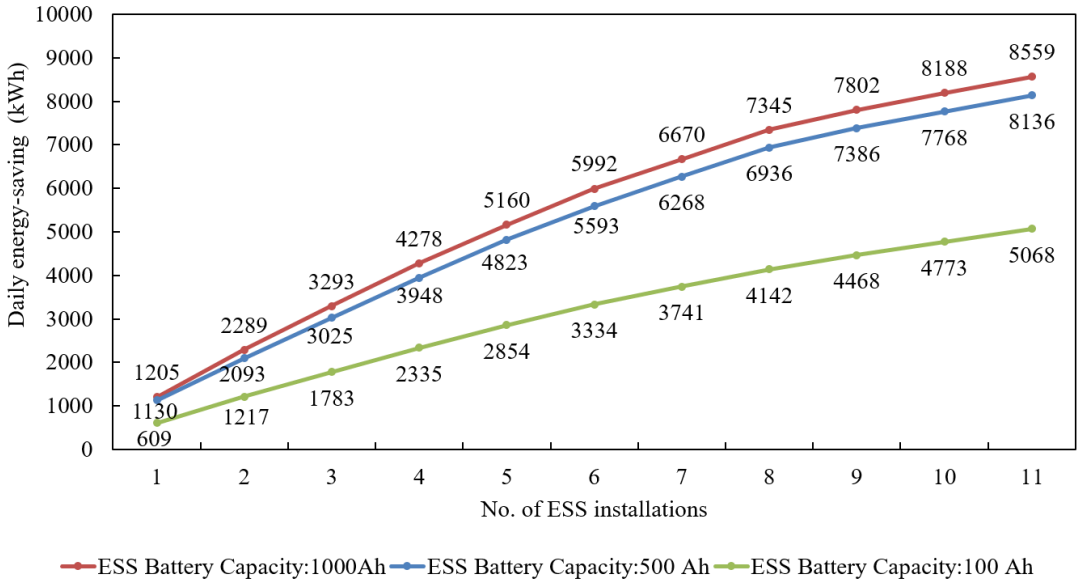

Figure 4-16 Daily electricity saving of centre stop ESS installations with different battery capacity

4.4 Economic feasibility of applying ESS on tram system

The introduction of an ESS can effectively deliver an energy-saving to the Supertram network, however the costs of the systems have not yet been addressed. Thus an economic evaluation has been conducted on ESS installations with different capacities and number of installations. Subsequently, a sensitivity study is presented to identify the influential factors to the economic evaluation. Since the final aim of this research is to integrate EVs as part of the ESS with the tram network, a further economic study was conducted to illustrate the economic benefit brought by utilizing the EVs batteries for the energy storage of the tram system.

In this chapter, the results presented in both Section 4.2 and Section 4.3 suggest that, no matter whether the tram system uses separate OCS or common OCS, installing ESS on one or more centre stops would deliver a better energy-saving than if the ESS is located elsewhere on the network. Moreover, Chapter 3 states that a common OCS is more energy-efficient than the

separate OCS. Therefore, this research considers the application of common OCS shall be or likely will be wider than that of the separate OCS. Thus, the economic feasibility study presented in this section was only conducted on the ESS applications on the tram system that uses the common OCS configuration.

The remainder of this chapter firstly introduces the method of the economic evaluation and the estimation of cost and income. It then presents the result of the economic feasibility of different ESS configurations, and examines the influential factors via the result obtained from the sensitivity study. Finally, the potential merit of using EV as ESS is also discussed.

It is worth noting that the content presented in this section has been published on Zhang, et al. [151].

4.4.1 Method of economic evaluation

The economic evaluation carried out in this chapter explores three aspects, payback period, net present value (NPV) and internal return rate (IRR). It aims to demonstrate when the investment will likely be recovered, how much profit will be generated at the end of the project, and determine the rate of return on the investment. The fundamental elements used to conduct the economic evaluation are the cost of installation and income generated. The cost includes the capital expenditure (CAPEX) and operational expenditure (OPEX), and income is considered as the monetary saving brought about by the energy saving. The details of the cost and income are described in subsection 4.4.2.

Net Present Value

NPV is the difference between the present value of cash inflows and the present value of cash outflows over a period of time [152]. It assumes the buying power of the same amount of money reduces in the future, and hence, the future income needs to be discounted accordingly for bringing it back to today's value [152]. The discount rate could be simply the inflation rate [153]. Alternatively, investors would assume their money can be invested elsewhere that generates profit. The discount rate then becomes the expected interest rate of the potential investment and is usually called, and used as, the nominal discount rate [152]. The NPV of an investment project is calculated via Equation 4-1 adapted from San Ong and Thum [153] and Žižlavský [152].

$$\text{NPV} = \sum_{t=0}^{n} \frac{R_t}{(1+i)^t} \qquad \text{Equation 4-1}$$

Where ***t*** is the number period in the unit of years, $\boldsymbol{R_t}$ is the net cash inflow during a single period of ***t***, and ***i*** is the discount rate. The *t* ranges from 0 to any value due to the asset life given and ranges from 0 to 5 in this study since the asset life was primarily assumed as five years. It is worth noting that $\boldsymbol{R_0}$, the net cash inflow in year zero, is considered negative in this case since the project only spends on initial investment but receives no income. When t>0, the $\boldsymbol{R_t}$ could be positive, equal to 0, or negative, depending on the magnitude of the expenditure and the income. For the discount rate *i*, it has been reportedly taken as 10-15% for big corporate projects, and was also set between 5-9% on some solar photovoltaic projects [152-154]. This research utilised a moderate value of 6% for the discount rate.

A positive NPV demonstrates that investment is economically feasible as profit is generated [153]. However, it only provides the absolute amount of profit generated during the appraised period and is not able to indicate the rate of return [155]. If two investments have the same amount of initial investment and the same estimated NPV but a different time scale, the one with a shorter time scale generates the profit quicker, and it is thereby potentially more preferable. Solely using the NPV is not able to provide an indicative comparison of the two investments [154].

Internal Rate of Return

The IRR is the rate of return of the current investment and is commonly used together with the NPV [155, 156]. IRR is calculated when the NPV is zero, and it can be expressed as Equation 4-2, that is adapted from Equation 4-1

$$0 = \sum_{t=0}^{n} \frac{R_t}{(1+\text{IRR})^t} \qquad \text{Equation 4-2}$$

Where ***t*** is the number period in the unit of years that leads to a NPV of zero, $\boldsymbol{R_t}$ is the net cash inflow during a single period of *t*.

In this research, the IRR was determined via the Excel IRR function. If the IRR equal to or greater than the discount rate, the return of the current investment meets or exceeds the investor's expectation, and hence the economic viability is proven [154].

Using the same example given in the NPV section, if two investments have the same amount of initial investment and the same estimated NPV but a different time scale, the one with a shorter time scale will have a higher IRR than the one with a longer time scale. Besides, if two investments have the same time scale and the same estimated NPV but a different initial investment, the one with a smaller initial investment will have a higher IRR than the one with a greater initial investment. Thus, IRR can be used to assess which investment is able to return quicker and better [156].

However, IRR is not able to be used on its own because it is not able to explain the absolute amount of profit generated [155]. If two investments have the same time scale and the same estimated IRR but a different initial investment, the one with a greater initial investment will have a higher absolute profit generated (NPV) than the one with a smaller initial investment.

Discount Payback Period

The discounted payback period (DPP) indicates the time taken to recover the initial investment with regards to potential depreciation over time. The annual income and annual OPEX are expected to be uniform before being discounted, and hence, the annual cash flow, which is the difference between the annual income and annual OPEX, is expected to be uniform as well. The DPP is calculated via Equation 4-3 [157].

$$DPP = \frac{ln[1 \div (1 - CAPEX \div ACF \times i)]}{ln(1 + i)} \qquad \text{Equation 4-3}$$

where the annual cash flow before being discounted is $\boldsymbol{ACF}$, and $\boldsymbol{i}$ is the discount rate.

In this study, the asset life, which is battery life, was primarily assumed as five years. A DPP that is smaller than the asset life helps to demonstrate economic feasibility. However, the DPP is not able to estimate any potential net income generated after the initial investment is recovered.

This paper considers that the economic feasibility is proven if the DPP is smaller than the asset life (battery life), and NPV are both positive, and the IRR is greater than the discount rate, simultaneously.

4.4.2 Cost and income

The CAPEX of the ESS considers the cost of the battery, the cost of the other components (i.e. converter, control units, site wiring, etc.), and the cost of installation. According to the economic analysis of energy storage system installation reported in various literatures [158-162], this paper gives reasonable mid-range assumptions of:

- The unit cost of the battery is estimated at £133 per kWh
- The cost of the other components is estimated to be 80% of the cost of the battery
- The cost of installation is estimated as £10,000 per ESS

Therefore, the CAPEX of each ESS installation can be calculated via Equation 4-4.

$$CAPEX = n \times [(1 + 80\%) \left(\frac{133 \times Battery\ Voltage \times Battery\ Capacity}{1000}\right) + 10000] \qquad \text{Equation 4-4}$$

where ***n*** is the number of ESS that will be installed, ***battery voltage*** is set as 390 V, ***battery capacity*** varies from 100 Ah, 500 Ah and 1,000 Ah, and ***1000*** is the conversion ratio between W to kW.

The OPEX per annum only considers the maintenance of the ESS and is assumed as 3% of the CAPEX [163, 164]. Therefore, the costs per ESS with different capacity are shown in Table 4-6.

Table 4-6 The costs per ESS

Capacity of battery	Cost of battery	Cost of other components	Cost of installation	CAPEX	OPEX per Annum
1000Ah (390kWh)	£51,870	£41,496	£10,000	£103,366	£3,101
500 Ah (195kWh)	£25,935	£20,748	£10,000	£56,683	£1,700
100 Ah (39kWh)	£5,187	£4,150	£10,000	£19,337	£580

The income is considered as the monetary -saving due to the electricity saved. The unit cost of electricity for this study is set at £53 per MWh [165]. The annual income related to the electricity-saving is calculated via Equation 4-5.

$$Annual\ Income = \frac{Daily\ Electricity\ Saving\ \times 365\ \times 53}{1000} \qquad \text{Equation 4-5}$$

where the ***Daily Electricity Saving*** of each ESS installation appraised is in the unit of kWh and is shown in Figure 4-16, ***53*** is the price (£) per MWh electricity, and ***1000*** is the conversion ratio from kWh to MWh.

4.4.3 Economic feasibility

The economics of different numbers of ESS installations are shown in Table 4-7. As shown, it is economically feasible to install ESSs with 500 Ah battery capacity at the top 6 identified best centre stops, and it is economically feasible to install ESSs with 100 Ah battery capacity on all centre stops. However, no 1,000 Ah ESS installation has been found to be economically viable. It is worth noting that, in order to demonstrate the impact of the different parameters on the economic evaluation, Table 4-7 and Table 4-10 to Table 4-20 highlight the NPV, IRR and DPP results, the uneconomic results (with NPV<0, IRR<6% and/or DPP>5) are highlighted by a superscript 'N'.

Table 4-7 The economics of different numbers of ESS installation with different ESS battery capacity

No. of ESS	ESS Battery Capacity:1000Ah			ESS Battery Capacity:500Ah			ESS Battery Capacity:100Ah		
	NPV (£)	IRR (%)	DPP (year)	NPV (£)	IRR (%)	DPP (year)	NPV (£)	IRR (%)	DPP (year)
1	-£18,251^{N}	-6.4%^{N}	6.3^{N}	£28,219	15.9%	3.2	£27,879	41.9%	1.9
2	-£46,339^{N}	-8.2%^{N}	6.8^{N}	£42,895	12.3%	3.5	£55,594	41.8%	1.9
3	-£80,945^{N}	-9.6%^{N}	7.2^{N}	£54,931	10.6%	3.6	£79,953	40.3%	1.9
4	-£117,099^{N}	-10.5%^{N}	7.5^{N}	£66,290	9.6%	3.7	£103,162	39.1%	2.0
5	-£161,696^{N}	-11.7%^{N}	7.9^{N}	£73,787	8.6%	3.8	£123,626	37.7%	2.0
6	-£210,269^{N}	-12.8%^{N}	8.3^{N}	£72,646	7.1%	4.0	£141,025	36.0%	2.1
7	-£271,489^{N}	-14.3%^{N}	8.9^{N}	£63,878^{N}	5.4%^{N}	4.2^{N}	£152,419	33.6%	2.2
8	-£332,897^{N}	-15.5%^{N}	9.4^{N}	£54,466^{N}	4.1%^{N}	4.4^{N}	£163,283	31.7%	2.3
9	-£412,102^{N}	-17.3%^{N}	10.4^{N}	£27,249^{N}	1.8%^{N}	4.7^{N}	£168,100	29.2%	2.4
10	-£497,068^{N}	-19.1%^{N}	11.5^{N}	-£5,453^{N}	-0.3%^{N}	5.1^{N}	£171,100	27.0%	2.5
11	-£583,288^{N}	-20.6%^{N}	12.6^{N}	-£39,335^{N}	-2.2%^{N}	5.4^{N}	£173,367	25.1%	2.6

^{N}: uneconomic results

Two most noticeable phenomenon found from Table 4-7 are that:

1) The greater the ESS battery capacity, the lower the economic feasibility
2) A greater number of ESS installations will also lower the economic feasibility

The ESS installation on Park Grange Croft (top 1 ESS installation shown in Table 4-3) is used as an example for demonstration. When the ESS battery capacity increases from 100 Ah to 1,000 Ah, the energy-saving (shown as $-E_{sub}$ in Figure 4-16) increases by 97%, and the CAPEX and OPEX per annum shown (in Table 4-6) both increase by 435%. When the ESS battery capacity increases, the energy-saving increases at a slower rate over time than the cost. Therefore, a greater ESS battery capacity will worsen the economic feasibility.

Regarding the second trend discovered, it could be attributed to multiple ESS installations consisting of the highest energy-saving centre stop ESS installations first. When the number of ESS installations increase, the total ESS battery capacity increases positively and linearly at the same rate, and so does the cost related CAPEX and OPEX. However, regarding the income related energy saving, when the number of ESS installations increase, more centre stop ESS installations with lower energy-saving are included, thus the increase of the total energy-saving and the income is thereby relatively slower. Therefore, when the number of ESS installations increase, the cost increases faster than the income, and hence leads to worse economics.

The economic evaluation aims to assist decision making over potential investment options. In the example where a single ESS installation is required, a 500 Ah ESS has a higher NPV but a smaller IRR than 100 Ah ESS. This means that the 500 Ah ESS will generate a greater profit than 100 Ah ESS at the end of the asset life, but its rate of return on investment is slower since it has a higher CAPEX. This indicates that a potential investor could thereby decide which option to invest in according to his/her own preference on the absolute value of profit or the flexibility of reinvestment.

4.4.4 Sensitivity study

In the economic evaluation, six variables could have substantial uncertainty and hence could heavily impact upon economic evaluation. They are the battery price which affects the cost of battery, the installation cost, the ratio between OPEX and CAPEX, electricity price, the battery life, and discount rate. This research also conducted the sensitivity study to examine the impact of these six variables on economic parameters, and subsequently to discover what is required and how to improve the economics. The testing approach was to apply a ±20% variation on one parameter to test in turns and then examine the change on NPV, IRR and DPP.

Since each ESS installation leads to varied $-E_{sub}$ (as shown in Table 4-3), the total $-E_{sub}$ delivered did not increase linearly when the number of ESS installations increased (as shown in Figure 4-16). Therefore, the above tested six parameters could potentially impact the economic appraisal of multiple ESS additions differently than how they affected the single ESS addition. Therefore, this study investigated how these parameters influence the economics of the single ESS addition and each multiple ESS addition (number of installation ranges from 2 to 11).

4.4.4.1 Sensitivity study for single ESS addition

The sensitivity study used the highest energy saving case of one ESS installation on Park Grange Croft (shown Table 4-3) as an example for illustration. The CAPEX and annual OPEX of the ESSs to install at Park Grange Croft have been listed in Table 4-6, and the undiscounted annual income and annual cash flow related to those ESS additions are listed in Table 4-8.

Table 4-8 The undiscounted annual income and annual cash flow related to the ESSs installed on Shalesmoor

Capacity of battery	Undiscounted Annual Income	Undiscounted Annual Cash Flow
1,000Ah (390kWh)	£23,307	£20,206
500 Ah (195kWh)	£21,856	£20,155
100 Ah (39kWh)	£11,789	£11,209

Impact of electricity price

The economic evaluations obtained from different electricity prices are shown in

Table 4-9. A higher electricity price leads to a higher current expenditure. Consequently, the same energy-saving would result in a higher cost saving. The electricity price substantially impacts upon all ESS regardless of capacity. In the base case, the electricity price is considered as a contract price which is discounted from normal market prices. If the UK average non-domestic electricity price of 2019, £122/MWh, is applied, the economics will be greatly increased [166].

Table 4-9 The economic evaluation based on different electricity price

Electricity Price (£/ MWh	ESS Battery Capacity:1000Ah			ESS Battery Capacity:500Ah			ESS Battery Capacity:100Ah		
	NPV (£)	IRR (%)	DPP (year)	NPV (£)	IRR (%)	DPP (year)	NPV (£)	IRR (%)	DPP (year)
£42.4	-£37,887^{N}	-14.0%^{N}	8.7	£9,806^{N}	5.8%^{N}	4.2^{N}	£17,947	28.2%	2.4
£53.0*	-£18,251^{N}	-6.4%^{N}	6.3	£28,219	15.9%	3.2	£27,879	41.9%	1.9
£63.6	£1,384^{N}	0.5%^{N}	4.9	£46,632	25.3%	2.6	£37,810	55.0%	1.5
£122.0	£109,564	31.8%	2.2	£148,078	71.1%	1.2	£92,529	122.1%	0.8

*: Base case, ^{N}: uneconomic results

The income generated via electricity saving is the product of the daily energy saving and electricity price as shown in Equation 4-5 and is only determined by the two as the rest of the components in the equation can be considered as constants. Therefore, the two factors share

the same effect on the economic appraisal. The same percentage variation given to the electricity price or energy saving will lead to the same change in economics.

Impact of battery price

The economic evaluations obtained for different battery prices are shown in Table 4-10. As can be seen, battery price substantially impacts the economics of the bigger capacity ESSs, but less-so, on the 100 Ah ESSs. This is because the battery cost contributes more to the capital costs of the 1,000 Ah ESS and 500 Ah ESS.

Table 4-10 The economic evaluation based on different battery price

Battery Price (£/kWh)	ESS Battery Capacity:1000Ah			ESS Battery Capacity:500Ah			ESS Battery Capacity:100Ah		
	NPV (£)	IRR (%)	DPP (year)	NPV (£)	IRR (%)	DPP (year)	NPV (£)	IRR (%)	DPP (year)
£106	£2,781^{N}	1.1%^{N}	4.8^{N}	£38,736	25.1%	2.6	£29,982	49.0%	1.7
£133*	-£18,251^{N}	-6.4%^{N}	6.3^{N}	£28,219	15.9%	3.2	£27,879	41.9%	1.9
£160	-£39,284^{N}	-12.1%^{N}	8.0^{N}	£17,703	8.9%	3.8	£25,775	36.0%	2.1

*: Base case, ^{N}: uneconomic results

Impact of battery life

The economic evaluations obtained from different battery life lengths are shown in Table 4-11. Battery life impacts both the NPV and IRR of all the ESS installations substantially but does not affect the payback period. This is because it controls the income-generating period, and hence controls the total amount of income generated during the battery life. However, it does not influence the rate of income generation and hence it will not change when the investment is recovered. Battery life is likely affected by the number of charging cycles. Battery life, and thereby the economics, could be potentially improved if the numbers of charging cycles can be reduced via a better system control and design.

Table 4-11 The economic evaluation based on different battery life

Battery Life (year)	ESS Battery Capacity:1000Ah			ESS Battery Capacity:500Ah			ESS Battery Capacity:100Ah		
	NPV (£)	IRR (%)	DPP (year)	NPV (£)	IRR (%)	DPP (year)	NPV (£)	IRR (%)	DPP (year)
4	-£33,351^{N}	-14.3%^{N}	6.3^{N}	£13,158	9.2%	3.2	£19,503	36.6%	1.9
5*	-£18,251^{N}	-6.4%^{N}	6.3^{N}	£28,219	15.9%	3.2	£27,879	41.9%	1.9
6	-£4,007^{N}	-1.2%^{N}	6.3^{N}	£42,428	19.9%	3.2	£35,780	44.9%	1.9

*: Base case, ^{N}: uneconomic results

Impact of installation cost

The economic evaluations obtained from different installation costs are shown in Table 4-12. Opposite to the battery price, the installation cost impacts more on the 100 Ah ESSs, but less on the 500 and 1,000 Ah capacities. This is because the installation cost is assumed to be a fixed cost and has a higher proportion of the capital cost in the 100 Ah ESSs.

Table 4-12 The economic evaluation based on different installation cost

Installation Cost (per ESS)	ESS Battery Capacity:1000Ah			ESS Battery Capacity:500Ah			ESS Battery Capacity:100Ah		
	NPV (£)	IRR (%)	DPP (year)	NPV (£)	IRR (%)	DPP (year)	NPV (£)	IRR (%)	DPP (year)
£8,000	-£15,999^{N}	-5.7%^{N}	6.1^{N}	£30,472	17.7%	3.0	£30,131	49.5%	1.7
£10,000*	-£18,251^{N}	-6.4%^{N}	6.3^{N}	£28,219	15.9%	3.2	£27,879	41.9%	1.9
£12,000	-£20,504^{N}	-7.1%^{N}	6.5^{N}	£25,967	14.2%	3.3	£25,626	35.6%	2.1

*: Base case, ^{N}: uneconomic results

Impact of OPEX

The economic evaluations obtained from different OPEX to CAPEX ratio cost are shown in Table 4-13. The higher the ratio, the worse the economic evaluation result. However, its impact on the overall economics is minor.

Table 4-13 The economic evaluation based on different OPEX to CAPEX ratio

OPEX: CAPEX	ESS Battery Capacity:1000Ah			ESS Battery Capacity:500Ah			ESS Battery Capacity:100Ah		
	NPV (£)	IRR (%)	DPP (year)	NPV (£)	IRR (%)	DPP (year)	NPV (£)	IRR (%)	DPP (year)
2.4%	-£15,639^{N}	-5.4%^{N}	6.1^{N}	£29,652	16.6%	3.1	£28,367	42.6%	1.9
3.0%*	-£18,251^{N}	-6.4%^{N}	6.3^{N}	£28,219	15.9%	3.2	£27,879	41.9%	1.9
3.6%	-£20,864^{N}	-7.3%^{N}	6.5^{N}	£26,787	15.1%	3.2	£27,390	41.3%	1.9

*: Base case, ^{N}: uneconomic results

Impact of discount rate

The economic evaluations obtained from different discount rates are shown in Table 4-14. A low discount rate leads to less depreciation when the future annual cash flow is discounted into the present value. Thus, a lower discount rate will lead to a better NPV and IRR, and ultimately, a shorter DPP. Moreover, the discount rate will have a greater impact on the high battery capacity project that recovers more energy and generates a higher income and cash flow. The discount rate is responsible for discounting the future cash flow into the present value. Hence, the variation of the discount rate will lead to a greater numerical change and potentially a greater percentage change to the NPV of projects with higher future cash flow, which are the

high CAPEX cases in this study. In the examples of the 500 Ah battery ESS and the 100 Ah battery ESS, the former has a higher annual cash flow than the latter as shown in Table 4-8. When the discount rate was reduced from 7.2% to 4.8%, the NPV of the former increased by £5,546 (22%), and of the latter increased by £3,084 (12%). Consequently, the 500 Ah battery ESS had a higher percentage increase on the IRR, and a higher percentage reduction on the DPP than the 100 Ah battery ESS, when the discount rate reduces. A lower discount rate will improve the economics of the high cash flow project to a greater extent.

Table 4-14 The economic evaluation based on different discount rate

Discount Rate	ESS Battery Capacity:1000Ah			ESS Battery Capacity:500Ah			ESS Battery Capacity:100Ah		
	NPV (£)	IRR (%)	DPP (year)	NPV (£)	IRR (%)	DPP (year)	NPV (£)	IRR (%)	DPP (year)
4.8%	-£15,399 ^{N}	-5.3%^{N}	6.0^{N}	£31,064	17.2%	3.1	£29,461	43.6%	1.8
6.0%*	-£18,251^{N}	-6.4%^{N}	6.3^{N}	£28,219	15.9%	3.2	£27,879	41.9%	1.9
7.2%	-£20,960^{N}	-7.4%^{N}	6.6^{N}	£25,518	14.6%	3.3	£26,376	40.3%	1.9

*: Base case, ^{N}: uneconomic results

Summary conclusions from the sensitivity study

As shown in Table 4-10 to Table 4-14, the change of the NPV, IRR, and DPP usually follows the pattern that when NPV increases, the IRR increases and the DPP reduces. Therefore, this research produced spider plots, to plot the change of NPV against the ratio of the changed value to the baseline value of a tested parameter. This was used to identify the most influential parameter (to the economic appraisal), which should have the steepest slope, among a number of tested parameters [167]. The spider plots of ESS with different battery capacities are shown in Figure 4-17. It is worth noting that, Figure 4-17(a) uses a different y axis compared to Figure 4-17(b) and Figure 4-17(c). It is because the baseline NPV of the 1,000 Ah ESS addition on Shalesmoor is negative and is considered as a financial loss, whereas a positive change in NPV indicates a larger financial loss and worse economics. However, a negative change of the NPV demonstrates a smaller financial loss and better economics. As aforementioned, if the battery price becomes lower, the economics improve, hence, as shown in Figure 4-17(a), when the battery price decreases from 100% to 80% of the baseline value, the NPV, would be reduced by approx. 75%, indicating that the financial loss could be reduced by 75%. In the cases of the 500Ah ESS and 100Ah ESS addition on Shalesmoor, the baseline NPVs were found to be both positive, as shown in Table 4-10 to Table 4-14. Therefore, the change in NPV is interpreted as "Change in profit" in Figure 4-17(b) and Figure 4-17(c), and the positive change in the NPV/"Change in Profit" indicates a better economic feasibility.

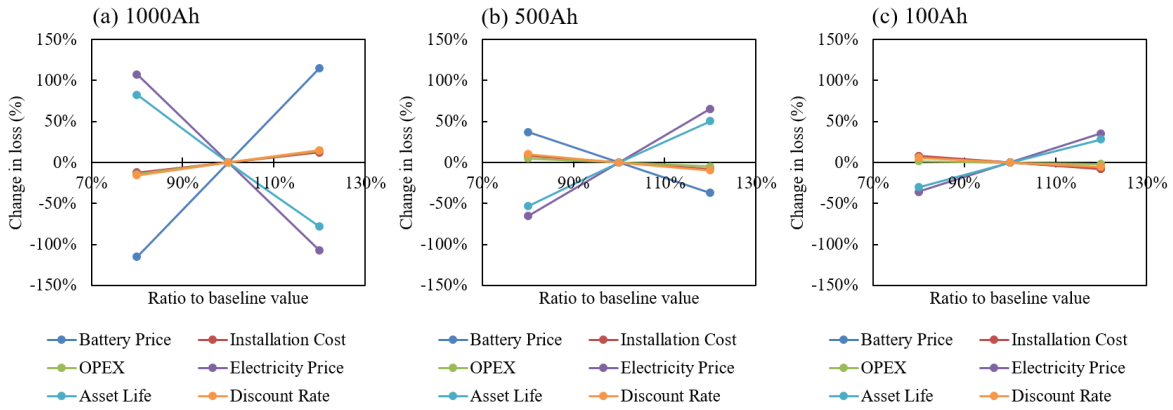

Figure 4-17 The spider-plot of the NPV of ESS additions with different battery capacity

As shown in Figure 4-17,

1) The electricity price and asset life heavily affect the NPV.
2) The battery price also substantially influences the NPV of the 1,000Ah and 500Ah ESS addition but mildly impacts the NPV of the 100Ah ESS since the battery cost accounts for less in the CAPEX compared to the former for ESS addition.
3) The installation cost, OPEX and discount rate only mildly influence the NPV.

As mentioned above, all the tested parameters should impact the IRR and DPP in a similar way as they influence the NPV. However, the variation asset life will only affect the NPV and IRR similarly but make no impact on DPP.

4.4.4.2 Sensitivity study for multiple ESS additions

As aforementioned, a ±20% variation was applied on one parameter to test in turns and then examine the change on NPV, IRR and DPP. Besides, the sensitivity study for multiple ESS additions utilized the absolute percentage change on NPV ($|\pm\%NPV|$), which was calculated via Equation 4-6, to demonstrate the importance of a parameter.

$$|\pm\%NPV| = \left|\frac{(NPV_{80\%} - NPV_{120\%})}{NPV_{100\%}}\right| \qquad \text{Equation 4-6}$$

where $\boldsymbol{NPV_{80\%}}$ is the NPV calculated when the parameter-to-test equals 80% of the base case value, $\boldsymbol{NPV_{120\%}}$ is the NPV calculated when the parameter-to-test equals 120% of the base case value, and $\boldsymbol{NPV_{100\%}}$ is the base case NPV. Using the 1,000 Ah single ESS addition for demonstration:

- The ±20% variation on battery price resulted in a $|\pm\%NPV|$ of 230% (based on data shown in Table 4-10), and

The ±20% variation on installation cost resulted in a $|\pm\%NPV|$ of 25% (based on data shown in

- Table 4-12).

The battery price is found influential to the economic appraisal, but the installation cost is not. Thus, the higher the $|\pm\%NPV|$, the more influential the parameter to the economic assessment. This study ranked the $|\pm\%NPV|$ obtained from sensitivity study conducted on each of the parameters-to-test and ESS additions with different numbers of installations, in descending order, as shown in Table 4-15.

Table 4-15 The ranking of the $|\pm\%NPV|$ on each ESS addition with different numbers of installation

Battery Capacity	No. of Installation	Ranking					
		Battery Price	Installation	OPEX	Electricity Price	Battery Life	Discount Rate
1000 Ah	1	1	6	5	2	3	4
	2	1	6	5	2	3	4
	3	1	6	4	2	3	5
	4	1	6	4	2	3	5
	5	1	6	4	2	3	5
	6	1	5	4	2	3	6
	7	1	5	4	2	3	6
	8	1	5	4	2	3	6
	9	1	5	4	2	3	6
	10	1	5	4	2	3	6
	11	1	5	4	2	3	6
500 Ah	1	3	5	6	1	2	4
	2	3	5	6	1	2	4
	3	3	5	6	1	2	4
	4	3	5	6	1	2	4
	5	3	5	6	1	2	4
	6	3	4	6	1	2	5
	7	3	4	6	1	2	5
	8	3	4	6	1	2	5
	9	2	4	6	1	3	5
	10	2	4	6	1	3	5
	11	2	4	6	1	3	5
100 Ah	1	4	3	6	1	2	5
	2	4	3	6	1	2	5
	3	4	3	6	1	2	5
	4	4	3	6	1	2	5
	5	4	3	6	1	2	5
	6	4	3	6	1	2	5
	7	4	3	6	1	2	5
	8	4	3	6	1	2	5
	9	4	3	6	1	2	5
	10	4	3	6	1	2	5
	11	4	3	6	1	2	5

As can be seen in Table 4-15, similar to the founding of the sensitivity study on the single ESS addition,

- The electricity price and asset life heavily affect the NPV of all the cases regardless of battery capacity and the number of installations;
- The battery price also substantially influences the NPV of the 1,000Ah and 500Ah ESS additions but mildly impacts the NPV of the 100Ah ESS;
- The installation cost, OPEX and discount rate only mildly influence the NPV;
- The change of number of addition only slight influences the importance of the parameter tested on the economic assessment.

The sensitivity study also examined whether the more beneficial conditions as

- A 20% lower battery price,
- A 20% higher electricity price, or
- A 20% longer asset life

would substantially alter the economics of the multiple ESS additions and lead to different decision making on the potential investments. The economics of each multiple ESS addition under each preferable condition was investigated and shown in Table 4-16, Table 4-17 and Table 4-18.

Table 4-16 The economics of the multiple ESS additions obtained at a 20% lower battery price

No of Installation	ESS Battery Capacity:1000Ah			ESS Battery Capacity:500Ah			ESS Battery Capacity:100Ah		
	NPV (£)	IRR (%)	DPP (year)	NPV (£)	IRR (%)	DPP (year)	NPV (£)	IRR (%)	DPP (year)
1	£2,781^{N}	1.1%^{N}	4.8^{N}	£38,736	25.1%	2.6	£29,982	49.0%	1.7
2	-£4,273^{N}	-0.9%^{N}	5.2^{N}	£63,928	21.1%	2.8	£59,801	48.9%	1.7
3	-£17,846^{N}	-2.5%^{N}	5.4^{N}	£86,480	19.2%	2.9	£86,263	47.2%	1.7
4	-£32,967^{N}	-3.4%^{N}	5.6^{N}	£108,356	18.1%	3.0	£111,575	45.9%	1.8
5	-£56,531^{N}	-4.8%^{N}	5.9^{N}	£126,369	17.0%	3.1	£134,142	44.4%	1.8
6	-£84,071^{N}	-6.0%^{N}	6.2^{N}	£135,745	15.3%	3.2	£153,645	42.6%	1.9
7	-£124,259^{N}	-7.6%^{N}	6.6^{N}	£137,493	13.4%	3.4	£167,142	40.0%	1.9
8	-£164,633^{N}	-8.9%^{N}	7.0^{N}	£138,598	11.9%	3.5	£180,109	37.9%	2.0
9	-£222,805^{N}	-10.9%^{N}	7.6^{N}	£121,897	9.4%	3.8	£187,030	35.3%	2.1
10	-£286,738^{N}	-12.8%^{N}	8.3^{N}	£99,712	7.0%	4.0	£192,133	32.9%	2.2
11	-£351,926^{N}	-14.5%^{N}	8.9^{N}	£76,346^{N}	4.9%^{N}	4.3^{N}	£196,504	30.8%	2.3

*: Base case, ^{N}: uneconomic results

Table 4-17 The economics of the multiple ESS additions obtained at a 20% higher electricity price

No of Installation	ESS Battery Capacity:1000Ah			ESS Battery Capacity:500Ah			ESS Battery Capacity:100Ah		
	NPV (£)	IRR (%)	DPP (year)	NPV (£)	IRR (%)	DPP (year)	NPV (£)	IRR (%)	DPP (year)
1	£1,384^{N}	0.5%^{N}	4.9^{N}	£46,632	25.3%	2.6	£37,810	55.0%	1.5
2	-£9,035^{N}	-1.5%^{N}	5.3^{N}	£77,013	21.2%	2.8	£75,425	54.9%	1.5
3	-£27,277^{N}	-3.1%^{N}	5.6^{N}	£104,225	19.3%	2.9	£109,012	53.1%	1.6
4	-£47,376^{N}	-4.1%^{N}	5.8^{N}	£130,625	18.2%	3.0	£141,219	51.7%	1.6
5	-£77,607^{N}	-5.4%^{N}	6.1^{N}	£152,391	17.1%	3.1	£170,131	50.1%	1.6
6	-£112,609^{N}	-6.6%^{N}	6.3^{N}	£163,791	15.4%	3.2	£195,366	48.2%	1.7
7	-£162,787^{N}	-8.2%^{N}	6.8^{N}	£166,038	13.5%	3.4	£213,395	45.4%	1.8
8	-£213,191^{N}	-9.5%^{N}	7.1^{N}	£167,513	12.0%	3.5	£230,787	43.2%	1.8
9	-£284,951^{N}	-11.5%^{N}	7.8^{N}	£147,621	9.5%	3.7	£240,924	40.4%	1.9
10	-£363,624^{N}	-13.3%^{N}	8.5^{N}	£121,149	7.1%	4.0	£248,881	37.9%	2.0
11	-£443,803^{N}	-15.0%^{N}	9.2^{N}	£93,259^{N}	5.0%^{N}	4.3^{N}	£255,957	35.7%	2.1

*: Base case, ^{N}: uneconomic results

Table 4-18 The economics of the multiple ESS additions obtained at a 20% longer

No of Installation	ESS Battery Capacity:1000Ah			ESS Battery Capacity:500Ah			ESS Battery Capacity:100Ah		
	NPV (£)	IRR (%)	DPP (year)	NPV (£)	IRR (%)	DPP (year)	NPV (£)	IRR (%)	DPP (year)
1	-£4,007^{N}	-1.2%^{N}	6.3^{N}	£42,428	19.9%	3.2	£35,780	44.9%	1.9
2	-£19,496^{N}	-2.9%^{N}	6.8^{N}	£69,046	16.5%	3.5	£71,371	44.7%	1.9
3	-£42,595^{N}	-4.3%^{N}	7.2^{N}	£92,582	14.9%	3.6	£103,042	43.3%	1.9
4	-£67,501^{N}	-5.1%^{N}	7.5^{N}	£115,329	14.0%	3.7	£133,371	42.1%	2.0
5	-£102,262^{N}	-6.2%^{N}	7.9^{N}	£133,567	13.0%	3.8	£160,495	40.7%	2.0
6	-£141,666^{N}	-7.3%^{N}	8.3^{N}	£141,721	11.6%	4.0	£184,043	39.1%	2.1
7	-£195,833^{N}	-8.7%^{N}	8.9^{N}	£140,972	10.0%	4.2	£200,579	36.8%	2.2
8	-£250,218^{N}	-9.8%^{N}	9.4^{N}	£139,471	8.7%	4.4	£216,497	35.0%	2.3
9	-£325,380^{N}	-11.5%^{N}	10.4^{N}	£117,185	6.6%	4.7	£225,357	32.7%	2.4
10	-£407,266^{N}	-13.2%^{N}	11.5^{N}	£88,497^{N}	4.5%^{N}	5.1^{N}	£232,096	30.5%	2.5
11	-£490,617^{N}	-14.7%^{N}	12.6^{N}	£58,430^{N}	2.8%^{N}	5.4^{N}	£237,978	28.7%	2.6

*: Base case, ^{N}: uneconomic results

Under the beneficial condition, the economics of all cases improve, particularly in the case of the 500Ah ESS. Under the based case condition, installing 500 Ah ESSs at the top 6 identified best centre stops is economically feasible (as shown in Table 4-7). With a 20% lower battery price or a 20% higher electricity price, it becomes economically feasible to install 500 Ah ESSs at the top 10 identified best centre stops (as shown in Table 4-16 and Table 4-17). Also, with a 20% longer battery life, it is economically viable to add 500 Ah ESSs at the top 9 identified best centre stops (as shown in Table 4-18). Still, adding more ESS degrades economic viability.

As shown in Table 4-7 and Table 4-16 to Table 4-18, in most cases either under the base case condition or the beneficial conditions, installing the 100Ah ESS would achieve the best NPV, IRR, and DPP among the three ESS with different capacities. However, similar to the base case, under each beneficial condition, choosing the 500Ah ESS leads to the best NPV if only one ESS will be added to the system. Besides, Once the battery price is reduced by 20% and when the number of ESSs added equals or is less than three, installing the 500Ah ESS will result in the best NPV. Also, Once the electricity price becomes 20% higher and when the number of ESSs added equals or is less than two, installing the 500Ah ESS will achieve the best NPV. However, installing 100Ah ESSs results in the best IRR and the shortest DPP in all cases.

4.4.5 The potential merit of using EVs for energy storage to the tram network

The battery purchase price is found to be an influential factor in the economic feasibility of ESS deployment. As the battery price is determined by the production technology and the market, it cannot be reduced from the customer perspective. However, if EVs can be used as part of the installed ESS, the capital investment costs of an ESS can be substantially reduced. A further economic feasibility study on a theoretical single ESS installation at Park Grange Croft was conducted to illustrate the potential merit of incorporating EVs into the energy storage system on the tram network. The EV batteries are expected to deliver the same energy storage capacity and the same energy-saving as the corresponding stationary ESS does, albeit the time that they are available (when the car is parked and connected to the system) is variable.

Taking this approach, the stationary battery is assumed being replaced by the EV battery but other components are remained. Hence, the cost of on battery is waived, thereby lowering the CAPEX and the OPEX related to maintenance of the ESS (shown in Table 4-6). Table 4-19 shows the cost breakdown of the ESS without a stationary battery.

Table 4-19 The costs per ESS without a stationary battery

Capacity of battery	Cost of battery	Cost of other components	Cost of installation	CAPEX	OPEX per Annum
1000Ah (390kWh)	£0	£41,496	£10,000	£51,496	£1,545
500 Ah (195kWh)	£0	£20,748	£10,000	£30,748	£922
100 Ah (39kWh)	£0	£4,150	£10,000	£14,150	£424

However, exploiting an EV battery as the ESS for the tram network is expected to contribute additional operating cycles to the EV battery which could potentially degrade the battery life

quicker than seen in normal EV use. Therefore, this research assumes that the tram service provider would provide the EV owners, who allow their EVs to be used as energy storage for the tram network, with incentives (e.g. discounted travel perhaps) to compensate for the use of their EV battery. The undiscounted annual cash flow of using EV batteries as the energy storage for the tram system (ACF_{EV}) is therefore calculated via Equation 4-7.

$$ACF_{EV} = Annual\ Income - OPEX_M - OPEX_C \quad \text{Equation 4-7}$$

where $\boldsymbol{OPEX_M}$ is the annual OPEX related to maintenance, and the $\boldsymbol{OPEX_C}$ is the annual OPEX related to the compensation provided to the EV owners.

This research estimates the compensation via scaling the energy-saving delivered, which can be considered as the braking energy firstly stored in the EV battery and subsequently discharged back to the tram network from the EV batteries. This research considered the electricity discharge is in unit of kWh_{ED} or $MWh_{ED,}$ and it subsequently provides a reasonable assumption on the degradation cost per unit electricity discharge, which is expressed as an aconynom of C_D and is in the unit of of £/kWh_{ED} or £/MWh_{ED}. Zhou, et al. [168] reported that, in concept, the C_D can be estimated by dividing the cost of the battery with the battery cycle life. The battery cycle life could be prolonged if the depth of discharge (DoD) is small, for example, Miao, et al. [169] reported that reducing the DoD from 20% to 10% will increase the potential life cycles of Li-ion battery from 2,000-9,000 to 6,000-15, 000. Zhou, et al. [168] reported a C_D of approx. £0.040-0.060/kWh_{ED} (£40-60/MWh_{ED}) for the Li-ion battery based on a battery cost of £128/kWh and a life cycle of 2,200 estimated from a rated DoD of 95%. This research therefore assumes:

- the DoD of the EV battery exploited for energy storage for the tram network could be regulated <20%
- according to Miao, et al. [169] the life cycle of the EV battery for this application is at a reasonable value of 6,000
- the life cycle is directly inversely proportional to the C_D

Hence, the estimated C_D could be potentially reduced to 2,200/6000=36.6% as £0.015-0.022/kWh_{ED} (£15-22/MWh_{ED}). This study thereby exploited a C_D of £0.018/kWh_{ED} to estimate the annual OPEX on compensation ($OPEX_C$) based the reduction of the energy supplied from the substation (-E_{sub} in Table 4-3) via Equation 4-8

$$OPEX_C = (-E_{sub}) \times 365 \times C_D \quad \text{Equation 4-8}$$

where the $-\boldsymbol{E_{sub}}$ is the reduction of the daily energy supplied from the substation shown (as -Esub) in Table 4-3, $\mathbf{365}$ is the number of days in a year, and $\boldsymbol{C_D}$ is the degradation cost per unit electricity discharge and is taken as £0.018/kWh$_{ED}$.

As shown in Equation 4-7, this study included annual OPEX related to the compensation into the economic evaluation of using EV batteries as ESS for the tram network. Besides, a ±20% variation is given to the C_D for studying the impact of the compensation cost on economics. Results are shown in Table 4-20.

Table 4-20 The economic evaluation based on ESS battery gets replaced by the EV battery

Battery Cost (£/kWh) and C_D (£/kWh$_{ED}$)	ESS Battery Capacity:1000Ah			ESS Battery Capacity:500Ah			ESS Battery Capacity:100Ah		
	NPV (£)	IRR (%)	DPP (year)	NPV (£)	IRR (%)	DPP (year)	NPV (£)	IRR (%)	DPP (year)
£0, £0	£40,173	24.1%	2.6	£57,432	52.8%	1.6	£33,721	65.6%	1.3
£0, £0.015	£13,499	8.7%	3.8	£32,418	31.7%	2.3	£20,229	41.6%	1.9
£0, £0.018	£6,830^N	4.5%^{N}	4.3^N	£26,164	26.1%	2.5	£16,856	35.3%	2.1
£0, £0.022	£162^N	0.1%^{N}	5.0^N	£19,911	20.3%	2.9	£13,483	28.9%	2.4
£133, £0*	-£18,251^N	-6.4%^{N}	6.3^N	£28,219	15.9%	3.2	£27,879	41.9%	1.9

*: Base case, ^{N}: uneconomic results

As can be seen from Table 4-20, using the EV battery for energy storage could improve the economics if the C_D is equal to or lower than the base case value of £0.018/kWh$_{ED}$, especially for the large capacity applications. The C_D that relates to the OPEX on compensation to EV owners has a bigger influence on economics than the OPEX on maintenance does. Using the EV battery for energy storage will reduce the CAPEX and the annual OPEX on maintenance by 27-50% (as shown in Table 4-6 and Table 4-19). At the same time, it also introduces additional OPEX for compensating the EV owners. Consequently, replacing the stationary ESS with EV battery will change the nature of the investment. As illustrated via the application with 500 Ah capacity and/or a C_D=£0.018/kWh$_{ED}$ in Figure 4-18,

1) In the stationary ESS case, the OPEX is only spent on maintenance and contributes 11% of the cost throughout the project
2) In the EV battery case, the total OPEX contributes 94% of the cost throughout the project due to the additional OPEX spent on compensation

Therefore, the C_D is considered an influential factor to the economic feasibility of using EVs for energy storage on the tram network.

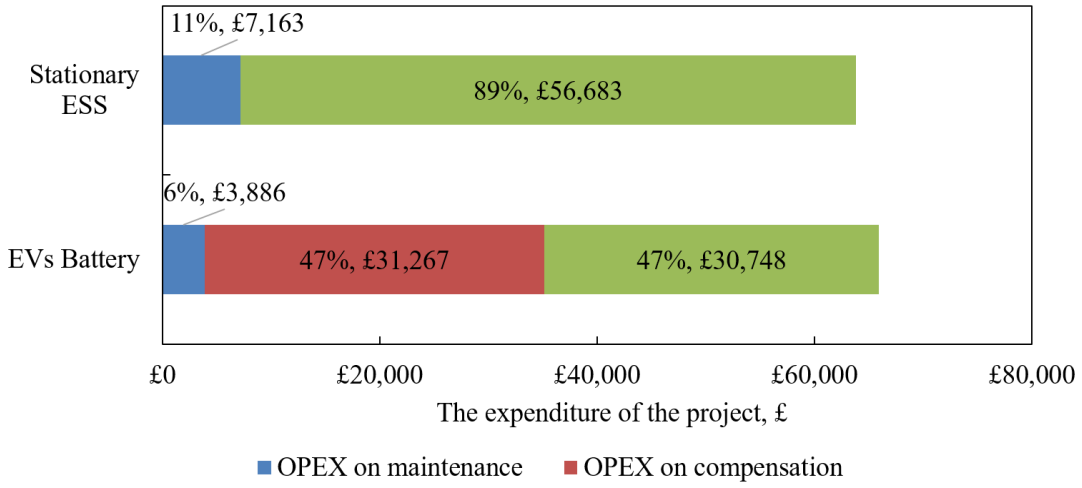

Figure 4-18 The breakdown of CAPEX and OPEXs of using Stationary ESS and EV battery for energy storage for the tram network

The determination of the C_D is profound as it requires comprehensive modelling and simulation of the state of charge (SoC), DoD, and the related potential degradation of capacity, etc. of the battery, that is tailored for different specific energy-storage scenarios. Besides, apart from the C_D, various factors could also impact the OPEX on compensation, for example, the reward (i.e. free or discounted parking or tram travel) to the EV owner, and/or the potential net electricity (from the braking energy of tram network) remained in the EV batteries, etc. If such rewards to be given by the tram operator to the EV owner could equal or be greater than the fee given by the tram operator to the EV owner for compensating the loss due to the degradation of the EV battery, then the OPEX on compensation could be eliminated, and finally, the economics could be further improved, as shown as the case with a battery cost of £0 and a C_D £0 in Table 4-20. This research considers using the EV battery as energy storage for the tram network, and demonstrates a promising option that could lead to better economic feasibility. Still, to provide a more reliable and comprehensive feasibility study for this exploitation, it requires further research on:

- investigating the SoC and DoD of the battery,
- determining the battery degradation,
- developing an intelligent control method that prevents the range anxiety of the EV drivers and minimises the battery degradation [117, 118, 120, 169], and

- studying the economic feasibility with careful consideration of all the available incentives to the EV owner [170].

4.5 Chapter summary

This chapter firstly introduces the design principle for and the structure of ESS system. The ESS has a converter module, a control module and an energy storage module that consists of a battery. By using the a double-closed loop control strategy, the ESS can be charged from tram braking energy, and discharge its energy to the tram system for traction uses according to the catenary voltage.

Furthermore, this chapter presents findings obtained from applying the ESS in separate OCS and common OCS. Although the systems added with the ESS used different power supply methods, the feature of the ESS addition on the energy saving were found to be similar. Generally, installing the ESS close to the mid point of the energy supply section likely results in the best energy saving performance. Therefore, multiple or a network-wide installation likely favours adding the ESS on the centre stops. Moreover, the higher maximum current, which is positively related to the discharge limit rate and battery capacity, will lead to a better energy saving. However, as the maximum current drawn by the tram is limited, a smaller ESS with an optimal discharge limit rate could be more efficient at energy saving than a larger capacity ESS.

Finally, this chapter shows the result of the economic feasibility study of applying an ESS on a tram network. It suggests that the economics stay viable when the number of 100 Ah ESS installations fully reaches the 11 available locations on the network in consideration, and the number of 500 Ah ESS installations reaches 6. However, no 1000 Ah ESS installations were found to be economically feasible under the base case assumptions. From the sensitivity study, both higher electricity prices and longer battery life are found to have positive impacts on the economics of all single ESS installations with various battery capacities. Higher battery purchase price, and higher installation costs both negatively impact the economics, the former has a greater impact on ESSs with a higher capacity, and the latter has a bigger influence on ESSs with a lower capacity. Similarly, the electricity price and asset life heavily and positively affect the economics of all the multiple ESSs addition. Meanwhile, the battery price also substantially negatively influences the economics of the multiple 1,000Ah and 500Ah ESSs additions but mildly impacts the economics of the multiple 100Ah ESSs additions. When the

ESS battery was replaced by EV batteries, and the cost of the battery was thereby removed, the economic feasibility improved substantially. High battery capacity installation would be able to generate a similar or greater profit compared to the low battery capacity ones. Using EVs for energy storage to the tram network could be more advantageous on the economic feasibility than the stationary ESS.

The following chapter will therefore consider the technical analysis of combining a stationary ESS with EV batteries which become available for energy storage on the tram system at various times during the day.

Chapter 5. Impact of the implementation of EV Energy Storage System

Previously, Chapter 4 investigated the energy-saving and economic feasibility of adding stationary ESSs to the tram network, to address the energy lost through braking events. It was found that an ESS installation can improve energy efficiency, but the high cost of the battery limits the economic feasibility in some cases. Thus, this chapter investigates the exploitation of EV batteries within an ESS as a method of reducing the high initial capital cost of the 'energy storage element' of the ESS, and subsequently examines the efficiency and financial impact on the tram system of this approach.

Compared to the conventional approach of stationary trackside ESS, using EVs as ESS is both novel and adventurous, since the connection between an EV and the tram system is temporary instead of permanent. In addition, both the EV battery and the tram system operate at DC, and therefore a dc-dc would be required as the EV charging / discharging interface. Thus, firstly, the modelling and simulation of the energy balance should be over a shorter period, hourly in the first instance, to accommodate the intermittent connection due to the EV mobility. Secondly, the study should investigate both a complete replacement of the stationary ESS with EVs, in addition to the integration of stationary ESS and EVs together at a single location. Hence, this chapter includes:

- Section 5.1 - analyses of the operating profile of the tram at different times during a day, and presents the hourly energy balance of a typical weekday, a Saturday and a Sunday.
- Section 5.2 - proposes an EV related ESS that only exploits an EV as the energy storage system, and analyses the impact of the EV availability on the energy balance.
- Section 5.3 - proposes an ESS that exploits both a stationary battery component and a number of EVs as mobile energy storage units, and reports a control method that integrates the two.
- Section 5.4 - compares the three types of ESSs (stationary ESS, a purely EV ESS and an ESS that consists of a stationary battery and EVs) and explains their different impacts on the system energy balance.
- Section 5.5 - studies the system operational and financial impacts of the proposed network-wide ESS installations.

5.1 Hourly energy balance of tram system

Since fundamentally, EVs are mobile, both car park operating hours, and the drivers' needs impact the length of time any given EV is available as an energy storage system for the tram network. As the availability of any given EV may be only one or two hours, it is important to understand the hourly energy balance of the Supertram since the hourly energy balance later forms a baseline from which to determine the impact of using EVs as an ESS on the tram system. It could be argued that a finer temporal division such as 30 minutes, or 10 minutes would allow more accurate determination of the EV availability. However, given that at certain times of the day, a tram is only available within a network section every 20 minutes, hourly intervals seem the most appropriate temporal split.

5.1.1 Analysis of operational data

As the energy balance is simulated based on the tram operational profile, this study firstly analyzes the tram profile during a day. As mentioned in Chapter 3, observation of the tram operation suggests that the tramcar operating profiles for the same journeys, but taken at different times, are generally the same if the number of tramcars stops remain similar. However, the Supertram operates a "stop by request system", and hence, the tram car would not stop if no one requests a stop to get off or on the tram. During the early morning, late evening, and night time when passenger numbers are low, tramcars could therefore omit stops due to no passengers embarking or alighting at a given stop. Omitting stops will lead to less regenerative braking events, and tram accelerations, which subsequently impacts the energy balance.

This section focuses on the tram journey between Halfway and Gleadless Townend on the Blue route for illustration. Figure 5-1(a) and Figure 5-1(b) show the velocity profiles of two tram journeys that departed at the same time during the Peak Period but on different days, and they indicate the overall profiles are similar with the tramcar stopping at every stop (as the velocity becomes zero). Velocity profiles of a tram journey that departed at the same time during off-peak periods, but on different days, are also similar as shown in Figure 5-1(c) and Figure 5-1(d). However, the velocity profiles of peak period and pff-peak period are very different from the peak period operating patterns, as shown in Figure 5-1(a) and Figure 5-1(c) that are both from one day, and in Figure 5-1(b) and Figure 5-1(d) that are both from a second day.

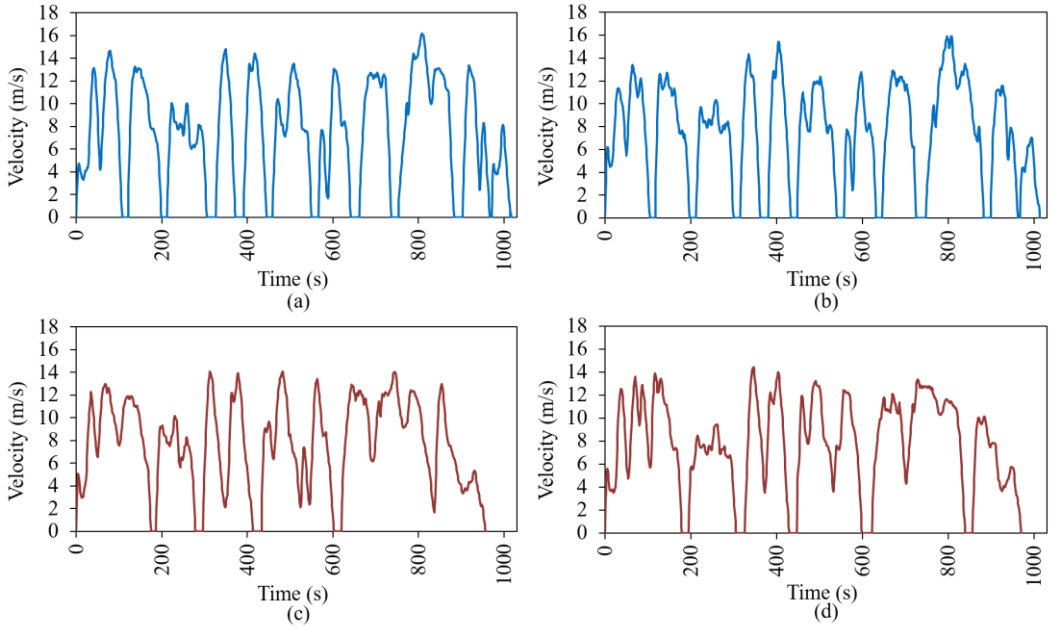

Figure 5-1 The speed profile of tram journey between Halfway and Gleadless Townend

Thus, this study subdivides the daily tram schedule and defines the segments as:

- Peak period: 07:00 to 20:00
- Off-peak period: 05:00 to 07:00 and 20:00 to 01:00 (+1)

Another sampling campaign was conducted which collected the tramcar's operational data, i.e. distance, velocity, and acceleration, using GPS data logging of journeys onboard a tram. This sampling was carried out during both peak periods and off-peak periods. Each day's sampling event thereby obtained two groups of data, the 'Peak Period Operational Data' (PPOD) and the 'Off-peak Period Operational Data' (OPOD). Both the PPOD and OPOD include the tramcar's operational data of every route in the whole network. Considering the tram departure timetable also varies between weekdays, Saturdays, and Sundays, the data sampling campaign was conducted on three different days, a typical weekday, a Saturday and a Sunday.

5.1.2 Simulation method

In order to simulate the hourly energy balance based on the travelling data collected at different time periods, this study optimized the simulation approach used in Chapter 3. Figure 5-2 shows the schematic of the process. As can be seen, there are three steps, 1) Data calculation, 2) Matlab modelling, and 3) Simulink modelling.

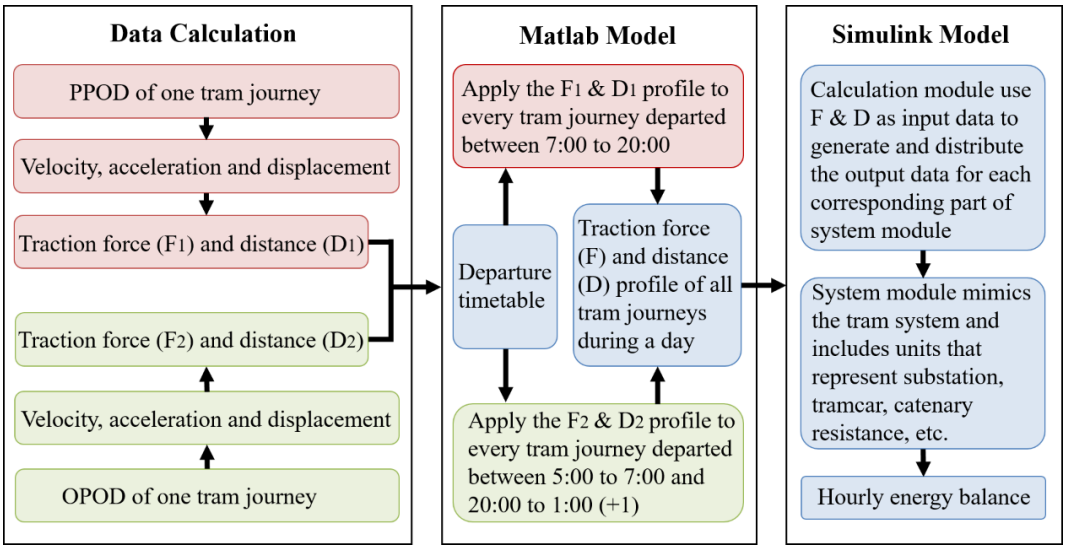

Figure 5-2 The schematic of simulation method

In the data calculation step, the PPOD and OPOD data, which contains the velocity, displacement, and acceleration recorded per second during one whole tram journey, is used to obtain the traction force and distance travelled, via a method developed from and similar to the method used in Chapter 3.

Those two sets of traction force and distance data were subsequently used in a Matlab model. Here, the model assigns the traction force and distance travelled, derived from the PPOD to every tram journey that departs between 07:00 and 20:00. Additionally, the traction force and distance travelled derived from the OPOD data is assigned to every tram journey that departs between 05:00-07:00 and 20:00-01:00(+1). Therefore, the traction force and travelling distance profile of every tram journey over a single day's operation was assembled.

Finally, the daily traction force and distance profile generated previously was used as an input to the Simulink model, which is the same as the one used in Chapter 3.

5.1.3 Hourly energy balance

The hourly energy balance of the whole tram system is obtained from the model and shown in Figure 5-3 with Figure 5-3(a) for the weekday, Figure 5-3(b) for the Saturday, and Figure 5-3(c) for the Sunday.

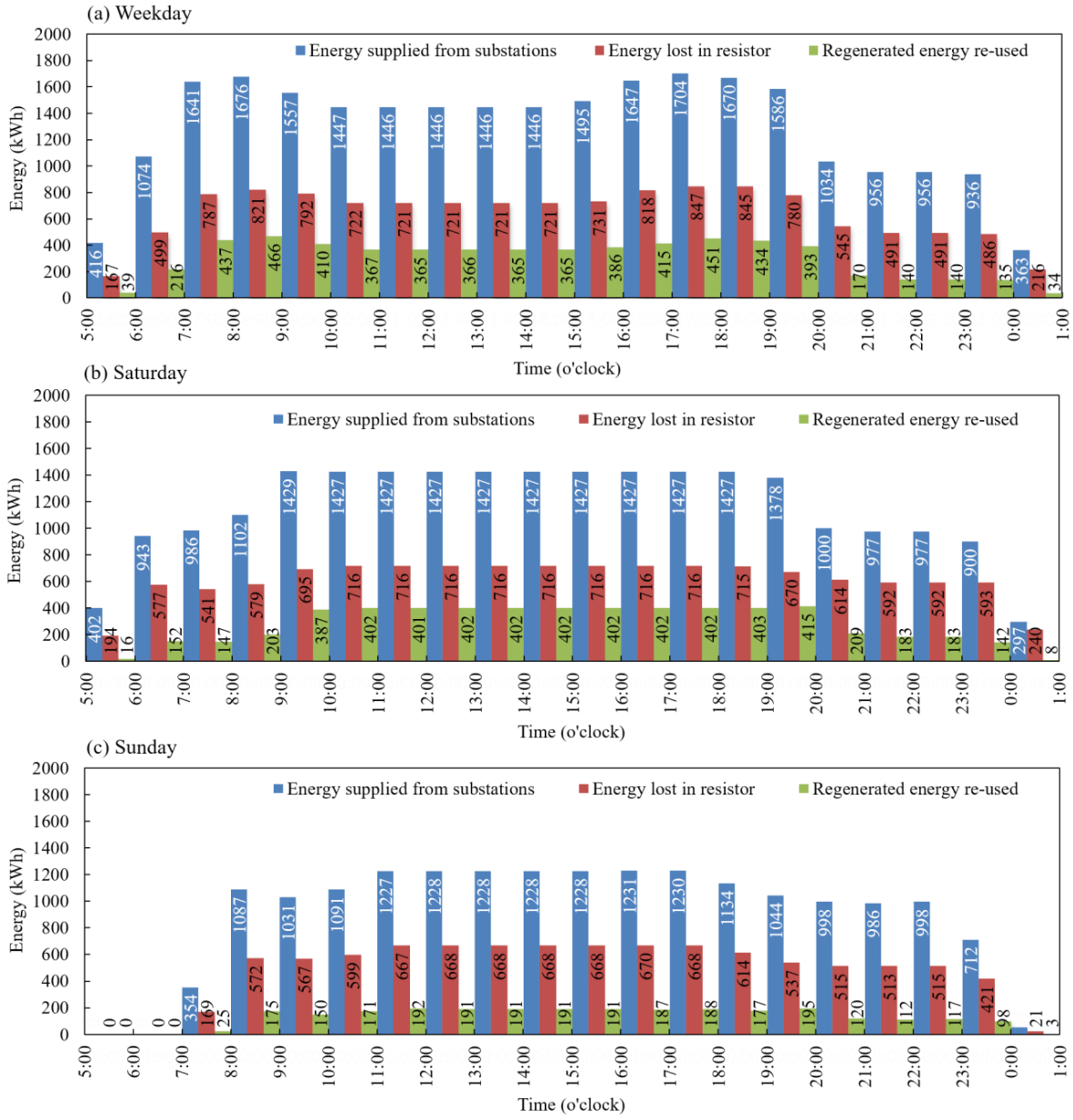

Figure 5-3 The hourly energy balance of the Supertram

As can be seen in Figure 5-3,

1) All three balances follow the pattern that the hour with higher energy supplied from the substation usually has the highest energy lost in the braking resistors. Typically, the energy lost in the resistors equals approximately half of the energy supplied from the substation.
2) In all three balances, the energy supplied from the substation during the peak period is found to be higher than that during the off-peak period.
3) All the energy consumed, wasted and recovered on Saturday and Sunday was found to be substantially lower than on a weekday, which is likely caused by fewer tram departures over the weekend compared to weekdays, especially on Sunday. Additionally, on weekdays

and Saturdays, the first departure is at around 5:00 AM, but on a Sunday this occurs at around 7:00 AM.

This research summed up the three hourly balances to acquire the daily energy balance of weekday, Saturday and Sunday and compared them with the mean energy balance result (common OCS) presented in Section 3.4.3 in Chapter 3, as shown in Figure 5-4.

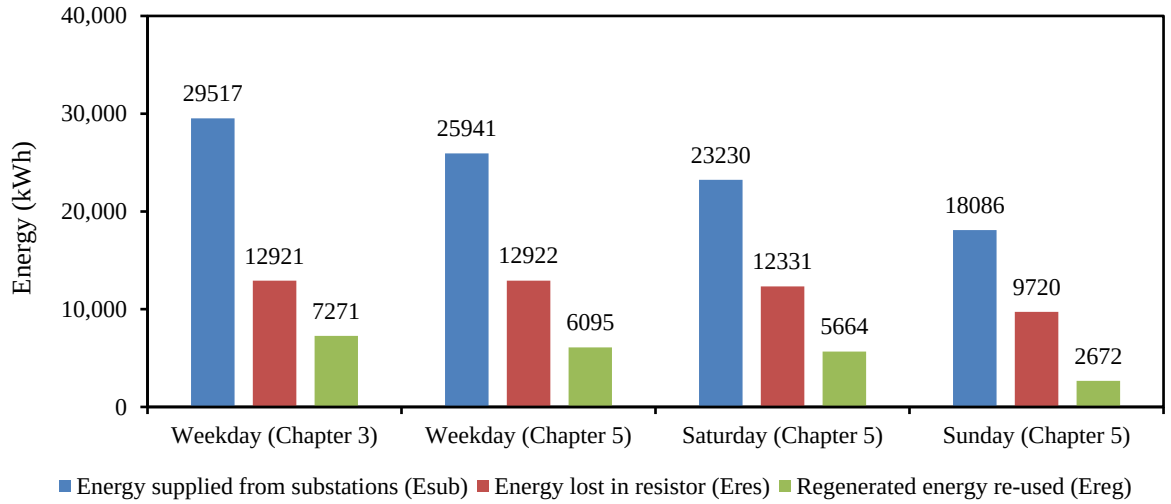

Figure 5-4 The daily energy balance obtained from different operational data

As aforementioned, the hourly balance presented in this chapter is obtained from a more explicit data set that considers the impact of the peak and off-peak period on the tram's operation, and thus, the corresponding daily energy balances obtained by summing up the hour balances are also influenced by the difference of tram travelling between the peak and off-peak period. As presented in Section 5.1.1, the peak period tram travelling could have more braking and acceleration than the off-peak period tram travelling, likely due to the heavy traffic on the road or more passengers' requests to stop. Hence, the more peak period tram travelling, or the busier peak period that also elevates the number of braking and acceleration due to heavy traffic, would result in a higher E_{res} associated with the more brakings and a higher E_{sub} associated with the more acceleration. In addition, the more frequent braking could also lead to a greater E_{reg}. Typically, the weekday is moderately busier than Saturday and is substantially more active than Sunday, and the weekday shares a similar number of departures with Saturday but has a substantially more departures than Sunday. Consequently, it has the highest E_{sub}, $E_{res,}$ and E_{reg} among the three, as shown in Figure 5-4. Since the daily energy balance presented in Chapter 3 was simulated only based on the peak period data, intrinsically, it would be related to more

brakings and acceleration and thereby have higher E_{sub}, E_{res} and E_{reg} than the other three balances acquired based on both peak and off-peak period data. As can be seen in Figure 5-4, the daily energy balance presented in Chapter 3 would normally have a higher E_{res}, E_{sub}, and E_{reg} than any other energy balance obtained in this chapter.

Regarding exploited EVs as the energy storage for tram, the expected time during which EVs are parked in car parks adjacent to the tram will likely match the period that the Supertram has a higher energy supplied from substations and therefore energy lost in the resistors, i.e. during peak periods on a weekday. Hence, the utilization of EVs as an ESS could appear a sensible approach to potentially recovering braking energy when the energy wastage is high, and also flatten the peak time load of the substation as seen by the utility grid.

5.2 Electric vehicle energy storage system

Conventional trackside ESS's usually only exploit a stationary battery as an energy store, and are termed Stationary Energy Storage Systems (SESS) in this chapter. This study considers there are two approaches to using EV batteries as energy storage, one is to solely replace the SESS with the mobile EV batteries, and the other is to use the EV batteries to only partially replace the capacity originally provided by the SESS. In this chapter, a system that only contains the EV batteries is termed an Electric Vehicle Energy Storage System (EVESS), and the system that combines the EV batteries together with a stationary battery is termed a Combined Energy Storage System (CESS).

5.2.1 Design of model

A detailed description of a standard SESS was reported in Chapter 4. The EVESS model used here is developed from that previously described SESS model, and the schematic of it is illustrated in Figure 5-5. Both models consist of two key components, the connection device, and the energy storage device.

A DC-DC converter is the main component of the connection device. This is mainly responsible for transferring the surplus braking energy produced on the tram system to the battery, and to feed the energy stored in the battery back to the tram system when required. The SESS only requires one connection device (DC-DC) to link the battery to the track, however the EVESS

could require multiple connection devices, as in a system with multiple EV's, each EV will require its own charger / interface.

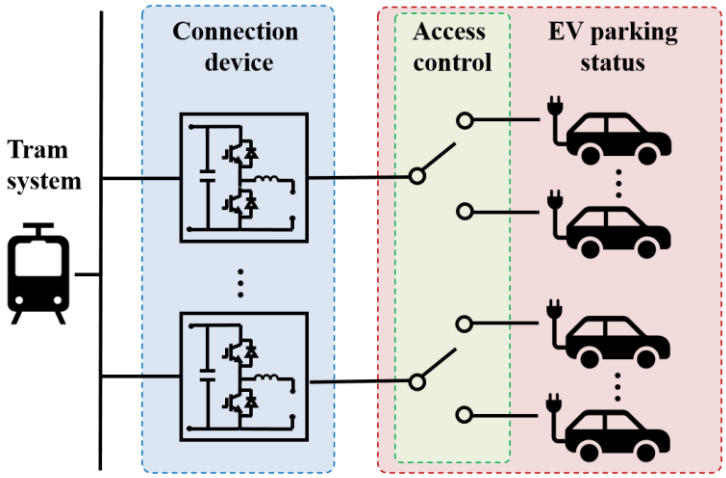

Figure 5-5 The schematic of the configuration of EVESS

The major difference between the SESS and the EVESS arrangement is on the energy storage side. The battery in the SESS is stationary, and hence, the SESS model only includes one battery unit of a fixed, predetermined, size. However, since EVs are mobile and their connection with the tram system is temporary, the EVESS model has multiple battery units in the model, each representing an EV. Additionally, the model also includes an Access Control unit for controlling the 'when' and 'how' to connect the battery units, to mimic the different parking statuses of the EV(s).

5.2.2 The influence of variables of electric vehicles parking status

Both the parking period of each EV, and the number of EVs parked at any given time impacts the EV availability, and the two also constrain each other. For example, during a 24-hour period, if each EV connects to the system for 2 hours, then one connection device can accommodate 12 EVs in sequence, if the parking duration per vehicle increases to 4 hours, the number of different EVs which can be accommodated with a single connection device reduces to 6. To accommodate the two variables related to the EV parking status and how this affects the energy recovery, different scenarios were considered.

This research initially focuses on the energy supply section between Carbrook and Nunnery Square, as an example for illustration. This track section has a typical, moderate length, and

passenger flow. Moreover, it also has a shopping park located at its center stop, which currently has a car park equipped with an EV charging point. As the example simulation presented in this section, and in the later Sections 5.3 and 5.4, are to demonstrate the design concepts and the characteristics of the different ESS, they are all conducted based on a tram weekday operating profile with the different ESS installed at the mid-point stop of the energy supply section.

For the purposes of this research, it is proposed that the EVs are parked in the car park during normal daytime working hours, and are therefore available to be plugged into the system to charge. Thus, this study initially assumed the parking period ranges between 08:00 and 18:00. Since, in this case, the car park is located next to the shopping center, the study assumed the minimum parking time is 2 hours, commensurate with a typical stay at a shopping center car park [171].

The characteristic of the EV battery could also impact energy recovery. Based on the typical specification of EV batteries (see section 4.3), it is assumed that the EV battery has a capacity of 100 Ah (39 kWh at 390V nominal) and has a limited charge and discharge rate of 2C. The capacity available to the study, namely the 'emptiness' of the EV battery (state of charge), could also impact the system energy recovery, and realistically could be at any level between full and empty when the car is plugged in. Thus, this study assumes that the State of Charge (SoC) of every EV to arrive is set to 50%, and the full state is regulated to a SoC of 95%, to protect the battery from overcharge.

This study also examined how variations of individual parking times and the total number of EVs parked impacts on the energy-saving for the system. Thus, the EV parking time was assumed to vary and be either 2 hours, 5 hours, or 10 hours. With regard to the total number of EVs parked, this study assumed two scenarios, 1) only one EV is parked on any given day for the allotted period, and 2) there are sufficient EVs parked to share the 10 hours parking period. In total, five combinations, which are illustrated in Figure 5-6, were considered and investigated.

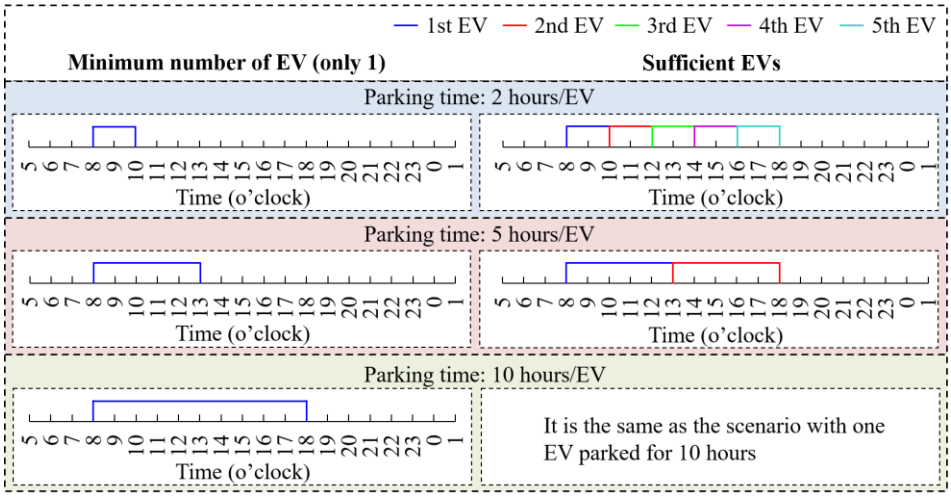

Figure 5-6 The scenarios studied for understanding the influence of variables in EV parking status to energy balance

Figure 5-7 shows the SoCs of the EV batteries of the five scenarios. Firstly, because the frequent traction and braking actions of the tram will take energy from, and export energy to the EV battery, the EV battery constantly switches between the discharging and charging mode. Therefore, its SoC exhibits a low level ripple. Indeed, the substation is much more capable of providing a great amount of energy to the tram system in a short period of time than the EV battery can, therefore, the amount of energy fed from the EV battery back to the tram system is relatively small. Overall, after every tramcar passes by, the energy flowing into the EV battery is larger than that taken from the battery. This leads to the EV battery being charged during its time connected to the tram system.

Figure 5-7 (a), (b) and (c) show the SoC of an EV battery of one EV parked for 2 hours, 5 hours, and 10 hours between 08:00 to 18:00, and it suggests that the EV battery would become fully charged within 2-3 hours. However, the EV battery can still provide some energy storage to the tram system even when it is fully charged, since the tram system can take energy from the battery when the tram accelerates, thereby creating room for the battery to absorb energy produced from the next braking event. However, this may not be an ideal operating scenario.

Figure 5-7 (d) and (e) show the SoC of each individual EV battery of the two EVs parked and the five EVs parked sequentially, respectively. As can be seen, if there were two EVs sharing the 10 hours parking period, the braking energy from the tram system was able to fully charge both. If there were five EVs sharing the 10 hours parking period, the braking energy was not able to fully charge every EV battery but could provide a substantial recharge to each of them

in turn. In this scenario, the amount of energy delivered to the EV would be dependent on the frequency of the tram braking events, which is in-turn dependent on the operating timetable which varies throughout the day.

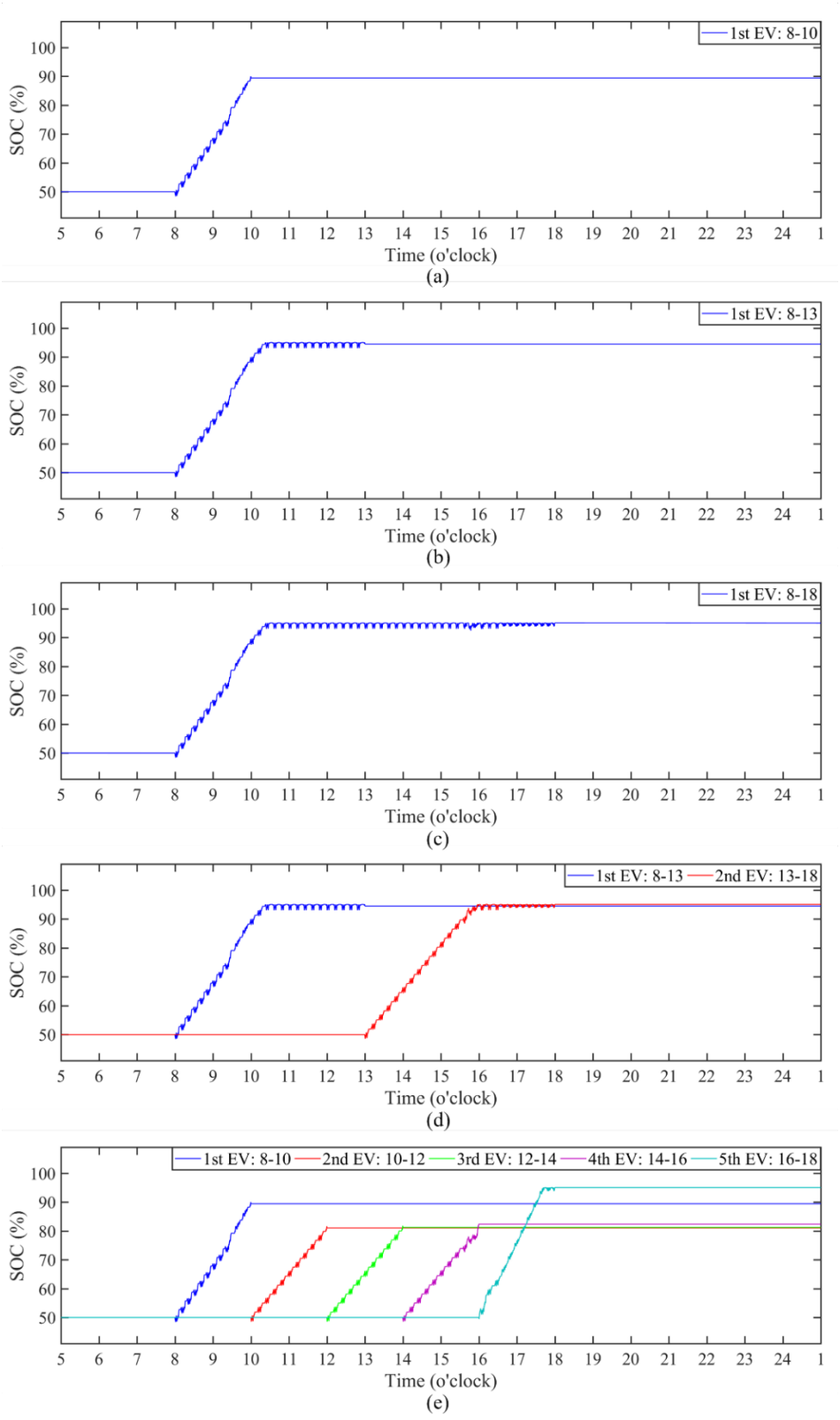

Figure 5-7 The SoC of EVs battery of the EVESSs equipped with on connection device but with different EV parking status

In principle, the EVESS serves to first collect the braking energy to reduce waste in the dump resistors on the tram system. Part of the energy collected will be later reused for tram traction and leads to a corresponding reduction in the energy supplied from the substation, in turn lowering the utility supply bill. Meanwhile, the rest of the energy collected will be stored in the EV battery and then removed from the system when the EV departs. The summary impact of the five scenarios of parking status on the daily energy balance of the energy supply section between Carbrook and Nunnery Square is therefore shown in Figure 5-8.

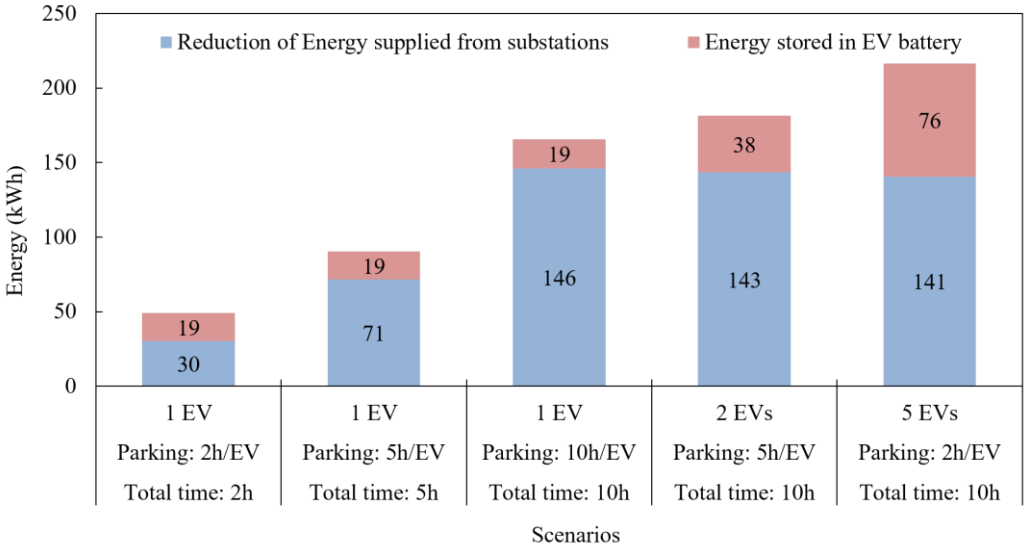

Figure 5-8 The energy saving and recovery delivered by the EVESSs equipped with one connection device, but with different EV parking status

The results suggest that:

1) The first three scenarios (from the left in Figure 5-8) demonstrate that when the number of EVs connected to the tram remained the same, the increase of parking time of the EV will increase the reduction of energy supplied from the substation. Since only one EV was connected in all three scenarios, the energy stored in and taken away by the EV in each scenario was the same, governed by the EV battery capacity and SoC on arrival.
2) In the last three scenarios, the total EV connection time was the same, 10 hours. To the tram system, no matter whether the EV parked/connected will change or not, there was always one EV serving as an ESS to share in the load of the substation. Hence, the reduction of energy supplied from the substation of all three scenarios was similar. However, if the turnover of parked EVs leads to more frequent refreshing of the energy storage, thus increasing the number of EVs parked during the period of interest, more energy would be stored in and removed by the EVs.

3) Conclusively, the total parking time of the EV, namely the total connection time of the EV impacts the reduction of energy supplied from the substation. The number of EVs parked affects the amount of energy eventually stored in the EVs when they depart.

5.2.3 The influence of the number of connection devices

The above study on the parking status suggests that the greatest energy saving was achieved via having 5 EVs, each parked for 2 hours, and the worst energy saving was achieved through having only one EV parked for 2 hours. In order to understand the impact of the number of connection devices on the energy balance, this study applied these two extremes on each of the three scenarios with different numbers (one, two, and three) of connection devices. Therefore, six sub-scenarios were formed and examined, as shown in Figure 5-9.

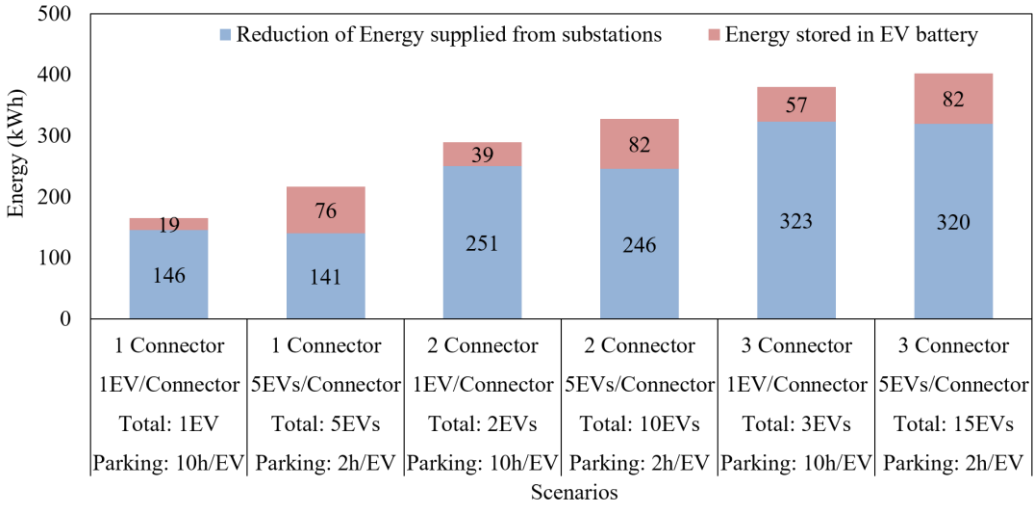

Figure 5-9 The energy saving and recovery delivered by the EVESSs with different number of connection devices and different EV availabilities

The result of reduction of energy supplied from substations and energy stored in EV batteries delivered by each sub-scenario are shown in Figure 5-9, which demonstrates:

1) The number of connection devices will positively affect the reduction of energy supplied from the substation. This is likely attributed to the individual EV battery discharging limit rate (2C) becoming scaled by the number of connection devices.
2) The refresh rate of the EVs parked positively affects the energy that could be removed by EVs. However, when the total number of EVs parked reaches a limit, the total energy gained by the EV batteries no longer increases, as this reaches the maximum that is available from the tram system. i.e. the total available energy capacity of all the EVs exceeds the energy available from the tram system braking events.

5.3 Combined energy storage system

The CESS is a further energy storage solution that utilises available parked EV batteries. However, it also includes two sub-systems, one is the stationary sub-system, equipped with a stationary battery, and the other is an EV sub-system that uses available EV batteries as energy storage. This study investigates the configuration of the two sub-systems to determine the combination that achieves the best synergy between the them.

5.3.1 Introduction of the design concept

In principal, the aim of the model design is to define how the sub-systems achieve the required energy exchange between each other, and with the tram system. The approach should allow the two sub-systems to absorb the braking energy when the tramcar brakes, and provide energy back to the network when the tramcar accelerates. Hence, the energy exchange between both sub-systems and the tram system should be bi-directional, as before. From the results shown in section 5.2, overall, the tram system gradually charges up any attached SESS, as there is more braking event energy available than is removed from the store with each acceleration event. The SESS, with only a stationary battery, acts as a closed system, and the battery gets fully charged quickly, requiring remedial action from the control system to enable it to continue to operate. Therefore, once the battery is full, it can't further store the braking energy, and thus surplus braking energy will be wasted, or control will be required to manage this excess charging. Thus, the introduction of a mobile EV battery can "open up" the system as the departure and arrivals of EVs will provide a convenient route for the removal of stored braking energy, and refresh and 'expand' the storage capacity, which in turn, should result in a better energy-saving performance. Thus, this study is designed to achieve an energy exchange where energy can flow from the SESS sub-system to the EVESS sub-system components.

As both sub-systems have to connect to the tram catenary, the connection between the two can also be via the tram catenary, and requires no separate independent link. This connection method not only keeps the cost of connecting the two sub-systems to a minimum but also enables the two sub-systems to be installed at different stops if required. For example, the center stop of an energy supply section is the best location for the stationary sub-system, and the installation is relatively convenient. However, the center stop might not have a car park, or might not be suitable for building a car park, or may have insufficient car flow. Hence, it might be better to install the EV sub-system elsewhere, but close by, on the network rather than at the

center stop. To achieve the expected energy exchange between the two systems, a smart control system that is different from the control approach used in standard SESS and EVESS's is required.

5.3.2 The smart control

The independent ESS, the SESS and EVESS, all use the catenary voltage as a control variable to control the DC-DC converter to charge or discharge the associated ESS. The nominal voltage of the tram catenary is 750V. When the tram system has surplus energy and the catenary voltage exceeds 760V, the ESS will enter into charging mode, removing energy from the tram system. When the tram requires energy (for traction) and the catenary voltage drops below 740V, the ESS will enter into discharging mode feeding energy into the tram system.

Therefore, to achieve spontaneous energy transfer from a stationary sub-system to an EV sub-system via the catenary, the discharging voltage of the stationary sub-system has to be higher than the charging voltage of the EV sub-system. Figure 5-10 illustrates the schematic of the controls.

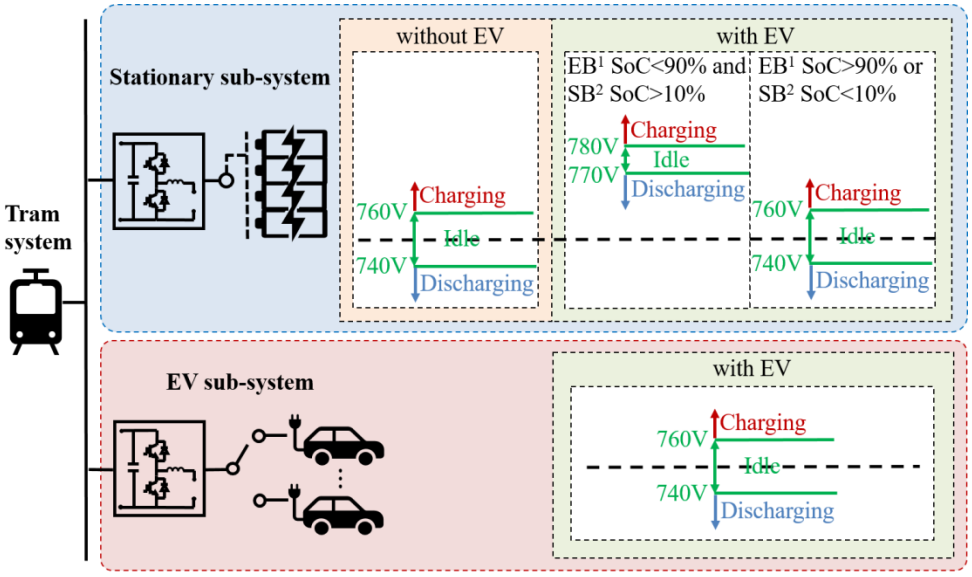

Figure 5-10 The schematic of the configuration and control of the CESS

When no EV is parked and attached to the system, and the CESS only has the stationary sub-system active, the stationary sub-system will not only collect the surplus braking energy but will also provide energy for tram traction when required. The charging and discharging voltage of limits are set at 760V and 740V respectively, as previously.

When there is an EV parked in the system, this study considered two scenarios:

1) When EV battery SoC is lower than 90% and the stationary battery SoC is greater than 10%, the system encourages the EV to charge from the energy stored in the stationary sub-system. Hence, the charging and discharging voltage of the EV sub-system is set at 760V and 740V as before. Concurrently, the voltage limits for the stationary sub-system are changed to 780V and 770V, respectively. This enables energy flow from the stationary sub-system to the EV sub-system, via the catenary.
2) When the EV battery SoC is greater than 90% or the stationary battery SoC is lower than 10%, the system no longer needs to provide energy from the SESS sub-system to the EV sub-system. The charging and discharging voltage of both sub-systems are returned to 760V and 740V respectively, and they function as before.

5.3.3 Scenario simulation

To verify the correct operation of the system, a CESS system, which is installed at the mid-point stop of the energy supply section between Carbrook and Nunnery Square, was simulated. The stationary sub-system has a stationary battery, which has a 100Ah capacity, a 2C limit discharge rate, and is initially set as full (SoC=95%, to protect the battery). For the EV sub-system, this study assumed five EVs were parked, and that each was parked for 2 hours, the EV batteries initially set as half full (SoC=50%), as before. The simulation results are shown in Figure 5-11. In detail, Figure 5-11(a) shows the SoC of each EV parked and connected to the EV sub-system, and Figure 5-11(b) shows the SoC of the stationary sub-system.

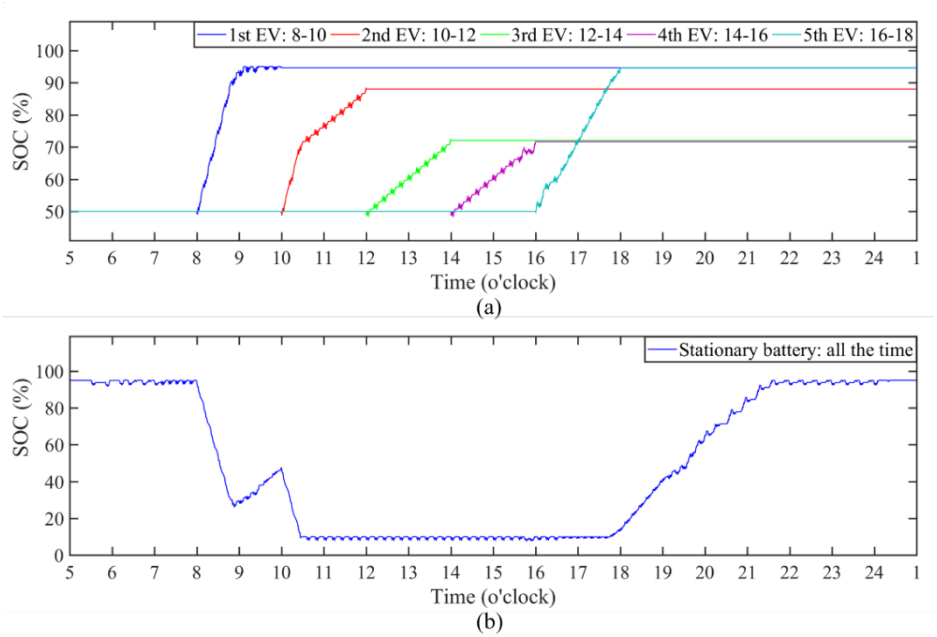

Figure 5-11 The SoC of the batteries in the CESS with a 100Ah stationary battery

As shown in Figure 5-11, during the first three hours of the simulation, no EVs were parked, and hence, only the stationary sub-system was active and responsible for providing energy storage to the tram system. From 08:00 to 10:00, the first EV parked and connected, the stationary sub-system discharged and the EV sub-system charged. Energy flowed from the stationary sub-system to the EV sub-system as required. After the EV was fully charged (with the 19-kWh of energy), the SoC of the EV remains around 95%. Meanwhile, the braking energy once again accumulates in the stationary sub-system until the next EV arrives. When the second EV arrives at 10:00, the stationary sub-system starts to charge the second EV until the SoC of the stationary subsystem falls below 10%. The SoC of the stationary battery then fluctuates slightly with normal operation of the energy buffering system, but mainly remains at 10%. In the meantime, the braking energy produced from the tram system gets accumulated in the EV battery until the second EV leaves and the third EV arrived at 12:00. The energy stored in the stationary sub-system is still approx. SoC=10%. As long as an EV was connected, the braking energy produced from the tram system would firstly accumulate in the EV. After the last EV leaves at 18:00, the braking energy then starts to accumulate in the stationary sub-system. It is worth noting that the charge rate of the 5th EV is faster than EV's 3 and 4, as the EV is parked during 'rush hour' when more trams pass through the section.

The result shown in this section demonstrates both sub-systems of the CESS can effectively exchange energy with the tram system. The stationary sub-system ensures full-time energy storage availability to the tram system, and the EV sub-system can successfully transfer the energy stored in the stationary sub-system to the connected EVs and therefore refresh the storage capacity for the stationary system.

5.4 Comparison of the three systems

The models of the EVESS and CESS have been demonstrated in Section 5.2 and Section 5.3. This chapter now compares the two, alongside the SESS, and aims to understand their impact on the daily energy balance. The previously used tram section between Carbrook and Nunnery Square was also used for this simulation.

5.4.1 Energy saving features of the three systems

To compare the energy-saving features of the three approaches, this chapter considers the operation of a SESS that has the same stationary battery as the CESS, and an EVESS, and exhibits the same EV parking pattern as before:

- The EVESS has five EVs parked in turn, and each 100Ah and parked for two hours, sequentially,
- The SESS has a stationary battery 100Ah,
- The CESS has the stationary sub-system with 100Ah battery, and EV sub-system with five EVs parked in turns, and each parking for two hours, sequentially.

The use of an ESS aims to recover the braking energy originally dissipated in the braking / dump resistors, and the energy recovered could be used to reduce the energy supplied from substations, or be stored inside the ESS. No matter how the recovered energy is used ultimately, it originates from the braking energy lost in the dump resistors. Hence, the energy-saving performance of an ESS can be assessed by how much less braking energy will be lost in the resistors. This section simulates the profile of braking energy lost in the resistors, when the three ESS systems are deployed, and compares them with the original system without any ESS, the results being shown in Figure 5-12. It is worth noting that the different ESSs added to the system were virtually installed at the mid-point stop of the energy supply section between Carbrook and Nunnery Square.

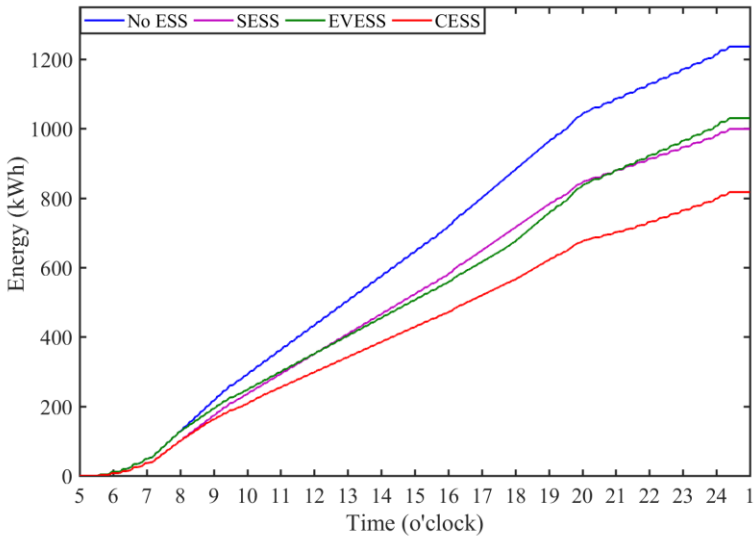

Figure 5-12 The profile of energy lost in dump resistor with different ESS scenarios

As can be seen in Figure 5-12:

1) Compared to the 'No ESS' case, any addition of an ESS will reduce the braking energy lost in the dump resistors, and therefore lead to greater recovery and reuse of the braking energy
2) The curves of 'EVESS' and 'No ESS' overlap between 05:00 to 08:00 and remain parallel after 18:00. This demonstrates the energy balance of the two cases are the same during

these periods, as the ‘EVESS’ has no EV connected to the system between 05:00 to 08:00 or after 18:00. Since both SESS and CESS have a stationary system that is constantly connected to the tram network, they have better performance on recovering the braking energy than is seen with the EVESS.

3) Compared to SESS, CESS had an additional EV sub-system. Thus, between 08:00 to 18:00, when there were EVs parked and connected, CESS recovered more braking energy than the SESS.

In summary of the energy-saving, the SESS can provide a full-time service to the tram system. However, it is a closed system, and it can only recover a limited amount of braking energy, without employing some means to regulate the SoC of the SESS, such as an auxiliary load. In contrast, the EVESS is an open system, and hence, its storage capacity can be constantly refreshed along with the come-and-go of the EVs. Nevertheless, due to the mobility of the EV, the time over which the EV is connected to the tram system is limited, and it thereby affects the recovery of braking energy. CESS, which combines the SESS and EVESS, keeps the strong points of both approaches, and compensates for their shortfalls. Thus, CESS can recover more braking energy than the other two approaches alone.

5.4.2 The effect of the three systems in application

Although this chapter has compared the energy-saving features of each ESS in turn, the merits and drawbacks of each ESS have to be demonstrated based on their energy-saving performance in a real-world application. In the previous simulation, the sub-systems in the CESS have the same capacity as the SESS and EVESS. But in reality, all three ESS could have different configurations and capacities. In order to compare the three ESSs under closer to real-world conditions, the following section details more simulations based on various configurations of each type of ESS.

For the stationary battery of the SESS, and of the stationary sub-system in the CESS, this section assumes the capacity varies from 100Ah to 500Ah and is initially fully charged. It also considered the number of EVs available to such schemes will generally continue to grow, and EVs will contribute a substantial proportion of the total car population in the coming years. Thus, for the EV-related scenario, this study assumes there are sufficient EVs to fully occupy

the 10 hours parking period and refresh after a period of two hours; and the EVs battery is 50% charged initially. In total, 11 configurations of three ESSs were studied, and these are:

- 1×EVESS scenario that has one EV charging point, and connects to five EVs sequentially, each connection lasting for 2 hours,
- 5×SESS scenarios, each has a stationary battery which varies from 100-500Ah in steps of 100Ah,
- 5×CESS scenarios, each has a stationary battery that varies from 100-500Ah in steps of 100Ah, and one EV charging point that connects to five EVs, each connection lasting for 2 hours, sequentially,
- all ESS were added to the mid-point stop of the energy supply section between Carbrook and Nunnery Square.

The energy that could be originally lost in the dump resistors but recovered by the ESSs will be used for the reduction of energy supplied from substations and stored into the EV batteries and into the stationary battery. This chapter therefore considers the energy re-used as the sum of the former two parameters. Table 5-1 shows the result of the comparison.

Table 5-1 The daily energy saving by different EVESS, SESSs and CESSs

System	Capacity of stationary battery (Ah)	Reduction of energy supplied from substations (kWh)	Net energy stored in EV battery (kWh)	Net energy stored in stationary battery (kWh)	The energy re-used (kWh)
EVESS	0	141	76	0	217
SESS	100	258	0	0	258
	200	341	0	0	341
	300	352	0	0	352
	400	355	0	0	355
	500	358	0	0	358
CESS	100	366	72	0	438
	200	441	76	-22	517
	300	467	83	-62	550
	400	485	93	-99	578
	500	502	94	-124	597

Table 5-1 shows that:

1) EVESS had the least braking energy recovered. This was because only the EV battery was available for energy recovery, and the connection time of the vehicles to the tram system

was only during a 10-hour period. Hence, this duration meant the energy exchange with the substation was very limited. The energy taken away by the EV was 76 kWh/d.

2) The braking energy recovered by the SESS, with any size of the stationary battery, is larger than by EVESS alone. This is because throughout the approx. 20 hours' operation, the stationary battery is continuously connected to the tram system and provides energy storage and bi-directional energy exchange. Since the battery was full at the beginning of the day and was full at the end of the day, the net energy flowed into the stationary battery is 0 kWh/d.
3) CESS has the best performance in terms of braking energy recovery. Since the CESS combines the strong points of the SESS and the EVESS, at any configuration, it has the best performance on the re-used energy than the other two ESS scenarios.
4) Amongst the different CESSs, a bigger stationary battery capacity leads to a greater braking energy recovery. However, as mentioned in Section 4.3.2, the available and accessible braking energy is limited. Likely, the CESS with a 100Ah stationary battery is able to recover a substantial proportion of the available braking energy. Hence, the increment of braking energy recovery (caused by the bigger stationary battery capacity) may be more gradual than the increment of the stationary battery capacity. In this case, when the stationary storage increased fivefold from 100Ah to 500Ah, the total energy re-used only increases by 37.2%.

In addition, this research found that the net energy stored in the stationary battery of the CESSs with larger stationary batteries is negative. Taking the CESS with a 500Ah stationary battery as an example for illustration. Figure 5-13(a) shows the SoC of each EV parked and connected to the EV sub-system, and Figure 5-13(b) shows the SoC of the stationary sub-system. As can be seen, all five connected EVs got fully charged, the CESS with a big stationary battery tends to overly provide its own energy to the tram network and the EVs. So that when there is no EV parked, the braking energy generated by the tram system cannot be used to recover this part of the energy that has been given out. Ultimately, the total braking energy that went into the stationary battery was smaller than the total energy that came out, leading to negative net energy stored in the stationary battery. Therefore extra energy can be supplied by the substations to charge the stationary battery when the tram section is not supplying a tram, and be used to fully charge the vehicles. This increases the energy drawn from the substations, but could be used to charge vehicles without the installation of charging infrastructure, although this is beyond the initial scope of this thesis.

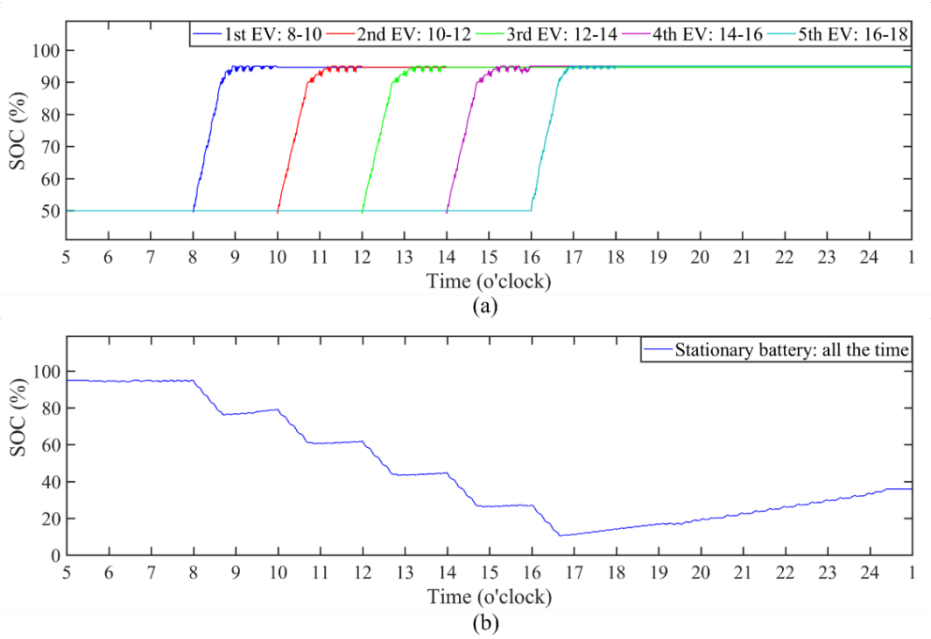

Figure 5-13 The SoC of the EV's and the battery in the CESS with a 500Ah stationary battery

No matter what the size of the stationary battery of a CESS, after a full day of operation, the remaining energy reserve in the stationary battery could differ from that at the start. This is because the parking status of the EVs influences the energy reserve in the stationary battery, and the parking status in real life could vary day to day. However, control of the stationary battery SoC can be carried out during periods of no tram movement, or overnight as required to maintain a fixed set point for the start of the next day's operations. The simulation conducted in this chapter assumed that there were enough EVs parked and connected to the system over a certain period of time during a day. In the cases of the CESSs with a bigger stationary battery, a negative net energy stored in a stationary battery was found after a day of operation, which suggests the energy re-used came from both the energy originally stored in the stationary battery and the braking energy collected from the tram system, rather than just the latter. The appraisal of energy saving performance only focuses on the braking energy collected from the tram system after a day of operation. Hence, this energy should be smaller than the energy re-used stated in Table 5-1. Consequently, the braking energy collected from the tram system by the CESSs with a 200-500Ah stationary battery only ranges from 473-495 kWh, which is only 8-13% larger than by the CESS with a 100Ah stationary battery.

In summary, for any configuration, the CESS shows better performance on energy saving than the SESS and EVESS. However, the steep growth of stationary battery capacity only results in the gradual growth of total braking energy recovery. As mentioned in Section 4.4.4, The capital

cost of the battery is influenced by the stationary battery capacity and is found to substantially negatively impact the economic feasibility of the application of the ESS system on tram. Thus, a CESS with a smaller stationary battery would be more economically acceptable.

5.5 Applying the energy storage system on the whole tram network

As presented in Section 5.2 to Section 5.4, EVs could be exploited as energy storage units for the tram network. Integrating the EVs and a stationary battery for energy storage is found to provide a better energy saving than when compared to using a SESS that has no EV element, and is a significant improvement on the EVESS that only utilizes EVs. To further study the merit of involving the EVs in the ESS, here we investigate the CESS and SESS, of similar capacities, added to each energy supply section, respectively. Subsequently, the energy saving delivered by and the economics of the addition of the ESSs were examined.

5.5.1 The energy-saving and energy recovery delivered by ESSs

To compare the CESS with the SESS, this investigation examines a 100 Ah SESS and a CESS with a 100Ah stationary battery and five EVs parked with a one-day period. Both of SESSs and the CESSs were installed in the mid-point stop of energy supply sections. The energy saving delivered by both the SESS and CESS to the corresponding energy supply section was therefore evaluated.

Regarding the modelling and simulation,

- The related battery in SESS and the battery of the stationary sub-system in the CESS were assumed to have a 100% SoC initially,
- The five EVs related to the CESS were assumed to be parked in turns between 08:00 to 18:00, each stay lasting for two hours, and each EV having a 100Ah battery, with an initial SoC=50%.

Here, the simulation is based on travelling data that includes the PPOD and OPOD of a weekday, a Saturday and a Sunday and was collected in the sampling campaign mentioned in Section 5.1. Since the simulated energy saving and recovery that includes the reduction of energy supplied from substation and the energy stored in EV battery varies between weekdays, Saturdays and Sundays, this study examined the energy saving and recovery on an annual basis.

In the UK, there are eight days of public holidays spread across the year. Among these eight days, the Supertram usually provides Saturday service on three days, Sunday service on four days, and no service on one day [125]. The yearly energy saving and recovery was calculated via Equation 5-1.

$$E_{year} = E_{Weekday} \times (5 \times 52 + 1 - 8) + E_{Sat} \times (52 + 3) + E_{Sun} \times (52 + 4) \quad \text{Equation 5-1}$$

where $\boldsymbol{E_{Weekday}}$, $\boldsymbol{E_{Sat}}$ and $\boldsymbol{E_{Sun}}$ are the daily energy saving and recovery simulated based on the weekday travelling data, the Saturday travelling data, and the Sunday travelling data, respectively.

The simulation results are summarized in Table 5-2 for each tram section in the network. As shown in Table 5-2, because of the different departure schedule and tram operational profiles, the SESS and CESS installed in different energy supply sections delivered different energy savings and recoveries. The reduction of energy supplied from the substation varied from 27 MWh/yr to 143 MWh/yr in the SESS cases, and 47 MWh/yr to 205 MWh/yr in the CESS cases. Generally, the SESS or CESS installed on an energy supply section that is shared by two lines will achieve a greater energy saving than the one installed on the energy supply section with only one line passing through. Compared to the SESS, each CESS can deliver a greater reduction on the energy supplied from substations. For a potential network-wide installation, the CESSs could provide 55% more energy saving to the tram than the SESSs alone could. Besides, since the CESS utilises the EV for energy storage, part of the energy recovered can be stored in and used by the EVs. Therefore, the total energy-saving and recovery delivered by all 11 CESSs is 92% more than by the 11 SESSs.

In the SESS case, the whole system installation has the reduction of energy supplied from substations ($-E_{sub}$) averaging at 2,356 kWh/d. It is substantially smaller than the 5,068 kWh/d, which is $-E_{sub}$ of the whole system installation simulated and presented in Figure 4-16 in Chapter 4. Such a difference is expected, and the reasons are:

- The base case energy balance obtained in this chapter considered the difference between peak period and off-peak period and between weekday, Saturday and Sunday. Meanwhile, the energy balance shown in Section 3.4.3 was used as the base case energy balance for the SESS study presented in Chapter 4. As discussed in Section 5.1.3, the latter was obtained purely based on the weekday's peak period tram travelling data that involves more braking

and thereby has higher energy lost in resistor than the former. The SESS aims to recover and re-use the energy lost in resistor. With lower energy lost in resistor in the base case, the SESSs explored in this chapter likely didn't access the same amount of energy originally lost in the resistor as the SESS studied in Chapter 4 did, and it thereby achieved a smaller -Esub.

- The SESS explored in Chapter 4 assumed its battery has an initial SoC=50%. The rationale was to allow the SESS to have a fair amount of headroom to absorb the braking energy to encourage recovery and re-use. With more experimental work was conducted, this research further discovered that the tram system could charge up the stationary battery with the braking energy if the battery is not full. This phenomenon results in the ending SoC being higher than the starting SoC. As the research conduct the energy-saving study and the subsequent economic appraisal on an annual basis, it would be beneficial to have the SoC staying at the same level before and after the everyday operation. Therefore, the SESS explored in this chapter was given a battery with an initial SoC=100%. Consequently, compared to the SESS investigated in Chapter 4, it has less headroom to potentially absorb and store the braking energy and thereby achieve a smaller -Esub.

Table 5-2 the energy saving and recovery delivered by the SESS and CESS

Energy supply sections	Centre stops	SESS	CESS	
		Reduction of energy supplied from substations (MWh/yr)	**Reduction of energy supplied from substations (MWh/yr)**	**Energy supplied to EV batteries (MWh/yr)**
Halfway-Crystal Peak	Waterthorpe	57	90	35
Crystal Peak-Birley Lane	Hackenthorpe	88	126	30
Birley Lane-Gleadless Townend	White Lane	27	47	32
Meadowhall-Carbrook	Tinsley	39	61	34
Carbrook-Nunnery Square	Attercliffe	89	129	28
Nunnery Square-Fitzalan Square	Hyde Park	33	57	34
Gleadless Townend-Arbourthorne Road	Manor Top	117	168	12
Arbourthorne Road-Fitzalan Square	Park Grange Croft	143	205	10
Fitzalan Square-The University of Sheffield	City Hall	82	147	34
The University of Sheffield-Langsett	Shalesmoor	88	141	34
Langsett-Middlewood	Hillsborough	98	161	34
Whole system		860	1332	317

5.5.2 The economic feasibility of the addition of ESSs

The economic evaluation of each ESS installation (at one location) was based on simulation results shown in Table 5-2, and covers Discounted Payback Period (DPP), Net Present Value (NPV), and Internal Return Rate (IRR) following the method mentioned in Chapter 4.

Based on reported literature [152, 153, 155, 157], this study assumed the capital expenditure (CAPEX) includes the cost of the stationary battery, of components such as the converter and controls, and installation cost. According to reported materials that are related to economic analysis of energy storage systems [150, 158-161], this paper assumes:

- For the SESS and the stationary sub-system of the CESS, the cost of the stationary battery is estimated at £133 per kWh, and the cost of its other components is assumed to be equivalent to 80% of the cost of the battery.
- For the EV sub-system of the CESS, there is no cost for the battery, and the cost of its other components is assumed to be equivalent to the SESS's.
- The installation cost of the SESS and the CESS is estimated as £10,000 per unit.
- The operational expenditure (OPEX) for maintenance equals to 3% of the CAPEX.

Each SESS has a CAPEX of £19,337 and an OPEX of £580 per annum. Each CESS has a CAPEX of £23,486 and an OPEX of £705 per annum.

The reduction of energy supplied from the substation delivered by the SESS and the CESS could bring financial benefit to the tram network via reducing the cost of purchasing electricity from the grid. This study thereby considers the income (generated by installing SESS and CESS) to the tram system from the cost reduction on purchasing electricity from the grid at a price of £53 per MWh that the tram operator pays to the grid [165].

Apart from reducing energy supplied from the substation, the CESS can also recover and supply energy to EVs. Therefore, tram operators could potentially generate revenue through selling the electricity to EV users. However, it is possible that the EV batteries could get degraded due to the V2X application, although this is the subject of other research [172, 173]. Therefore, the economic feasibility study on the CESS considers two scenarios:

1) the electricity stored in the EV is assumed to be complementary to the EV users in order to encourage them to connect their EVs to the CESS,

2) the electricity stored in the EV is assumed to be sold to the EV users at £53 per MWh (£0.053 per kWh). Although the electricity is no longer free to EV users, it is still approx. £0.140 per kWh cheaper than the reported domestic electricity price of £0.193 per kWh [174]. the saving of £0.140 per kWh is considered reasonable compensation for the possible degradation (due to V2G use) cost per unit electricity discharge at £0.015–0.060 per kWh [168].

Hence, this study used a typical discount rate of 6% and assumed a moderate asset life of 5 years to firstly assess the economic feasibility of:

- each individual SESS installation location,
- each individual CESS location if the electricity stored in the EV is assumed to be complementary to the EV users,
- each individual CESS location if the electricity stored in the EV is assumed to be sold to the EV users at £ 0.053 per kWh.

It is worth noting that the economic feasibility is considered with a DPP<5 years, a positive NPV, and an IRR>6%. The economics and the related ranking of each individual installation are listed in Table 5-3.

Table 5-3 The economics of each individual SESS and CESS installations

Energy supply sections	SESS				CESS (free electricity to EV)				CESS (electricity to EV charged)			
	Rank	NPV	IRR	DPP (yr)	Rank	NPV	IRR	DPP (yr)	Rank	NPV	IRR	DPP (yr)
Halfway-Crystal Peak	8	-£9,064[N]	-18.5%[N]	11.1[N]	8	-£6,419[N]	-10.1%[N]	7.3[N]	8	£1,283[N]	1.9%[N]	4.7[N]
Crystal Peak-Birley Lane	6	-£2,222[N]	-4.1%[N]	5.8[N]	7	£1,705[N]	2.5%[N]	4.6[N]	7	£8,378	11.6%	3.5
Birley Lane-Gleadless Townend	11	-£15,834[N]	-39.7%[N]	N/A[N]	11	-£16,020[N]	-29.8%[N]	27.2[N]	11	-£8,811[N]	-14.3%[N]	8.9[N]
Meadowhall-Carbrook	9	-£13,055[N]	-29.4%[N]	25.8[N]	9	-£12,813[N]	-22.2%[N]	13.9[N]	9	-£5,248[N]	-8.2%[N]	6.8[N]
Carbrook-Nunnery Square	4	-£2,003[N]	-3.7%[N]	5.7[N]	6	£2,250[N]	3.3%[N]	4.5[N]	6	£8,515	11.8%	3.5
Nunnery Square-Fitzalan Square	10	-£14,380[N]	-33.9%[N]	73.3[N]	10	-£13,620[N]	-24.0%[N]	15.8[N]	10	-£5,922[N]	-9.3%[N]	7.1[N]
Gleadless Townend-Arbourthorne Road	2	£4,430	7.6%	4.0	2	£10,962	15.0%	3.2	4	£13,684	18.4%	3.0
Arbourthorne Road-Fitzalan Square	1	£10,084	16.6%	3.1	1	£19,424	25.4%	2.6	1	£21,623	28.0%	2.4
Fitzalan Square-The University of Sheffield	7	-£3,414[N]	-6.4%[N]	6.3[N]	4	£6,370	9.0%	3.8	3	£14,008	18.8%	3.0
The University of Sheffield-Langsett	5	-£2,099[N]	-3.9%[N]	5.7[N]	5	£4,986	7.1%	4.0	5	£12,484	16.9%	3.1
Langsett-Middlewood	3	£23[N]	0.0%[N]	5.0[N]	3	£9,575	13.2%	3.4	2	£17,220	22.7%	2.7

[N]: uneconomic results

It is worth noting that the SESS explored in this chapter does not have the economics as good as the SESS studied in Chapter 4 does due to the former achieving less energy saving, and the potential cause of this incident has been explained in Section 5.5.1. As can be seen in Table 5-3, only two out of eleven SESSs were economically feasible as they had a DPP<5 years and a positive NPV plus IRR>6%. However, the number of economically feasible CESSs is five, if the electricity stored in the EVs is free to EV users; and seven if that electricity is charged to EV users. Compared to SESS, CESS has a higher CAPEX and OPEX, but CESS can recover enough profitable energy, which then generates a higher income to cover that extra CAPEX and OPEX. Consequently, CESS performs better on energy saving and also has more favourable economics than the SESS. It is worth noting that most of the CESS installations share the similar ranking in the two different scenarios, whether electricity to EVs is free or charged. Still, the CESS installation at the mid-point stops of energy supply sections: Gleadless Townend-Arbourthorne Road, Fitzalan Square-The University of Sheffield, Langsett-Middlewood rank differently, which is because the ranking regarding the amount of profitable energy varies in the two scenarios. In detail, the CESS installed in Gleadless Townend-Arbourthorne Road was simulated to deliver the second greatest energy-saving and thereby has the second-best economics. However, it only supplied 12 MWh to the EV on an annual basis, which is only approx. a third of that from the CESS installed in Fitzalan Square-The University of Sheffield or Langsett-Middlewood energy supply sections. Thus, when the electricity supplied to the EV could be used to generate profit, the CESS installed in Gleadless Townend-Arbourthorne Road section therefore generates less profit than the other two CESSs installed elsewhere, and thus its ranking dropped from second to fourth.

On both energy saving and economics, CESS is more advantageous than the SESS. Therefore, the study about the network wide ESS installation only focuses on the CESS. Although some of the CESS installations are found to have poor returns, the network-wide installation could still be economically feasible since the income generated from economically viable ones could cover the deficit brought by the non-economically viable ones. This research thereby studied the optimal solution of a network-wide installation and aimed to maximise the energy-saving by installing as many CESS as possible if the economic feasibility is still proven. The logic of the study is to include the CESS with the best economics (listed in Table 5-3) first, and to examine which installation could change the economics of the whole installation to unfeasible and should thereby be excluded. For example, if only three CESSs would be added to the system,

- for a scenario that offers electricity to EVs free of charge, the CESSs should be added to the mid-point stops of Arbourthorne Road-Fitzalan Square, Gleadless Townend-Arbourthorne Road and Langsett-Middlewood, which have the top three best economics in the category,
- for a scenario that charges for the electricity supplied to EVs, the CESSs should be added to the mid-point stops of Arbourthorne Road-Fitzalan Square, Langsett-Middlewood and Fitzalan Square-The University of Sheffield, which have the top three best economics in the category.

Table 5-4 shows the economic feasibility of different numbers of CESS installations.

Table 5-4 Economic of CESSs excluded the selling of electricity to EV users

No. of CESS installations	CESS (free electricity to EV)			CESS (electricity to EV charged)		
	NPV	IRR	DPP (yr)	NPV	IRR	DPP (yr)
1	£19,424	25.4%	2.6	£21,623	28.0%	2.4
2	£30,386	20.3%	2.9	£38,843	25.4%	2.6
3	£39,960	17.9%	3.0	£52,851	23.2%	2.7
4	£46,330	15.8%	3.2	£66,536	22.0%	2.7
5	£51,316	14.1%	3.3	£79,020	21.0%	2.8
6	£53,566	12.3%	3.5	£87,535	19.5%	2.9
7	£55,271	11.0%	3.6	£95,913	18.4%	3.0
8	£48,852	8.6%	3.8	£97,196	16.5%	3.1
9	£36,038^{N}	5.7%^{N}	4.2^{N}	£91,949	14.0%	3.3
10	£22,418^{N}	3.2%^{N}	4.5^{N}	£86,026	11.9%	3.5
11	£6,398^{N}	0.9%^{N}	4.9^{N}	£77,215	9.8%	3.7

^{N}: uneconomic results

As shown in columns under “CESS (free electricity to EV)” in Table 5-4, if the electricity stored in EVs is free to EV users, a full network-wide installation (No. of CESS installation=11) is not economically viable as it has an IRR that is smaller than the 6% discount rate. However, the plan (No. of CESS installation=8) that excludes the mid-point stops installations on energy supply sections of Meadowhall-Carbrook, Nunnery Square-Fitzalan Square and Birley Lane-Gleadless Townend which have the poorest economics (as shown Table 5-2), was found economically viable. It is worth noting that the CESSs installed on the Meadowhall-Carbrook, Nunnery Square-Fitzalan Square and Birley Lane-Gleadless Townend sections, together only contribute to 12% of the total reduction of energy supplied from substations (as shown Table 5-2). Hence, if the electricity given to the EV users is free of charge, a partial network-wide installation that excluded Meadowhall-Carbrook, Nunnery Square-Fitzalan Square and Birley Lane-Gleadless Townend is an optimal solution as it leads to a satisfactory energy saving and still maintains a fair return on investment.

If the electricity given to the EV users is no longer free and generates revenue for the tram operator (even at a low level, as discussed), then it provides extra income and improves the economics of the CESS. Even though including the selling of electricity to EV users does not help to make any individual CESS installations economically viable (Table 5-3), it enables a full network-wide installation (No. of CESS installation=11, columns under "CESS (electricity to EV charged)" in Table 5-4), which can successfully pay back the initial investment in less than four years, generate a profit during the asset life, and give out an IRR greater than the 6% discount rate.

The addition of CESS for braking energy recovery not only brings economic benefits to the tram service provider but also results in a carbon emission saving. As reported, generating one kWh of electricity results in a direct emission of 0.231 kg CO_2 [150]. If the electricity given to the EV users is complementary, the economically viable partial network wide CESS installation could provide:

- the tram with an electricity saving of 1,167 MWh per annum, which results in reducing the CO_2 emission by 270 metric tonnes.
- the EV users with an electricity saving of 217 MWh per annum since the EV's electricity demand can be fulfilled by the recovered braking energy, corresponding to a 50 metric tonnes reduction on the CO_2 emission.

If the electricity given to the EV users is charged, the economically viable full network-wide CESS installation could provide:

- the tram with an electricity saving of 1,332 MWh per annum, which results in reducing the CO_2 emission by 308 metric tonnes.
- the EV users with an electricity saving of 317 MWh per annum to the grid, which results in reducing the CO_2 emission by 73 metric tonnes.

5.5.3 Sensitivity study of the economic evaluation of the CESSs' addition

As discussed in the sensitivity study of the economic evaluation of the SESSs' addition (shown in Section 4.4.4), each variable considered has a different impact on the economics. Therefore, a similar sensitivity study was also conducted to gain insight into how each variable influences the economics of the CESSs' addition, and the variables considered include:

- The battery price, which influences the CAPEX of the stationary battery

- The cost of the EV sub-system, which was assumed to be 80% of the stationary battery used in the stationary sub-system
- The installation cost
- The OPEX ratio to the total CAPEX, which was assumed to be 3%
- The electricity price, which the tram service operator pay to the grid
- The asset life
- The discount rate
- The electricity price, which the EV used to pay to the tram service operator

The sensitivity study examines economic evaluations with the electricity stored and taken away by the EVs free or charged for. Additionally, since the electricity stored in the EV could be different which thereby impacts the potential income from the sale of electricity to the EV, the sensitivity study used the full network-wide installation for illustration. Similar to the sensitivity study conducted in Section 4.4.4, the approach was to apply a ±20% change to one variable in turn and subsequently reviews the impact on the NPV, IRR and DPP.

Impact of the cost relating variables

The economic evaluations obtained for different battery prices, cost of the other components of the EV sub-system, installation cost, and OPEX ratios to the total CAPEX are shown in Table 5-5.

Table 5-5 The economic evaluation based on different cost relating variables

Variables	Value	CESS (free electricity to EV)			CESS (electricity to EV charged)		
		NPV	IRR	DPP (yr)	NPV	IRR	DPP (yr)
Battery Price (per kWh)	£106	£39,817^{N}	5.8%^{N}	4.2^{N}	£110,634	15.5%	3.2
	£133	£6,398^{N}	0.9%^{N}	4.9^{N}	£77,215	9.8%	3.7
	£160	-£27,021^{N}	-3.3%^{N}	5.6^{N}	£43,796	5.1%	4.3
EV sub-system: Battery	64%	£16,681^{N}	2.3%^{N}	4.6^{N}	£87,498	11.4%	3.6
	80%	£6,398^{N}	0.9%^{N}	4.9^{N}	£77,215	9.8%	3.7
	96%	-£3,885^{N}	-0.5%^{N}	5.1^{N}	£66,932	8.3%	3.9
Installation Cost (per installation)	£8,000	£31,178^{N}	4.5%^{N}	4.3^{N}	£101,995	13.9%	3.3
	£10,000	£6,398^{N}	0.9%^{N}	4.9^{N}	£77,215	9.8%	3.7
	£12,000	-£18,382^{N}	-2.3%^{N}	5.4^{N}	£52,435	6.3%	4.1
OPEX: CAPEX	2.4%	£12,927^{N}	1.7%^{N}	4.7^{N}	£83,745	10.6%	3.6
	3.0%	£6,398^{N}	0.9%^{N}	4.9^{N}	£77,215	9.8%	3.7
	3.6%	-£132^{N}	0.0%^{N}	5.0^{N}	£70,686	9.0%	3.8

^{N}: uneconomic results

As can be seen, both battery price and the installation cost can substantially impact the economics, no matter whether the electricity supplied to the EV is charged for or not. A ±20% variation of the battery price could result in a ±0.5-0.7 year change in the DPP, and an approx. ±£34,000 change in the NPV, and ±4-6% numerical change in the IRR, respectively. When the ±20% variation was applied to the installation cost,a ±0.4-0.6 year change in the DPP, an approx. ±£25,000 change in the NPV, and ±3-5% numerical change in the IRR would occur. However, the ratio of the EV sub-system to the stationary battery and the OPEX to the total CAPEX influence the economics less. The ±20% change of either of them alters the DPP less than ±£0.3 years, the NPV less than ±£10,000, and the IRR less than ±1.6%.

Different costings influence the economics differently as different costings form different proportions of the total expenditure, which is the sum of the OPEX and CAPEX. Since the OPEX is assumed to be 3% of the total CAPEX, the total expenditure is dominated by the CAPEX, and hence, the OPEX has a small influence on the total expenditure and the economics. The CAPEX consists of the battery cost, the cost of the other component in the stationary sub-system, the EV sub-system, and the installation cost. In the base case, the installation cost contributed 43% of the CAPEX, thereby substantially impacting the CAPEX. Although the battery cost only contributes 22% of the CAPEX in the base case, it was used to estimate the cost of the other component in the stationary sub-system and of the EV sub-system. Therefore, the battery cost influences 57% of the CAPEX. Consequently, both the battery and installation costs, which dominate the CAPEX, can heavily affect the economic evaluation with a ratio of CAPEX to total expenditure.

Impact of the variables relating to income / cost streams

The economic evaluations obtained for different electricity prices paid to the grid and charged to the EV users are shown in Table 5-6.

The elevation of the electricity price on the one paid to the grid and charged to the EV users would deliver a higher cost-saving on the electricity bill and generate more income from the sale of electricity. Although both electricity prices used in the base case were the same, the ±20% change of them would create a different impact on the economic feasibility. As shown in Table 5-2, the energy-saving delivered by the site wide CESS installation is >300% more than the electricity export to the EVs, and therefore the potential income from the energy-saving dominates the total income, and has a greater impact on the economic evaluation. As a result,

the ±20% change of the electricity price paid to the grid could lead to a ±0.6-1.7 year change in DPP, a ±£60,000 change in NPV, and an approx. ±8% numerical change in IRR. Meanwhile, the ±20% change of the electricity price does not impact the scenario offering the free electricity to the EVs users and only results in a ±0.2 year change in DPP, a ±£14,000 change in NPV, and an approx. ±1.7% numerical change in IRR on the scenario charging for the electricity to the EVs.

Table 5-6 The economic evaluation based on income relating variables

Variables	Value	CESS (free electricity to EV)			CESS (electricity to EV charged)		
		NPV	IRR	DPP (yr)	NPV	IRR	DPP (yr)
Electricity Price (paid to the grid, per kWh)	£0.042	-£53,081[N]	-7.5%[N]	6.6[N]	£17,736[N]	2.3%[N]	4.6[N]
	£0.053	£6,398[N]	0.9%[N]	4.9[N]	£77,215	9.8%	3.7
	£0.064	£65,877[N]	8.4%[N]	3.9[N]	£136,694	16.8%	3.1
Electricity Price (charged to EVs, per kWh)	£0.042	£6,398[N]	0.9%[N]	4.9[N]	£63,052	8.1%	3.9
	£0.053	£6,398[N]	0.9%[N]	4.9[N]	£77,215	9.8%	3.7
	£0.064	£6,398[N]	0.9%[N]	4.9[N]	£91,379	11.5%	3.5

[N]: uneconomic results

Impact of the other variables

The economic evaluations obtained for different asset life and discount rates shown in Table 5-7.

Table 5-7 The economic evaluation based on income relating variables

Variables	Value	CESS (free electricity to EV)			CESS (electricity to EV charged)		
		NPV	IRR	DPP (yr)	NPV	IRR	DPP (yr)
Asset Life (yr)	4	-£40,567[N]	-6.7%[N]	4.9[N]	£17,687[N]	2.8%[N]	3.7[N]
	5	£6,398[N]	0.9%[N]	4.9[N]	£77,215	9.8%	3.7
	6	£50,704[N]	5.7%[N]	4.9[N]	£133,373	14.2%	3.7
Discount Rate	4.8%	£15,269[N]	2.0%[N]	4.7[N]	£88,460	11.1%	3.6
	6.0%	£6,398[N]	0.9%[N]	4.9[N]	£77,215	9.8%	3.7
	7.2%	-£2,026[N]	-0.3%[N]	5.0[N]	£66,538	8.6%	3.8

[N]: uneconomic results

As can be seen, longer asset life and a smaller discount rate improves the economics. The asset life affects the total amount but not the rate of income generated throughout the project. Therefore, it only impacts the NPV and IRR but not the DPP, and extending it will produce more income. In this study, the asset life has a strong impact on the economics as its ±20% change result in a ±£45,000-65,000 change in NPV, and an approx. ±5-8% numerical change in IRR. The discount rate impacts the depreciation of the future cash flow. Therefore, lower the discount rate, the better the economics. However, the impact of the discount rate is not

substantial as its ±20% change only lead to a ±0.2-0.3 year change in DPP, a ±£8,000-11,000 change in NPV, and an approx. ±1.2% numerical change in IRR.

In summary, among the eight tested variables, the battery price, the installation cost, electricity price paid to the grid, and the asset life were found to substantially influence the economics.

5.6 Chapter summary

This chapter successfully describes the hourly energy balance of the Supertram system on a weekday, a Saturday and a Sunday. Generally, the energy consumed, wasted and recovered on a weekend are less than those on the weekdays. Still, all the energy balances suggest that there is a large amount of braking energy lost in the onboard dump resistor, especially during the peak period which has a higher passenger flow. Such a finding strengthens the potential for using EVs as energy storage for light rail systems, due to EVs being expected to be parked at tram stops during the peak period.

This chapter then presented an EVESS model. It subsequently identifies that EV parking time and the number of EVs parked will both impact the EVESS's performance on energy saving. The EV parking time is found to be positively related to the reduction of energy supplied from the substation, and the number of EVs parked positively influences the energy that could be finally stored in the EV batteries.

The chapter also presents a CESS model, which includes a stationary sub-system that is similar to the SESS and an EV sub-system that is similar to the EVESS. A smart control system is proposed, which uses the tram catenary to connect the sub-systems and prioritises EV charging. In the comparison of CESS, SESS, and EVESS, the CESS has the greatest total energy reused within the system, which combines a reduction of energy supplied from the substation and the net energy stored in, or delivered to, EVs.

Finally, this chapter compares the energy and economic performance of installing a SESS or a CESS onto each energy supply section of an urban tram network. The addition of the CESS delivered a substantial reduction of energy supplied from the substation of each energy supply section, and the CESS performs better than the SESS on both the energy saving and economic feasibility. The economic evaluation was carried out to determine a practical solution for the

CESS installation, and it also appraised the impact of whether to charge the EV user for the electricity recovered and stored in the EV. If the braking energy delivered to the EVs is free of charge, although only five out of 11 individual CESS installations are individually economically viable, a partial network-wide installation that excludes the three CESSs with the lowest energy saving and poorest return was found to be economically feasible. Such a solution manages to maintain a reasonable energy saving and provides a good carbon emission saving. If the braking energy delivered to the EVs is charged to the EV users and generates income for the tram operator, seven out of eleven individual CESS installations were found individually economically viable and the economics of a full network-wide installation was then proven; thus achieving even better energy savings and carbon emission savings. From the sensitivity study, this chapter also finds that the battery price, the installation cost, electricity price paid to the grid, and the asset life are substantially influential to the economics of the network-wide CESS installation.

Chapter 6. Conclusions and future work

This chapter firstly summarizes the work conducted and reviews the outcome and contribution of this research, chapter by chapter, in Section 6.1. At the end, Section 6.2 discusses the work that could be done to further develop this research topic in the future.

6.1 Conclusion

This research aims to use the EV battery as the energy storage system to recover the braking energy from the tram system to achieve the bidirectional energy exchange between light rail and road and promote the overall energy efficiency of the electrified transportation system. As the literature reviews suggested that

- The energy balance for different urban light rail systems are case-specific, and the modelling and simulation of it seldomly focuses on a whole network study;
- The stationary battery ESS, which can be considered a static battery EV, is commonly used for braking energy recovery for urban light-rail, and its capacity, installation location and number of installations are found impacting the energy-saving performance and thereby are worthwhile to be optimized
- EVs have been applied as energy storage for different electric facilities and markets, and recent research has been proposed a concept of exploiting EVs for the urban light-rail. Still, such a concept has been proven on an existing system, via modelling and simulation.

Thus, this research proposes three objectives as

- Objective 1 - To investigate the energy balance of the tram network, especially the energy demand for traction and the distribution of the braking energy, via an adequate methodology.
- Objective 2 - To add ESS into the system and examine its impact on energy balance and to determine the optimal configuration of stationary ESS with regards size and location and consideration of economic feasibility.
- Objective 3 - To explore the technical feasibility and the optimal solution for including EVs into the rail network via a full or partial replacement of the stationary ESS, and to assess its merit on the energy balance and the economic feasibility.

Through the modelling and simulation study conducted based on the Sheffield Supertram system, this research has fulfilled all the objectives proposed and made five key contributions to knowledge, as being presented below.

A new modelling and simulation method to model the tram system

As presented in Chapter 3, this research constructed a model that has a number of modules mimicking the operation of the Supetram's crucial components, such as the substations, the power supply catenary, the tram, and so on, in Simulink. Moreover, due to the constraints on limited access to the operational data and the facilities of the Supertram, this research developed a new method that uses the tram operational data, which included the speed, distance and acceleration and was collected via a dedicated GPS device, as the fundamental variable for the Simulink simulation.

This new modelling and simulation method successfully estimated the daily energy balance, which indicated the energy supplied from the substation, the energy lost on the resistor, and the energy recovered via regenerative braking energy, as shown in Section 3.4. Furthermore, the method has been validated as the simulated current and voltage trend matches the designed range. With a further explicit GPS data sampling campaign, this modelling and simulation method is able to estimate the hourly energy balance, as shown in Section 5.1. Such a function enables the modelling and simulation of a system that involves EVs, which is mobile and might only connect to the system for hours instead of all day long.

Furthermore, this modelling and simulation method is easy to use for the ESS study. The number, the capacity, the installation location of ESS to add to the system can be easily adjusted and modified. Such merit allows this research to conduct comprehensive investigations to gain insight into the different ESS additions.

In summary, this modelling and simulation method associated with GPS data sampling is convenient to exploit as it requires no physical system modification and has good extensibility for the subsequent ESS study. Therefore, this new approach would suit studying systems that are difficult to modify.

The insight into the difference between the "Common system" and "Separate System" energy supply methods

The urban light rail systems could be operated in a separate OCS arrangement (“Separate System")or a common OCS arrangement (“Common system”). The difference between the two is that the separate OCS prohibits energy exchange between the uplink and downlink within the energy supply section, but the common OCS allows that. Although these two energy supply method have been widely applied on the urban light-rail system around the globe, they have not been compared for the energy performance based on the same system. In Chapter 3, this research simulated the daily energy balance of the Supertram with these two different OCS’s. Generally, the sum of energy lost on the resistor and energy recovered via regenerative braking accounts for most braking energy.

The result suggested that the sum of the energy lost on the braking resistors and energy recovered via regenerative braking were found similar in both cases. It thereby indicates the amount of braking energy in the two systems were similar. However, the common OCS allows the energy exchange between the uplink and downlink, and consequently provides more opportunities for the tramcars to access and utilize the braking energy produced from both the uplink and downlink than the separate OCS does. Thus, the common OCS only dissipated 64% of its braking energy in the dump resistors but the separate OCS dissipated more than 90%. The energy recovered through re-use of the common OCS is approx. 300% more than of the separate OCS. With more braking energy being re-used, the common OCS required approx. 14% less energy supplied from the substation than the separate OCS. Thus, this research discovered that the “Common System” is more energy-efficient than the “Separate System” under the Supertram set-up.

In summary, this research successfully compared the two energy supply method on one existing system and discovered the “Common System” is more advantageous for energy efficiency. Such a finding could be referential to future modification and construction of the tram energy supply system.

The insight into the impact of ESS specification and installation on energy saving

This research successfully designed a SESS system consisting of a converter module, a control module, and an energy storage module that includes a battery for modelling and simulation. A double-closed loop control strategy was applied to control the energy exchange between SESS and the tram, and the catenary voltage served as the key signal that triggers the charging and discharging of the SESS.

This research then explored the optimal ESS addition strategy, and it firstly focused on the stationary ESS and later on the EV related ESS. As presented in Section 4.4 and Section 5.5, the approach was to add the ESS with different capacities in the same location and the ESSs with the same capacity in different locations and then test and compare the energy-saving performance. All the ESSs additions could successfully reduce the energy supplied from the substation, reduce energy lost in resistors, and increase the amount of regenerated energy re-used.

Regarding the location, even though the ESS installed at the substation stops could cover two adjacent energy supply sections, the ESS installed at the stops that are close to the mid-point of the energy supply section is instead likely to deliver the best energy-saving performance. Furthermore, adding the ESS on the centre stops would have better energy savings in multiple or network-wide installations.

Regarding the capacity, a bigger battery capacity will lead to a higher maximum current and discharge limit rate, and hence, a better energy saving. Nevertheless, the maximum current drawn from/by the tram is limited. Besides, although the battery capacity is positively related to energy saving, the increase of battery capacity may not result in the same extent of increase in energy-saving since the accessible braking energy is limited. Compared to a large ESS, a smaller ESS with an optimal discharge limit could be more efficient at energy-saving.

In summary, this research discusses how installation location and capacity of the ESS could influence energy-saving performance, and the finding would hint the future design and addition of ESS.

The technically feasible EV related ESS

This research designed two ESSs involving the EV, the EVESS that solely uses the EVs for energy storage, and the CESS that combines the EV sub-system and a sub-system equipped with a stationary battery.

This research proved the technical feasibility of the EVESS via modelling and simulation. It then studied the feature of the EVESS and discovered that a longer EV connection (to the tram

system) time would lead to better energy saving and a greater number of EVs parked would result in a greater braking energy recovery as the energy get taken away by the EVs.

This research proposed an innovative connection method for the CESS by using the catenary to link the EVs and stationary sub-systems, and it allows the EVs and the stationary sub-system to be installed in different locations. Moreover, this research developed a smart control for the CESS, prioritizing EV charging to allow more energy to flow from the tram and the stationary sub-system to the EV, refreshing the stationary sub-system's capacity and promoting energy-saving.

In comparing the CESS, SESS, and EVESS, the CESS was found to achieve the greatest total energy re-used as it combines the merit of the SESS, providing consistent connection to the tram system, and of the EVESS, being able to take away the braking energy to refresh the storage capacity.

In summary, this research proved the technical feasibility of the EV related ESS, the EVESS and CESS. Besides, it designed the smart control for the CESS that improved the energy recovery and reuse for the tram and simultaneously benefited EV users with battery charging. This outcome proved the viability of energy exchange between rail and road and could potentially stimulate future research on Vehicle-to-Rail.

The ESS addition strategy with consideration of economic feasibility

As aforementioned, the bigger the ESS capacity and/or a greater number of ESS addition can better the energy saving. However, such measures will also increase the initial investment.

This research conducted the economic appraisals, which focus on NPV, IRR and DPP and involves sensitivity study, on the addition of SESS firstly. The results suggest that even though the bigger capacity ESSs and a greater number of ESS addition can recover more energy, the energy recovered can not generate enough income to cover the greater investment. Exploiting smaller capacity SESS and potentially conducting a partial network wide-addition would help achieve economic viability or lead to better investment returns. The sensitivity study considers both electricity prices and the battery life positively and substantially influence all the SESS installations with different capacities. Meanwhile, the battery price was found to negatively

and strongly impact the economics of SESS installation with a higher capacity. The installation cost, OPEX, and the discount rates used are all found to negatively but mildly affect the economics.

This research conducted another economic appraisal on SESS and CESS, both with 100Ah stationary battery, via the same approach but based on different simulated energy-saving performances. Unlike the SESSs study, although the CESS requires a higher investment than the SESS, it recovers much more energy that generates enough income to offset the additional investment. It is worth noting that this research also projected how the potential income generated from the energy given to EV influences the economics. If the energy given to the EVs is charged, the economics will improve. Still, similar to the SESS study mentioned in the last paragraph, a full network-wide addition could be economically feasible, but a partial network-wide addition would yield the best investment returns. The related sensitivity study advised the battery price, installation cost, the electricity price paid to the grid, and the battery life can substantially impact the economics of the CESS addition.

In summary, this research examined how various factors, such as specification, number of installations, potential cost and income, affect the economic feasibility of different ESS additions. The method used could help understand the sweet spots and hurdles of the commercialization of innovative technology. It thereby could support the decision-making that aims to balance satisfying technical performance and acceptable economics.

6.2 Future work

This finding and the outcomes of this project demonstrate the potential technical feasibility and the merit of the energy exchange between rail and road. This research topic could be further developed, and areas to investigate may include the following:

1) Although this research proved the technical feasibility of using EVs as the energy storage for the tram via simulation, it would be beneficial to validate the method, control, and design via experiments with the actual electrical devices.

2) This research combined the EV sub-system with a stationary battery sub-system to create a CESS. The CESS was designed as a whole but its two key sub-systems could be installed in different locations of the tram system since the two are connected via the catenary. Therefore, in reality, the physical or geographical condition would require the two sub-systems to be installed in different locations. In this sense, it would be beneficial to understand how installing the two sub-systems in different locations could affect the energy-saving performance.

3) This study investigated the technical and economic feasibility of the CESS with a stationary sub-system possessing a 100Ah battery. As discussed in 4.4 and 5.5, a smaller battery unit could recover less braking energy, but on the other hand, it could have better economic feasibility due to the lower initial investment required. Therefore, it would be useful to conduct further technical and economic feasibility on CESS with a stationary sub-system that holds a battery with different capacities in order to gain insight into the optimal battery capacity for the stationary subsystem.

4) The degradation of EV batteries due to the V2G application has been studied previously [117-121]. Exploiting the EV and its battery for the energy exchange between rail and road is a new topic, and the impact of such an application on the battery life has yet to be investigated but is worthwhile to be explored.

5) This research proposed to offer free energy to the EV user to encourage their participation in the scheme, and the financial benefit to the EV owners was discussed. The willingness of the EV owner could impact the available number of EVs that could be connected for the energy storage for rail, whether a higher or a lower amount of incentive could be given for the encouragement, etc., and eventually affect the technical and economic feasibility of the integration of EV and rail. It could be diverse but has not been examined here. Thus, it would be meaningful to conduct further study to understand the attitude, concerns and willingness of the EV owner.

References

[1] UK Paliament. (2008). *Climate Change Act 2008*. Available: http://www.legislation.gov.uk/ukpga/2008/27/pdfs/ukpga_20080027_en.pdf

[2] BEIS, "2020 UK greenhouse gas emissions: provisional figures - data tables," ed, 2021.

[3] BEIS, "2017 UK greenhouse gas emissions: provisional figures - data tables," ed. London, UK, 2020.

[4] European Commission, "Electrification of the Transport System," European Commission, Brussell, Belgium2017, Available: http://ec.europa.eu/newsroom/horizon2020/document.cfm?doc_id=46372.

[5] BEIS, "Electricity generation and supply in Scotland, Wales, Northern Ireland and England, 2004 to 2019 - data tables," ed. London, UK, 2020.

[6] L. Butcher, S. Hinson, and D. Hirst, "Electric vehicles and infrastructure," The House of Commons Library, London, UK2018.

[7] Department for Transport, "TSGB0101: Passenger transport by mode from 1952," D. f. Transport, Ed., ed, 2020.

[8] Department for Transport, "TSGB0401: Domestic freight transport by mode," ed, 2020.

[9] European Environment Agency. (2020, 24-06-2021). *New registrations of electric vehicles in Europe* [Online]. Available: https://www.eea.europa.eu/data-and-maps/indicators/proportion-of-vehicle-fleet-meeting-5/assessment

[10] UK Government. (2020, 01-01-2021). *Government takes historic step towards net-zero with end of sale of new petrol and diesel cars by 2030* [Online]. Available: https://www.gov.uk/government/news/government-takes-historic-step-towards-net-zero-with-end-of-sale-of-new-petrol-and-diesel-cars-by-2030

[11] N. Carey and C. Steitz. (2021, 16-07-2021). *EU proposes effective ban for new fossil-fuel cars from 2035*. Available: https://www.reuters.com/business/retail-consumer/eu-proposes-effective-ban-new-fossil-fuel-car-sales-2035-2021-07-14/

[12] UK Government, "The ten point plan for a green industrial revolution," London, UK2020, Available: https://assets.publishing.service.gov.uk/government/uploads/system/uploads/attachment_data/file/936567/10_POINT_PLAN_BOOKLET.pdf.

[13] Office of Rail and Road. (n.d., 01-02-2022). *Mainline network*. Available: https://www.orr.gov.uk/about/who-we-work-with/railway-networks/mainline-network

[14] Office of Rail and Road. (n.d., 01-02-2022). *Underground railways*. Available: https://www.orr.gov.uk/about/who-we-work-with/railway-networks/underground-railways

[15] Office of Rail and Road. (n.d., 01-02-2022). *Light rail and tramways*. Available: https://www.orr.gov.uk/about/who-we-work-with/railway-networks/light-rail-tramways

[16] S. Frey, *railway electrification system and engineering*, First Edition ed. Dehli, India: White Word Publications, 2012.

[17] Stagecoach. (2017, 01-11-2017). *Vehicle Information* [Online]. Available: https://www.stagecoachbus.com/supertram/vehicle-information

[18] A. Baxter, "Network Rail A Guide to Overhead Electrification," Alan Baxter & Associates LLP, London, UK2015.

[19] Office of Rail and Road, "Table 6320 - Infrastructure on the mainline," ed, 2020.

[20] Office of Rail and Road, "Table 6105 - Estimates of passenger and freight energy consumption and carbon dioxide equivalent (CO2e) emissions," ed, 2020.

[21] J. Disney, W. Rossiter, and D. J. Smith, "Nottingham Express Transit:The role of green innovation in the drive for sustainable mobility through improved public transport," vol. 19, no. 1, pp. 56-68, 2018.
[22] London-road-croydon.org. (2013, 01-02-2022). *2–8 London Road, part 3: West Croydon Station in the 1900s*. Available: https://london-road-croydon.org/history/0006-west-croydon-station-1900s.html
[23] J. K. Srivastava, V. K. Singh, and A. K. J. J. E. S. Singhal, Comput. Sci. Eng. Technol., "Review on railway traction power supply system," vol. 2, no. 4, pp. 1236-1250, 2013.
[24] Stagecoach. (n.d., 01-02-2022). *Working near the Supertram network*. Available: https://www.stagecoachbus.com/supertram/working-near-supertram-network
[25] P. Stanton. (2021, 01-02-2022). *Controlling Docklands' traction*. Available: https://www.railengineer.co.uk/controlling-docklands-traction/
[26] Strathclyde Partnership for Transport. (n.d., 01-02-2022). *Celebrating 125 years of Subway*. Available: https://www.spt.co.uk/125/
[27] (2006). *EDINBURGH TRAM (LINE ONE) BILL - Environmental Statement - Non-Technical Summary*. Available: https://archive2021.parliament.scot/S2_Bills/Edinburgh%20Tram%20(Line%20One)%20Bill/line1-NTS.pdf
[28] Transport for Greater Manchester. (n.d., 01-02-2022). *Working safely near Metrolink*. Available: https://tfgm.com/public-transport/tram/working-safely
[29] Transport for West Midlands, "Working safely next to West Midlands," ed, n.d.
[30] UKtram. (n.d., 01-02-2022). *London Tramlink*. Available: https://uktram.org/systems/london-tramlink/
[31] UKtram. (n.d., 01-02-2022). *Blackpool Tramway*. Available: https://uktram.org/systems/blackpool-tramway/
[32] Department for Transport and Driver and Vehicle Licensing Agency, "VEH0130: Licensed plug-in cars, LGVs and quadricycles by local authority: United Kingdom," ed, 2021.
[33] Department for Transport and Driver and Vehicle Licensing Agency, "VEH0101: Licensed vehicles by body type (quarterly): Great Britain and United Kingdom," ed, 2021.
[34] Department for Transport and Driver and Vehicle Licensing Agency, "VEH0133: Licensed ultra low emission vehicles by body type and propulsion or fuel type: United Kingdom," ed, 2021.
[35] UK Government. (2018, 2018-08-03). *Low-emission vehicles eligible for a plug-in grant* [Online]. Available: https://www.gov.uk/plug-in-car-van-grants
[36] DEFRA, "UK plan for tackling roadside nitrogen dioxide concentrations: detailed plan," Department for Environment, Food & Rural Affairs and Department for Transport, London, UK2017, Available: https://assets.publishing.service.gov.uk/government/uploads/system/uploads/attachment_data/file/633270/air-quality-plan-detail.pdf.
[37] National Grid ESO, "Future Energy Scenarios (FES) 2021," 2021, Available: https://www.nationalgrideso.com/document/202851/download.
[38] National Grid ESO, "Future Energy Scenarios 2021 Data Workbook," ed, 2021.
[39] V. R. Vuchic, *Urban transit systems and technology*. John Wiley & Sons, 2007.
[40] C. Gavin, "Seasonal variations in electricity demand," Department of Energy & Climate Change, London, UK2014, Available: https://assets.publishing.service.gov.uk/government/uploads/system/uploads/attachment_data/file/295225/Seasonal_variations_in_electricity_demand.pdf.

[41] A. González-Gil, R. Palacin, and P. Batty, "Sustainable urban rail systems: Strategies and technologies for optimal management of regenerative braking energy," *Energy Conversion and Management*, vol. 75, pp. 374-388, 2013.
[42] M. Khodaparastan, A. A. Mohamed, and W. Brandauer, "Recuperation of Regenerative Braking Energy in Electric Rail Transit Systems," *IEEE Transactions on Intelligent Transportation Systems*, vol. 20, no. 8, pp. 2831-2847, 2019.
[43] M. Popescu and A. Bitoleanu, "A Review of the Energy Efficiency Improvement in DC Railway Systems," *Energies*, vol. 12, no. 6, 2019.
[44] Department for Transport, "VEH0170: Ultra low emission vehicles registered for the first time: United Kingdom," ed, 2021.
[45] BMW. (2020, 01-06-2021). *TECHNICAL DATA OF THE BMW i3*. Available: https://www.bmw.co.uk/en/all-models/bmw-i/i3/2020/technical-data.html
[46] Kia. (2021). *e-Niro Specification*. Available: https://www.kia.com/content/dam/kwcms/kme/uk/en/assets/vehicles/e-Niro/Specification/e-niro-specification.pdf
[47] Nissan. (2021). *Nissan Leaf*. Available: https://www-europe.nissan-cdn.net/content/dam/Nissan/gb/brochures/Vehicles/Nissan_Leaf_UK.pdf
[48] Renault. (n.d., 01-06-2021). *DRIVING RANGE, BATTERY & CHARGING RENAULT ZOE E-TECH ELECTRIC*. Available: https://www.renault.co.uk/electric-vehicles/zoe/battery.html
[49] Electric Vehicle Database. (n.d., 01-06-2021). *Tesla Model 3 Standard Range Plus*. Available: https://ev-database.org/car/1485/Tesla-Model-3-Standard-Range-Plus
[50] Electric Vehicle Database. (n.d., 01-06-2021). *Tesla Model 3 Long Range Dual Motor*. Available: https://ev-database.org/car/1525/Tesla-Model-3-Long-Range-Dual-Motor
[51] Tesla. (n.d., 01-07-2021). *Design Your Model 3*. Available: https://www.tesla.com/en_gb/model3/design#overview
[52] Jaguar. (2021, 01-06-2021). *ALL-ELECTRIC JAGUAR I-PACE SPECIFICATION AND PRICE GUIDE*. Available: https://www.jaguar.co.uk/Images/Jaguar-I-PACE-Specification-And-Price-Guide-1X5901910000SGBEN01P_tcm634-609065.pdf
[53] BMW. (n.d., 01-06-2021). *The BMW 3 Series Saloon: Engines & Technical Data*. Available: https://www.bmw.co.uk/en/all-models/3-series/saloon/2020/technical-data.bmw-330e-saloon.html
[54] Mercedes-Benz. (n.d., 01-06-2021). *A250e hatchback*. Available: https://www.mercedes-benz.co.uk/passengercars/mercedes-benz-cars/models/a-class/hatchback-w177/plugin-hybrid/key-stats.module.html
[55] Department for Transport, "NTS0303: Average number of trips, stages, miles and time spent travelling by main mode: England," ed, 2020.
[56] Department for Transport, "NTS0308: Average number of trips by trip length and main mode: England," ed, 2020.
[57] J. Mullan, D. Harries, T. Bräunl, and S. Whitely, "The technical, economic and commercial viability of the vehicle-to-grid concept," *Energy Policy*, vol. 48, pp. 394-406, 2012.
[58] W. Kempton, J. Tomic, S. Letendre, A. Brooks, and T. Lipman, "Vehicle-to-grid power: battery, hybrid, and fuel cell vehicles as resources for distributed electric power in California," 2001.
[59] S. E. Letendre and W. Kempton, "The V2G concept: A new model for power?," *Public Utilities Fortnightly*, vol. 140, no. 4, pp. 16-27, 2001.
[60] A. W. Thompson, "Economic implications of lithium ion battery degradation for Vehicle-to-Grid (V2X) services," *Journal of Power Sources*, vol. 396, pp. 691-709, 2018.

[61] N. S. Pearre and H. Ribberink, "Review of research on V2X technologies, strategies, and operations," *Renewable and Sustainable Energy Reviews*, vol. 105, pp. 61-70, 2019.
[62] A. W. Thompson and Y. Perez, "Vehicle-to-Everything (V2X) energy services, value streams, and regulatory policy implications," *Energy Policy*, vol. 137, 2020.
[63] B. Tarroja, L. Zhang, V. Wifvat, B. Shaffer, and S. Samuelsen, "Assessing the stationary energy storage equivalency of vehicle-to-grid charging battery electric vehicles," *Energy*, vol. 106, pp. 673-690, 2016.
[64] M. A. Laughton and M. G. Say, *Electrical engineer's reference book*. Elsevier, 2013.
[65] B. Destraz, P. Barrade, A. Rufer, and M. Klohr, "Study and simulation of the energy balance of an urban transportation network," in *2007 European conference on power electronics and applications*, 2007, pp. 1-10: IEEE.
[66] S. Açıkbaş and M. Söylemez, "Catenary system paralleling and its effect on power consumption and regenerated energy recuperation," in *4th International Conference on Electrical and Electronics Engineering (ELECO 2005)*, 2005, pp. 17-21.
[67] M. Z. Chymera, A. C. Renfrew, M. Barnes, and J. Holden, "Modeling Electrified Transit Systems," *IEEE Transactions on Vehicular Technology*, vol. 59, no. 6, pp. 2748-2756, 2010.
[68] A. Kara, K. Mardikyan, and S. Baran, "Application of regenerative braking energy to Istanbul metro operation system," in *2012 Electrical Systems for Aircraft, Railway and Ship Propulsion*, 2012, pp. 1-3: IEEE.
[69] J. Yang, Y. Hou, R. Song, and T. Yuan, "Modeling and analysis of the electrical braking energy of urban railway vehicles," *Simulation*, vol. 91, no. 11, pp. 989-997, 2015.
[70] Z. Tian *et al.*, "Energy evaluation of the power network of a DC railway system with regenerating trains," *IET Electrical Systems in Transportation*, vol. 6, no. 2, pp. 41-49, 2016.
[71] R. Barrero, X. Tackoen, and J. Van Mierlo, "Stationary or onboard energy storage systems for energy consumption reduction in a metro network," *Proceedings of the Institution of Mechanical Engineers, Part F: Journal of Rail Rapid Transit*, vol. 224, no. 3, pp. 207-225, 2010.
[72] J. Kubín and A. Richter, "Efficiency of mechanical energy recovery from a tram by different input conditions," in *2012 15th International Power Electronics and Motion Control Conference (EPE/PEMC)*, 2012, pp. DS1c. 6-1-DS1c. 6-5: IEEE.
[73] S. l. Ac¸ ikbas¸ and M. T. So¨ ylemez, "Parameters affecting braking energy recuperation rate in DC rail transit," in *ASME/IEEE Joint Rail Conference*, 2007, vol. 4787, pp. 263-268.
[74] C. Gong, S. Zhang, F. Zhang, J. Jiang, and X. Wang, "An Integrated Energy-Efficient Operation Methodology for Metro Systems Based on a Real Case of Shanghai Metro Line One," *Energies*, vol. 7, no. 11, pp. 7305-7329, 2014.
[75] J. F. Chen, R. L. Lin, and Y. C. Liu, "Optimization of an MRT train schedule: reducing maximum traction power by using genetic algorithms," *IEEE Transactions on power systems*, vol. 20, no. 3, pp. 1366-1372, 2005.
[76] H. Lee *et al.*, "Capacity optimization of the supercapacitor energy storages on DC railway system using a railway powerflow algorithm," *International Journal of Innovative Computing, Information and Control*, vol. 7, no. 5, pp. 2739-2753, 2011.
[77] R. Teymourfar, B. Asaei, H. Iman-Eini, and R. Nejati fard, "Stationary super-capacitor energy storage system to save regenerative braking energy in a metro line," *Energy Conversion and Management*, vol. 56, pp. 206-214, 2012.
[78] F. Shahnia, M. Sarhangzadeh, M. B. Sharifian, and S. H. Hosseini, "Induction motor characteristics and applications for DC electrified railway systems," 2005.

[79] L. Streit and P. Drabek, "Energy efficiency of tram emulation with energy storage system," in *2012 15th International Power Electronics and Motion Control Conference (EPE/PEMC)*, 2012, pp. DS1e. 6-1-DS1e. 6-3: IEEE.
[80] L. Streit and P. Drabek, "Simulation model of tram with energy storage system," in *2013 International Conference on Applied Electronics*, 2013, pp. 1-4: IEEE.
[81] F. Du, J. He, L. Yu, M. Li, Z. Bo, and A. Klimek, "Modeling and simulation of metro DC traction system with different motor driven trains," in *2010 Asia-Pacific Power and Energy Engineering Conference*, 2010, pp. 1-4: IEEE.
[82] L. Yu, J. He, H. Yip, F. Du, Z. Bo, and J. Hu, "Simulation of regenerative braking in DC railway system based on MATLAB/Simulink," in *45th International Universities Power Engineering Conference UPEC2010*, 2010, pp. 1-5: IEEE.
[83] S. Ruigang, Y. Tianchen, Y. Jian, and H. Hao, "Simulation of braking energy recovery for the metro vehicles based on the traction experiment system," *Simulation*, vol. 93, no. 12, pp. 1099-1112, 2017.
[84] V. Brazis, L. Latkovskis, and L. Grigans, "Simulation of trolleybus traction induction drive with supercapacitor energy storage system," *Latvian Journal of Physics Technical Sciences*, vol. 47, no. 5, p. 33, 2010.
[85] A. González-Gil, R. Palacin, P. Batty, and J. P. Powell, "A systems approach to reduce urban rail energy consumption," *Energy Conversion and Management*, vol. 80, pp. 509-524, 2014.
[86] D. Cornic, "Efficient recovery of braking energy through a reversible dc substation," in *Electrical systems for aircraft, railway and ship propulsion*, 2010, pp. 1-9: IEEE.
[87] H. Ibaiondo and A. Romo, "Kinetic energy recovery on railway systems with feedback to the grid," in *Proceedings of 14th International Power Electronics and Motion Control Conference EPE-PEMC 2010*, 2010, pp. T9-94-T9-97: IEEE.
[88] V. Gelman, "Braking energy recuperation," *IEEE Vehicular Technology Magazine*, vol. 4, no. 3, pp. 82-89, 2009.
[89] V. Gelman, "Energy Storage That May Be Too Good to Be True: Comparison Between Wayside Storage and Reversible Thyristor Controlled Rectifiers for Heavy Rail," *IEEE Vehicular Technology Magazine*, vol. 8, no. 4, pp. 70-80, 2013.
[90] EvoEnergy. (2020, 25-07-2021). *Selling electricity back to the grid* [Online]. Available: https://www.evoenergy.co.uk/news-updates/selling-electricity-back-to-the-grid/
[91] N. Ghaviha, J. Campillo, M. Bohlin, and E. Dahlquist, "Review of Application of Energy Storage Devices in Railway Transportation," *Energy Procedia*, vol. 105, pp. 4561-4568, 2017.
[92] B. Dunn, H. Kamath, and J.-M. Tarascon, "Electrical energy storage for the grid: a battery of choices," *Science*, vol. 334, no. 6058, pp. 928-935, 2011.
[93] P. Arboleya, P. Bidaguren, and U. Armendariz, "Energy is on board: Energy storage and other alternatives in modern light railways," *IEEE Electrification Magazine*, vol. 4, no. 3, pp. 30-41, 2016.
[94] F. Meishner and D. U. Sauer, "Wayside energy recovery systems in DC urban railway grids," *eTransportation*, vol. 1, p. 100001, 2019.
[95] M. Steiner, M. Klohr, and S. Pagiela, "Energy storage system with ultracaps on board of railway vehicles," in *2007 European conference on power electronics and applications*, 2007, pp. 1-10: IEEE.
[96] V. I. Herrera, H. Gaztañaga, A. Milo, A. Saez-de-Ibarra, I. Etxeberria-Otadui, and T. Nieva, "Optimal energy management and sizing of a battery--supercapacitor-based light rail vehicle with a multiobjective approach," *IEEE Transactions on Industry Applications*, vol. 52, no. 4, pp. 3367-3377, 2016.

[97] R. Barrero, X. Tackoen, and J. Van Mierlo, "Improving energy efficiency in public transport: Stationary supercapacitor based Energy Storage Systems for a metro network," in *2008 IEEE Vehicle Power and Propulsion Conference*, 2008, pp. 1-8: IEEE.
[98] M. Ceraolo and G. Lutzemberger, "Stationary and on-board storage systems to enhance energy and cost efficiency of tramways," *Journal of Power Sources,* vol. 264, pp. 128-139, 2014.
[99] Z. Gao, J. Fang, Y. Zhang, L. Jiang, D. Sun, and W. Guo, "Control of urban rail transit equipped with ground-based supercapacitor for energy saving and reduction of power peak demand," *International Journal of Electrical Power & Energy Systems,* vol. 67, pp. 439-447, 2015.
[100] R. Lamedica, A. Ruvio, L. Palagi, and N. Mortelliti, "Optimal Siting and Sizing of Wayside Energy Storage Systems in a DC Railway Line," *Energies,* vol. 13, no. 23, p. 6271, 2020.
[101] J.-y. Park, J.-H. Heo, S. Shin, and H. Kim, "Economic evaluation of ESS in urban railway substation for peak load shaving based on net present value," *Journal of Electrical Engineering Technology,* vol. 12, no. 2, pp. 981-987, 2017.
[102] D. Roch-Dupré, Á. J. López-López, R. R. Pecharromán, A. P. Cucala, and A. Fernández-Cardador, "Analysis of the demand charge in DC railway systems and reduction of its economic impact with Energy Storage Systems," *International Journal of Electrical Power Energy Systems,* vol. 93, pp. 459-467, 2017.
[103] W. Kempton and J. Tomić, "Vehicle-to-grid power fundamentals: Calculating capacity and net revenue," *Journal of power sources,* vol. 144, no. 1, pp. 268-279, 2005.
[104] W. Kempton and J. Tomić, "Vehicle-to-grid power implementation: From stabilizing the grid to supporting large-scale renewable energy," *Journal of power sources,* vol. 144, no. 1, pp. 280-294, 2005.
[105] K. Clement-Nyns, E. Haesen, and J. Driesen, "The impact of vehicle-to-grid on the distribution grid," *Electric Power Systems Research,* vol. 81, no. 1, pp. 185-192, 2011.
[106] S. Habib, M. Kamran, and U. Rashid, "Impact analysis of vehicle-to-grid technology and charging strategies of electric vehicles on distribution networks–a review," *Journal of Power Sources,* vol. 277, pp. 205-214, 2015.
[107] S. Lefeng, L. Zhengfa, P. Yongjian, C. Qi'an, and Systems, "A reserve dispatch paradigm considering vehicle-to-grid reserve," *Electric Power Components,* vol. 44, no. 5, pp. 471-479, 2016.
[108] L. Drude, L. C. P. Junior, and R. Rüther, "Photovoltaics (PV) and electric vehicle-to-grid (V2G) strategies for peak demand reduction in urban regions in Brazil in a smart grid environment," *Renewable Energy,* vol. 68, pp. 443-451, 2014.
[109] L. Udrene and G. Bazbauers, "Role of vehicle-to-grid systems for electric load shifting and integration of intermittent sources in Latvian power system," *Energy Procedia,* vol. 72, pp. 156-162, 2015.
[110] Aalborg University. (2021, 01-02-2021). *Introduction*. Available: https://www.energyplan.eu/
[111] C. D. White and K. M. Zhang, "Using vehicle-to-grid technology for frequency regulation and peak-load reduction," *Journal of Power Sources,* vol. 196, no. 8, pp. 3972-3980, 2011.
[112] F. Mwasilu, J. J. Justo, E.-K. Kim, T. D. Do, and J.-W. Jung, "Electric vehicles and smart grid interaction: A review on vehicle to grid and renewable energy sources integration," *Renewable and Sustainable Energy Reviews,* vol. 34, pp. 501-516, 2014.

[113] D. B. Richardson, "Electric vehicles and the electric grid: A review of modeling approaches, Impacts, and renewable energy integration," *Renewable and Sustainable Energy Reviews*, vol. 19, pp. 247-254, 2013.
[114] H. Lund and W. Kempton, "Integration of renewable energy into the transport and electricity sectors through V2G," *Energy policy*, vol. 36, no. 9, pp. 3578-3587, 2008.
[115] G. Haddadian, N. Khalili, M. Khodayar, and M. Shahiedehpour, "Security-constrained power generation scheduling with thermal generating units, variable energy resources, and electric vehicle storage for V2G deployment," *International Journal of Electrical Power Energy Systems*, vol. 73, pp. 498-507, 2015.
[116] A. Ul-Haq, C. Cecati, and E. A. Al-Ammar, "Modeling of a photovoltaic-powered electric vehicle charging station with vehicle-to-grid implementation," *Energies*, vol. 10, no. 1, p. 4, 2017.
[117] C. Guenther, B. Schott, W. Hennings, P. Waldowski, and M. A. Danzer, "Model-based investigation of electric vehicle battery aging by means of vehicle-to-grid scenario simulations," *Journal of Power Sources*, vol. 239, pp. 604-610, 2013.
[118] K. Uddin, M. Dubarry, and M. B. Glick, "The viability of vehicle-to-grid operations from a battery technology and policy perspective," *Energy Policy*, vol. 113, pp. 342-347, 2018.
[119] D. M. Hill, A. S. Agarwal, and F. Ayello, "Fleet operator risks for using fleets for V2G regulation," *Energy Policy*, vol. 41, pp. 221-231, 2012.
[120] J. Geske and D. Schumann, "Willing to participate in vehicle-to-grid (V2G)? Why not!," *Energy Policy*, vol. 120, pp. 392-401, 2018.
[121] P. V. Radu, M. Lewandowski, and A. Szelag, "On-Board and Wayside Energy Storage Devices Applications in Urban Transport Systems—Case Study Analysis for Power Applications," *Energies*, vol. 13, no. 8, p. 2013, 2020.
[122] A. Millner *et al.*, "Plug in electric vehicles and the grid," in *2014 IEEE NewNEB DC Utility Power Conference and Exhibition (NewNEB)*, 2014, pp. 1-6: IEEE.
[123] M. Brenna, M. Longo, and W. Yaïci, "Modelling and simulation of electric vehicle fast charging stations driven by high speed railway systems," *Energies*, vol. 10, no. 9, p. 1268, 2017.
[124] A. Fernandez-Rodriguez *et al.*, "Charging electric vehicles using regenerated energy from urban railways," in *2017 IEEE Vehicle Power and Propulsion Conference (VPPC)*, 2017, pp. 1-6: IEEE.
[125] Stagecoach. (2021). *Welcome to Supertram* [Online]. Available: https://www.stagecoachbus.com/supertram#tab7
[126] G. Morita, T. Konishi, S. Hase, Y. Nakamichi, H. Nara, and T. Uemura, "Verification tests of electric double-layer capacitors for static energy storage system in DC electrified railway," in *2008 International Symposium on Power Electronics, Electrical Drives, Automation and Motion*, 2008, pp. 1017-1022: IEEE.
[127] T. Hirano, S. Kikuchi, T. Suzuki, and H. Hayashiya, "Evaluation of energy loss in dc traction power supply system," in *2015 17th European Conference on Power Electronics and Applications (EPE'15 ECCE-Europe)*, 2015, pp. 1-6: IEEE.
[128] A. López-López, R. Pecharromán, J. García-Matos, A. Fernández-Cardador, and A. Cucala, "Optimal deployment of energy storage systems in a dc-electrified railway system," *WIT transactions on the built environment*, vol. 127, pp. 603-614, 2012.
[129] Supertram, "Supertram report for internal use of university of Sheffield only," 2017.
[130] Stagecoach. (2021). *Vehicle information* [Online]. Available: https://www.stagecoachbus.com/supertram/vehicle-information

[131] S. C. Walpole, D. Prieto-Merino, P. Edwards, J. Cleland, G. Stevens, and I. Roberts, "The weight of nations: an estimation of adult human biomass," *BMC public health,* vol. 12, no. 1, pp. 1-6, 2012.
[132] W. J. Davis, *The tractive resistance of electric locomotives and cars*. General Electric, 1926.
[133] B. P. Rochard and F. Schmid, "A review of methods to measure and calculate train resistances," *Proceedings of the Institution of Mechanical Engineers, Part F: Journal of Rail Rapid Transit,* vol. 214, no. 4, pp. 185-199, 2000.
[134] H. S. Hansen, M. U. Nawaz, and N. Olsson, "Using operational data to estimate the running resistance of trains. Estimation of the resistance in a set of Norwegian tunnels," *Journal of Rail Transport Planning Management,* vol. 7, no. 1-2, pp. 62-76, 2017.
[135] A. Rupp, H. Baier, P. Mertiny, and M. Secanell, "Analysis of a flywheel energy storage system for light rail transit," *Energy,* vol. 107, pp. 625-638, 2016.
[136] S. Yi, *Principles of railway Location and Design*. Academic Press, 2017.
[137] P. Hu, R. Chen, H. Li, and Y. Liang, "Train operation traction energy calculation and saving in urban rail transit system," in *2012 Second International Conference on Instrumentation, Measurement, Computer, Communication and Control*, 2012, pp. 505-507: IEEE.
[138] A. Frilli, E. Meli, D. Nocciolini, L. Pugi, A. Rindi, and Management, "Energetic optimization of regenerative braking for high speed railway systems," *Energy Conversion,* vol. 129, pp. 200-215, 2016.
[139] S. Hillmansen and C. Roberts, "Energy storage devices in hybrid railway vehicles: a kinematic analysis," *Proceedings of the Institution of Mechanical Engineers, Part F: Journal of Rail Rapid Transit,* vol. 221, no. 1, pp. 135-143, 2007.
[140] H. Alnuman, D. Gladwin, and M. Foster, "Electrical modelling of a DC railway system with multiple trains," *Energies,* vol. 11, no. 11, p. 3211, 2018.
[141] P. V. Radu and Z. Drazek, "Analysis of wayside energy storage devices for DC heavy rail transport," in *MATEC Web of Conferences*, 2018, vol. 180, p. 04001: EDP Sciences.
[142] P. J. Grbović, P. Delarue, P. Le Moigne, and P. Bartholomeus, "The ultracapacitor-based controlled electric drives with braking and ride-through capability: Overview and analysis," *IEEE Transactions on Industrial Electronics,* vol. 58, no. 3, pp. 925-936, 2010.
[143] W. Dewei, Z. Kun, W. Shenrong, Y. Zhongping, and Y. Xiaojie, "Power distribution control strategy of on-board supercapacitor energy storage system of railway vehicle," in *2011 International Conference on Materials for Renewable Energy & Environment*, 2011, vol. 1, pp. 664-668: IEEE.
[144] Z. Gao, J. Fang, Y. Zhang, and D. Sun, "Control strategy for wayside supercapacitor energy storage system in railway transit network," *Journal of Modern Power Systems Clean Energy,* vol. 2, no. 2, pp. 181-190, 2014.
[145] Y. Jiang, J. Liu, W. Tian, M. Shahidehpour, and M. Krishnamurthy, "Energy Harvesting for the Electrification of Railway Stations: Getting a charge from the regenerative braking of trains. A," *IEEE Electrification Magazine,* vol. 2, no. 3, pp. 39-48, 2014.
[146] S.-D. Kim and K.-h. Choi, "A Study on the Efficiency of Energy Storage System Applied to the Power Traction System of DC Electric Railway," *Journal of International Council on Electrical Engineering,* vol. 2, no. 2, pp. 225-230, 2012.
[147] BMW. Technical specifications [Online]. Available: https://www.press.bmwgroup.com/global/article/attachment/T0284828EN/415571
[148] Tesla. (2021). *Model S* [Online]. Available: https://www.tesla.com/en_gb/models

[149] T. Zhang, R. Zhao, E. E. F. Ballantyne, and D. A. Stone, "Increasing urban tram system efficiency, with battery storage and electric vehicle charging," *Transportation Research Part D: Transport and Environment*, vol. 80, 2020.
[150] H. Nikolas *et al.*, "2020 Government greenhouse gas conversion factors for company reporting - Methodology Paper for Conversion factors - Final Report," London, UK, 2020, Available: https://assets.publishing.service.gov.uk/government/uploads/system/uploads/attachment_data/file/901692/conversion-factors-2020-methodology.pdf.
[151] T. Zhang, E. E. F. Ballantyne, R. Zhao, and D. A. Stone, "Technical and economic feasibility of increasing tram system efficiency with EV batteries," *Transportation Research Part D: Transport and Environment*, vol. 91, 2021.
[152] O. Žižlavský, "Net present value approach: method for economic assessment of innovation projects," *Procedia-Social Behavioral Sciences*, vol. 156, pp. 506-512, 2014.
[153] T. San Ong and C. H. Thum, "Net present value and payback period for building integrated photovoltaic projects in Malaysia," *International Journal of Academic Research in Business Social Sciences*, vol. 3, no. 2, p. 153, 2013.
[154] M. S. H. Lipu and T. Jamal, "Techno-economic analysis of solar Concentrating power (CSP) in Bangladesh," *Int. J. Adv. Renew. Energy Res*, vol. 2, no. 5, pp. 750-762, 2013.
[155] L. Juhász, "Net present value versus internal rate of return," *Economics Sociology*, vol. 4, no. 1, pp. 46-53, 2011.
[156] A. Gallo, "A refresher on internal rate of return," *Harvard Business Review Digital Articles*, vol. 2, 2016.
[157] H. E. Marshall, *Recommended Practice for Measuring Simple and Discounted Payback for Investments in Buildings and Building Systems*. National Bureau of Standards, 1984.
[158] K. Ardani, E. O'Shaughnessy, R. Fu, C. McClurg, J. Huneycutt, and R. Margolis, "Installed cost benchmarks and deployment barriers for residential solar photovoltaics with energy storage: Q1 2016," National Renewable Energy Lab.(NREL), Golden, CO (United States)2016.
[159] W. J. Cole and A. Frazier, "Cost projections for utility-scale battery storage," National Renewable Energy Lab.(NREL), Golden, CO (United States)2019.
[160] K. Mongird *et al.*, "Energy storage technology and cost characterization report," Pacific Northwest National Lab.(PNNL), Richland, WA (United States)2019.
[161] L. Goldie-Scot. (2019). *A Behind the Scenes Take on Lithium-ion Battery Prices* [Online]. Available: https://about.bnef.com/blog/behind-scenes-take-lithium-ion-battery-prices/
[162] X. Li, K. J. Chalvatzis, and P. Stephanides, "Innovative energy islands: life-cycle cost-benefit analysis for battery energy storage," *Sustainability*, vol. 10, no. 10, p. 3371, 2018.
[163] C. Rahmann, B. Mac-Clure, V. Vittal, and F. Valencia, "Break-even points of battery energy storage systems for peak shaving applications," *Energies*, vol. 10, no. 7, p. 833, 2017.
[164] L. Wingren and J. Johnsson, "Battery Energy Storage Systems as an alternative to gas turbines for the fast active disturbance reserve," 2018.
[165] T. West, "2015-2018 Electricity Purchasing Case Study By Pulse Business Energy and Nottingham Express Transit," London, UK, 2017, Available: http://pulsebusinessenergy.co.uk/wp-content/uploads/Pulse-Business-Energy-and-Nottingham-Express-Transit-Performance-Report.pdf.
[166] BEIS, "Gas and electricity prices in the non-domestic sector," ed. London, UK, 2020.

[167] S. A. El-Temtamy and T. S. Gendy, "Economic evaluation and sensitivity analysis of some fuel oil upgrading processes," *Egyptian Journal of Petroleum*, vol. 23, no. 4, pp. 397-407, 2014.
[168] C. Zhou, K. Qian, M. Allan, and W. Zhou, "Modeling of the cost of EV battery wear due to V2G application in power systems," *IEEE Transactions on Energy Conversion*, vol. 26, no. 4, pp. 1041-1050, 2011.
[169] Y. Miao, P. Hynan, A. Von Jouanne, and A. Yokochi, "Current Li-ion battery technologies in electric vehicles and opportunities for advancements," *Energies*, vol. 12, no. 6, p. 1074, 2019.
[170] G. R. Parsons, M. K. Hidrue, W. Kempton, and M. P. Gardner, "Willingness to pay for vehicle-to-grid (V2G) electric vehicles and their contract terms," *Energy Economics*, vol. 42, pp. 313-324, 2014.
[171] O. McDonald, "Re-Think! Parking on the High Street: Guidance on Parking Provision in Town and City Centres," Association of Town & City Management, British Parking Association, Parking Data & Research International and Springboard Research Ltd2013, Available: https://www.britishparking.co.uk/write/Documents/Re-thinking_Car_Parking.pdf.
[172] S. B. Peterson, J. Apt, and J. Whitacre, "Lithium-ion battery cell degradation resulting from realistic vehicle and vehicle-to-grid utilization," *Journal of Power Sources*, vol. 195, no. 8, pp. 2385-2392, 2010.
[173] D. Wang, J. Coignard, T. Zeng, C. Zhang, and S. Saxena, "Quantifying electric vehicle battery degradation from driving vs. vehicle-to-grid services," *Journal of Power Sources*, vol. 332, pp. 193-203, 2016.
[174] Ofgem, "Infographic: Bills, prices and profits," 2021, Available: https://www.ofgem.gov.uk/publications/infographic-bills-prices-and-profits.

Appendix A Tram travelling profile

The travelling profile of the tram journeys from Halfway to malin Bridge (Blue Line), from Middlewook to Meadowhall (Yellow Line) and from Cathedral to Herding Park (Purple Line) are shown in Figure A-1, Figure A-2 and Figure A-3, respectively.

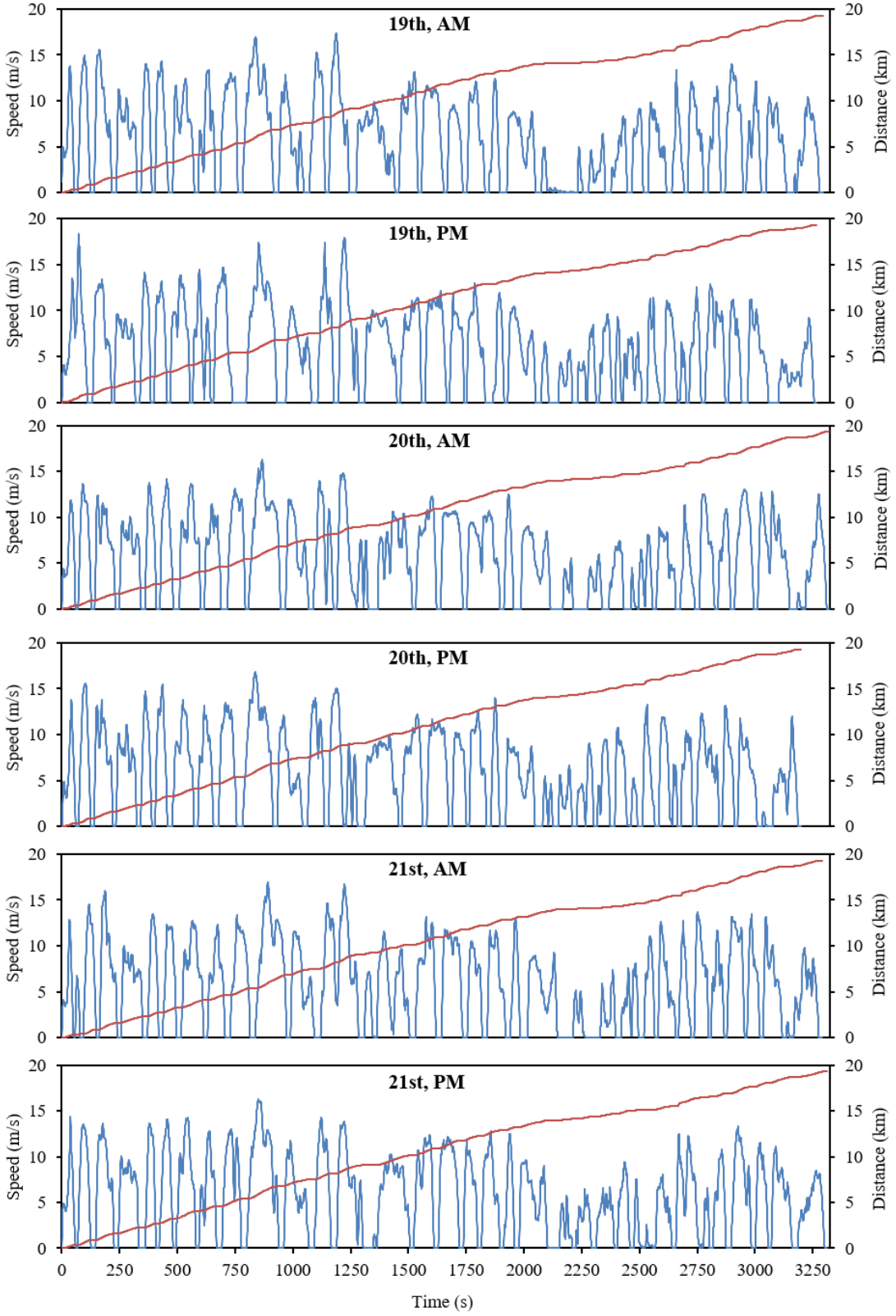

Figure A-1 The speed and distance profile of the tram journey from Halfway to Malin Bridge (Blue Line)

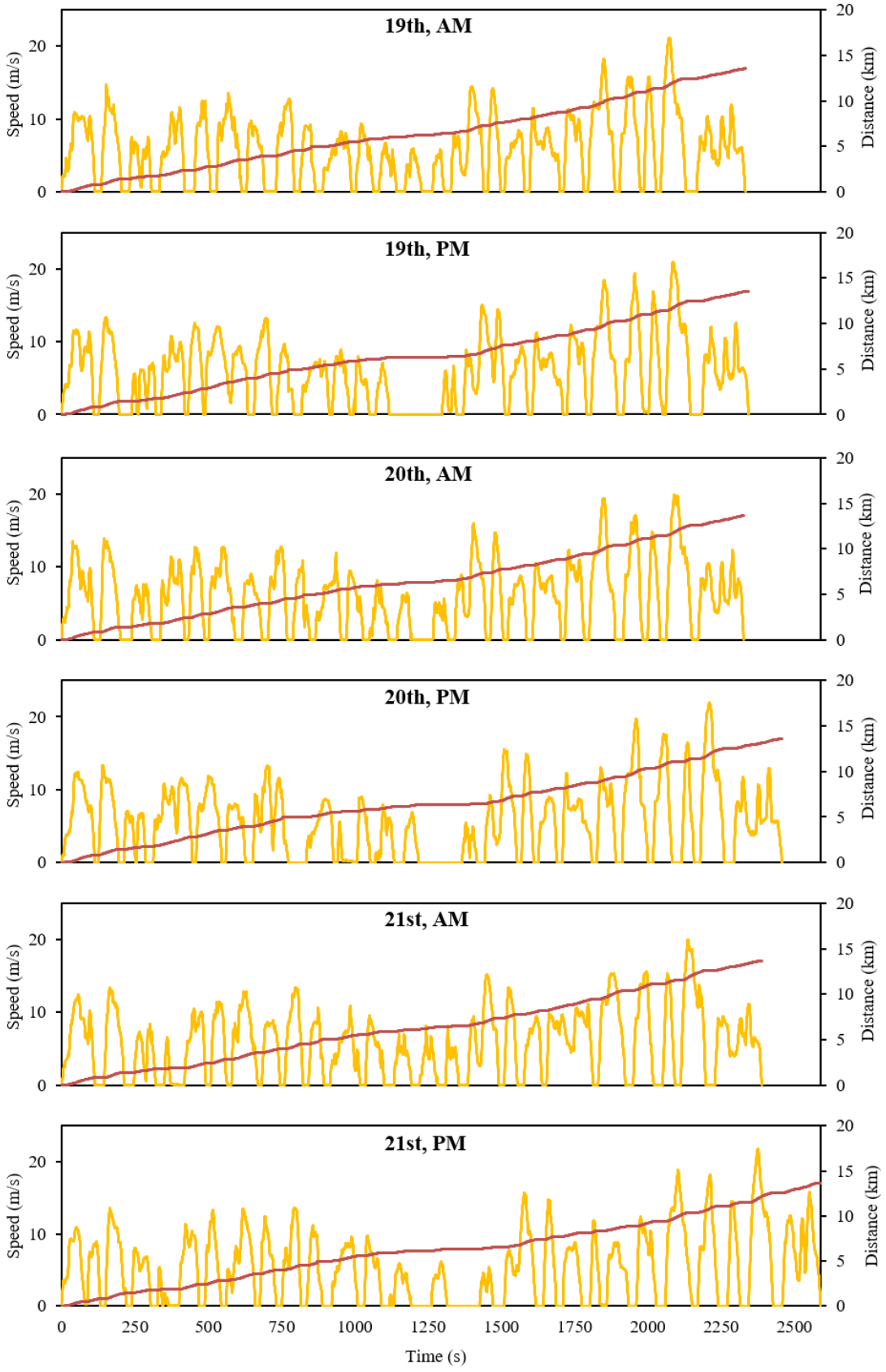

Figure A-2 The speed and distance profile of the tram journey from Middlewook to Meadowhall (Yellow Line)

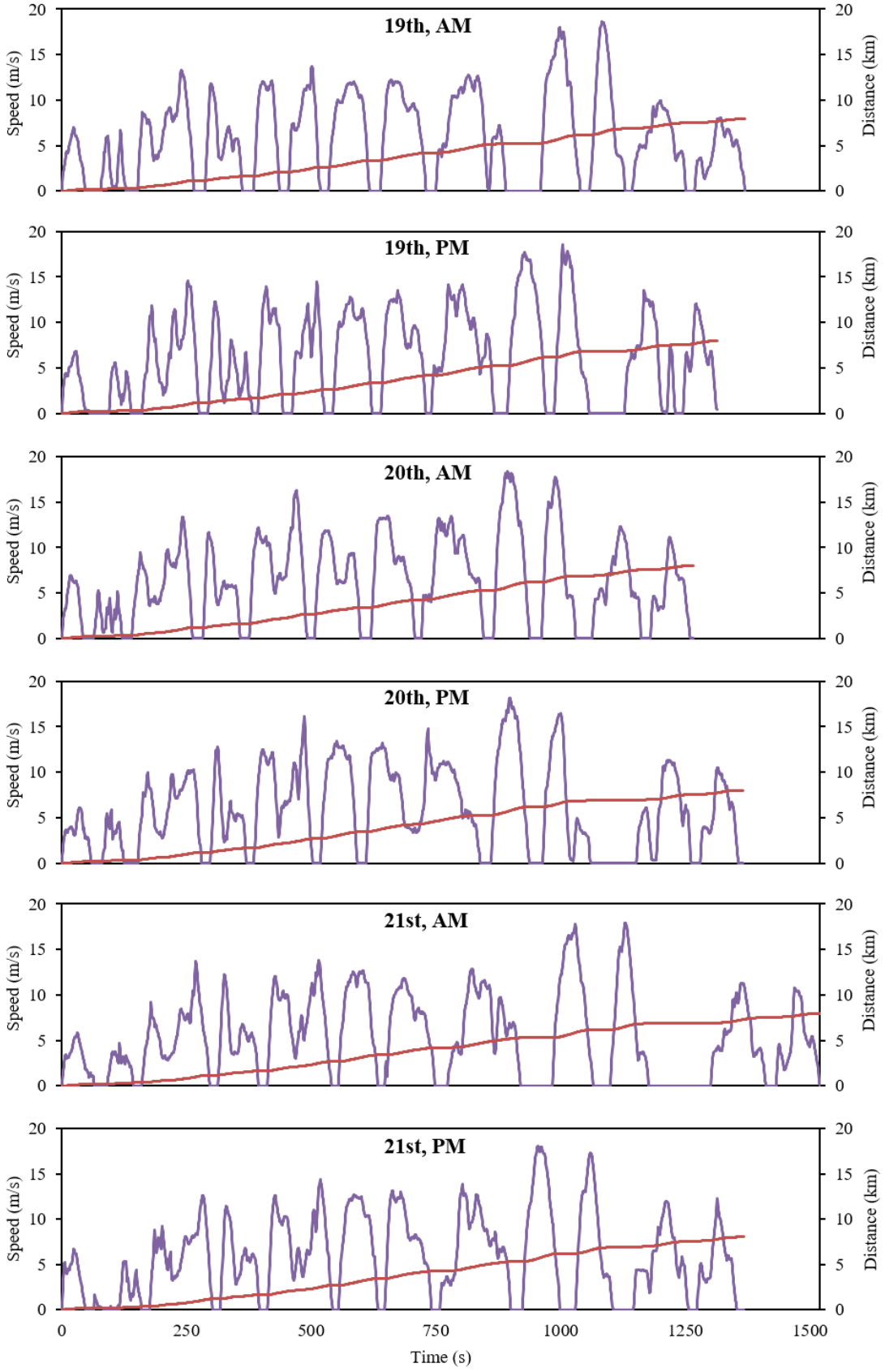

Figure A-3 The speed and distance profile of the tram journey from Cathedral to Herding Park (Purple Line)